The Pennsylvania State University

The Graduate School

Department of Cellular & Molecular Physiology

INVESTIGATIONS OF POLYAMINE FUNCTION USING TRANSGENIC MOUSE MODELS WITH SPERMIDINE SYNTHASE AND S-ADENOSYLMETHIONINE DECARBOXYLASE OVEREXPRESSION

A Dissertation in

Physiology

by

Chenxu Shi

Submitted in Partial Fulfillment
of the Requirements
for the Degree of

Doctor of Philosophy

December 2011

The dissertation of Chenxu Shi was reviewed and approved* by the following:

David J. Feith
Assistant Professor of Cellular and Molecular Physiology
Dissertation Advisor
Chair of Committee

Anthony E. Pegg
Evan Pugh Professor Emeritus of Cellular and Molecular Physiology and Pharmacology

Lisa M. Shantz
Associate Professor of Cellular and Molecular Physiology

Edward J. Gunther
Associate Professor of Medicine

Scot R. Kimball
Professor of Cellular and Molecular Physiology

Barbara A. Miller
Professor of Pediatrics and Biochemistry and Molecular Biology

Leonard S. Jefferson, Jr.
Evan Pugh Professor and Chair of Cellular and Molecular Physiology

* Signatures are on file in the Graduate School

ABSTRACT

Polyamines, including putrescine, spermidine, and spermine, are ubiquitous polycationic compounds that are essential for cell growth and differentiation. To better understand cellular function of polyamines, two transgenic mouse models with either widespread constitutive overexpression of spermidine synthase (SpdS) or regulated expression of S-adenosylmethionine decarboxylase (AdoMetDC) in the skin were created and characterized.

SpdS is a polyamine biosynthetic enzyme, and it transfers an aminopropyl group from decarboxylated S-adenosylmethionine (dcAdoMet) to putrescine to produce spermidine. We generated a transgenic mouse line that overexpresses human spermidine synthase from a composite cytomegalovirus- immediate early gene enhancer/chicken β-actin promoter (CAG) in order to determine the impact of elevated SpdS activity on murine development and physiology, and to enable simultaneous overexpression of SpdS and other polyamine biosynthetic enzymes by combining transgenic models. CAG-SpdS mice were viable and fertile and exhibited a reduced tissue spermine:spermidine ratio that correlated with the level of SpdS activity. We also demonstrated that the combined overexpression of both SpdS and spermine synthase (SpmS) in CAG-SpdS/CAG-SpmS bitransgenic mice did not impair murine viability or lead to overt developmental abnormalities but instead normalizes the elevated tissue spermine:spermidine ratios of CAG-SpmS mice. Finally, upon breeding of CAG-SpdS mice to MHC (α-myosin heavy chain)-AdoMetDC mice with a >100-fold increase in cardiac AdoMetDC activity, CAG-SpdS/MHC-AdoMetDC bitransgenic animals were produced at the expected frequency and exhibited cardiac polyamine levels comparable to MHC-AdoMetDC littermates.

Taken together these results indicate that SpdS levels are unlikely to exert significant regulatory effects on cellular polyamine content and function.

Previous studies suggest that the increased levels of polyamines, especially putrescine, play a critical role in skin tumor development. AdoMetDC is a rate-limiting enzyme in the polyamine biosynthetic pathway. It catalyzes the decarboxylation of S-adenosylmethionine (AdoMet) to generate dcAdoMet that serves as the aminopropyl donor for the production of spermidine and spermine from the precursor putrescine. We utilized the Tet-off system to generate transgenic mice with regulated expression of AdoMetDC in skin basal keratinocytes directed by the Keratin 5 promoter to enhance our understanding of the role played by AdoMetDC in controlling polyamine levels and of polyamine function in epithelial carcinogenesis. We found that untreated transgenic mice displayed a 7 to 8-fold increase in epidermal and dermal AdoMetDC activity at 7 weeks of age, and a corresponding increase in the enzymatic product dcAdoMet levels. These mice also exhibited a thin fur phenotype that could be eliminated by doxycycline treatment. A skin chemical carcinogenesis experiment on these mice demonstrated that AdoMetDC overexpression resulted in a 46% reduction in tumor multiplicity compared to controls after 25 weeks of tumor promotion. A further study of tumor growth upon transgene silencing by doxycyline suggested that the tumor suppressive effect was the result of blocking the growth of initiated cells at a microscopic, dormant but still viable state in the skin. These findings will help with future development of polyamine-targeted therapies to prevent and treat cancer.

TABLE OF CONTENTS

LIST OF FIGURES

LIST OF TABLES

LIST OF ABBREVIATIONS

AdoMetDC - *S*-adenosylmethionine decarboxylase

hAdoMetDC - human *S*-adenosylmethionine decarboxylase

AdoMet - *S*-adenosylmethionine

dcAdoMet - decarboxylated *S*-adenosylmethionine

AZ - antizyme

AZI - antizyme inhibitor

CAG - composite cytomegalovirus immediate early gene enhancer-chicken β-actin promoter

DFMO - α-difluoromethylornithine

DMBA - 7,12-dimethylbenz[a]anthracene

Dox - doxycycline

eIF5A - eukaryotic initiation factor 5A

FACS - fluorescence-activated cell sorting

HA - hemagglutinin

HPLC - high-performance liquid chromatography

IRES - internal Ribosome Entry Site

K5 - Keratin 5

K6 - Keratin 6

MAT - methionine adenosyltransferase

MEK - mitogen-activated protein kinase/extracellular signal-regulated kinase

MGBG - methyglyoxal bis(guanylhydrazone)

MHC - α-myosin heavy chain

MTA - 5’-methylthioadenosine

MYC - myelocytomatosis viral oncogene homolog

ODC - ornithine decarboxylase

ORS - outer root sheath

PAO - acetylpolyamine oxidase

Put - putrescine

RLU – relative luciferase units

ROS - reactive oxygen species

Spd - spermidine

Spm – spermine

SMO - spermine oxidase

SpdS - spermidine synthase

SpmS- Spermine synthase

SSAT - spermidine/spermine N^1-acetyltransferase

TPA - 12-*O*-tetradecanoyl-phorbol-13-acetate

uORF - upstream open reading frame

5’-UTR - 5’- untranslated region

3’-UTR - 3’- untranslated region

ACKNOWLEDGEMENTS

I will always be grateful to my mentor, Dr. David Feith for his advice and guidance throughout the course of my graduate studies. Without his exceptional scientific insights, endless support and patience, I would not be able to finish my thesis research. I also would like to express my deep gratitude to my former mentor, Dr. Anthony Pegg for giving me the opportunity to work in his lab, for his insightful advice and invaluable input to my projects, and for his continuing serving on my committee after his retirement. I want to give my special thanks to Dr. Lisa Shantz, Dr. Edward Gunther, Dr. Scot Kimball and Dr. Barbara Miller for their very helpful insights and different scientific perspectives, and for their time and effort to serve on my committee.

I extend my appreciation to members of the Feith/Pegg lab both past and present, especially Pat Welsh, Chethana Prakashagowda, Suzanne Sass-Kuhn for their excellent technical support; Dr. Diane McCloskey, Dr. Natalia Loktionova, Dr. Xiaojing Wang, Dr. Sreenivas Kanugula and Dr. Qingming Fang for generously donating their time to help me with my projects, thesis, and presentations.

I would like to acknowledge Dr. Janet Sawicki for providing the pCX-EGFP plasmid, Dr. Masaru Okabe for permission to use this construct in our experiments, Dr. Lewis Chodosh for providing the inducible TetO vector, Dr. Adam Glick for providing the K5-tTA mice, Tom Salada of the Penn State University Transgenic Mouse Facility for the transgene microinjections, Fan He of the Penn State Public Health Sciences for doing the statistical analysis on tumor studies, and Dr. Tim Cooper of the Penn State Comparative Medicine for scoring mouse hair follicle morphogenesis stages and hair follicle cycling phases.

I thank my friends, especially Dr. Jiafen Hu, Dr. James Olopade and Xuequn Wu for their help and encouragement during my graduate studies.

I am forever grateful to my parents, my brother and my sister for their love, support and understanding over these years.

Chapter I

Introduction

Polyamine metabolism

The polyamines putrescine, spermidine and spermine are cationic molecules (**Fig. 1-1**) that are found in all eukaryotic cells and are clearly essential to growth and development (reviewed in (Pegg, 2009a; Wallace et al., 2003)).

The pathway for polyamine metabolism has been well established (**Fig. 1-2**) (Pegg 1988; Tabor&Tabor 1984; reviewed in (Pegg, 2009a; Wallace et al., 2003)). Using arginine and methionine precursors, mammalian polyamine biosynthesis is achieved by the combined function of two decarboxylases, ornithine decarboxylase (ODC, EC 4.1.1.17) and *S*-adenosylmethionine decarboxylase (AdoMetDC, EC 4.1.1.50), and two distinct aminopropyltransferases, spermidine synthase (SpdS, EC 2.5.1.16) and spermine synthase (SpmS, EC 2.5.1.22). ODC catalyzes the conversion of ornithine to putrescine, while AdoMetDC converts S-adenosylmethionine (AdoMet) to decarboxylated S-adenosylmethionine (dcAdoMet). The decarboxylation of AdoMet irreversibly commits it to polyamine biosynthesis rather than cellular methylation reactions. SpdS transfers an aminopropyl group from dcAdoMet to putrescine to produce spermidine and SpmS transfers an aminopropyl group from dcAdoMet to spermidine to produce spermine. The aminopropyl transfer reaction also produces 5'-methylthioadenosine (MTA) which is normally rapidly degraded and removed from the cells. Spermidine and spermine are inter-converted and can also be degraded back to putrescine by acetylation followed by oxidation through the spermidine/spermine N^1-acetyltransferase/acetyl-polyamine oxidase (SSAT/PAO) pathway. The oxidation by PAO also yields stoichiometric amounts

of H_2O_2 and N-acetyl-3-aminopropanaldehyde. Spermine can also be directly oxidized to spermidine by spermine oxidase (SMO, also referred to as PAO1).

In addition to *de novo* synthesis, catabolism and inter-conversion, intracellular polyamine levels can also be adjusted by uptake and efflux through the polyamine transport systems (reviewed in (Pegg, 2009a; Wallace et al., 2003). The systems are not well characterized in mammalian cells currently. It is thought that the majority of polyamine transport is carrier-mediated, energy-dependant and saturable and polyamines can also be taken up by endocytosis. Most mammalian cells appear to have two types of carriers, one for putrescine and the other one for spermidine and spermine. These carriers are not highly specific and they can also transport related compounds such as methylglyoxal bis-guanylhydrazone (MGBG, an AdoMetDC inhibitor) and polyamine analogs. Recently, an alternative two-step model was proposed where polyamines are first imported by a plasma membrane carrier, and then sequestered into pre-existing polyamine-sequestering vesicles via a H^+-coupled vesicular transporter (Soulet et al., 2004). Polyamine can also be exported from the cell in a selective and regulated manner. Putrescine and N^1-acetylspermidine are the major polyamines exported from the cell. Studies with selective uptake inhibitors indicate that the outward transporters are separate from the inward transporters and they have distinct modes of action (Huang et al., 2005; Kusano et al., 2008).

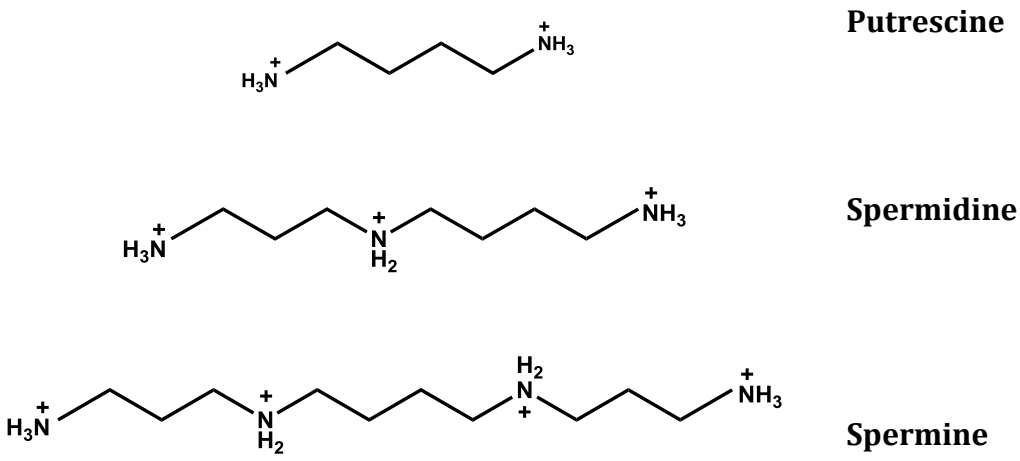

Fig. 1-1 Structures of polyamines

At physiological pH, they are positively charged.

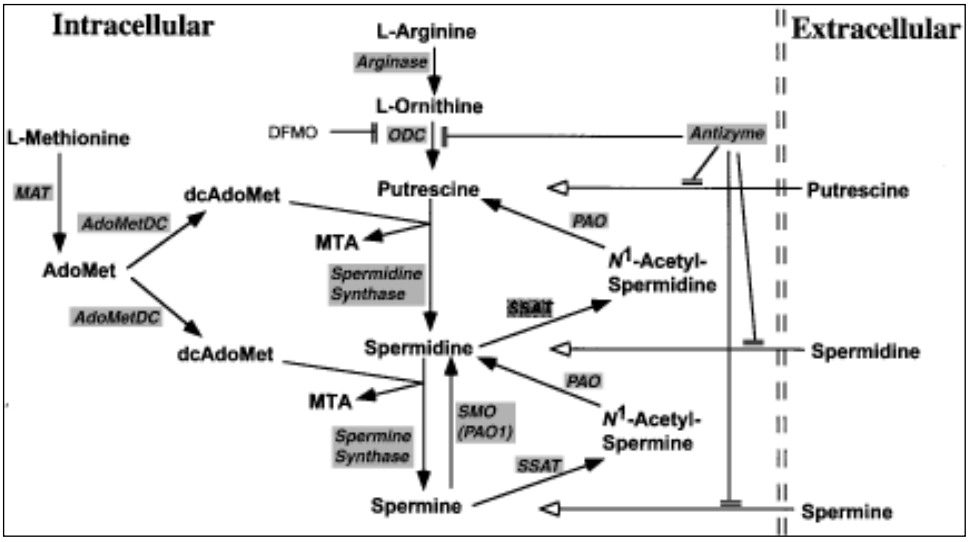

Fig. 1-2 Mammalian polyamine metabolic pathway (From (Pegg et al., 2003))

ODC, ornithine decarboxylase; PAO, polyamine oxidase; AdoMet, S-adenosylmethionine; dcAdoMet, decarboxylated AdoMet; MAT, methionine adenosyltransferase; MTA, 5'-methylthioadenosine; and SSAT, spermidine/spermine-N^1-acetyltransferase; DFMO, α-difluoromethylornithine.

Regulation of polyamine metabolism

Polyamines are present at millimolar concentrations in most cells and their content is tightly regulated to maintain levels that permit critical biological processes by biosynthesis, catabolism, uptake and efflux.

Polyamine biosynthetic rates are regulated through the two decarboxylases, ODC and AdoMetDC, while polyamine catabolic rates are controlled largely by SSAT. All of the three enzymes are present at very low levels in the absence of an inducing stimulus, have very short half-lives, and are under multi-level regulation (reviewed in (Pegg, 2009a; Wallace et al., 2003)).

ODC is regulated at the levels of transcription, translation, mRNA stability and protein degradation (reviewed in (Pegg, 2006), (Nowotarski and Shantz, 2010)). *Odc* gene transcription is induced by hormones, growth factors and tumor promoters through specific sequences in the promoter region. ODC mRNA translation is negatively regulated by its long and GC-rich 5' UTR, while 3'UTR may facilitate translation. Both transcription and translation are also inversely regulated by intracellular polyamine levels. RNA-binding protein human antigen R (HuR) is found to be able to bind to the ODC 3'-UTR and stabilize the ODC mRNA in a nonmelanoma skin cancer model. ODC protein has a half-life of about 30 minutes in most mammalian cells and its degradation is regulated by antizyme (AZ), which binds noncovalently to the ODC monomer, inactivating it and targeting it for degradation by the 26S proteasome in a ubiquitin-independent manner. AZ synthesis is increased by high intracellular polyamine levels by triggering a +1 frameshift needed to pass the internal stop codon on the AZ mRNA; AZ

degradation is increased by low intracellular polyamine levels. Antizyme inhibitor (AZI) has a greater affinity for AZ than ODC and can negate AZ functions.

AdoMetDC is the other decarboxylase in polyamine biosynthesis and its function and regulation will be described in detail in a later section.

SSAT, like ODC, has a half-life of about 30 minutes. It is also highly regulated at several levels and inducible by some hormones, cytokines and polyamine analogues (reviewed in (Pegg, 2008)). Mostly importantly, it is readily responsive to intracellular spermidine and spermine levels in order to maintain polyamine homeostasis. This regulation by polyamines involves transcription of *Sat1* gene encoding SSAT, correct processing and stabilization of the transcript, mRNA translation and protein degradation.

Polyamine uptake can be suppressed by the protein AZ, so mammalian polyamine biosynthesis and uptake are linked through AZ. Polyamine export is regulated by AZ and the growth status of the cell. It decreases in response to growth stimuli and increases in response to growth repression.

Physiological role of polyamines

It has been well established that polyamines are absolutely required for cell growth and differentiation (Pegg, 1988; Pegg and McCann, 1982; Tabor and Tabor, 1984). Polyamine levels have been found to positively correlate with cell growth in bacterial, yeast and mammalian cell lines and tissues. Depletion of intracellular polyamine levels by the specific and irreversible inhibitor α-difluoromethylornithine (DFMO) of ODC results in cell growth arrest, which can be reversed by the addition of exogenous polyamines. On the other hand, elevated polyamine levels are associated with rapid cell growth and proliferation.

Numerous studies have been done to elucidate how polyamines affect cellular processes. Due to the fact that the majority of polyamines interact with polyanionic molecules including DNA, RNA, proteins and phospholipid membranes and it is impossible to measure the concentrations of free versus bound forms of polyamines, and they are readily interconverted by polyamine metabolic enzymes, the specific biological function of polyamines remain largely unclear. However, it is known that polyamines play an important role in many critical biological processes such as DNA replication, gene transcription, mRNA translation, modulation of ion channels and protection from oxidative stress (Pegg, 2009a; Rider et al., 2007; Wallace et al., 2003). By binding to DNA, polyamines can induce bending and local conformational change of DNA; polyamines can also modulate binding of transcription factors to DNA response elements and thus regulate DNA transcription (Panagiotidis et al., 1995; Peng and Jackson, 2000; Shah et al., 2001). Polyamines have also been shown to affect translation in several ways, one of which is that spermidine is required for the post-translational hypusine modification to produce active eukaryotic translation initiation factor 5A (eIF-5A) (Park, 2006; Park et al., 2010; Wolff et al., 2007), which is essential for growth in yeast (Chattopadhyay et al., 2002). Polyamines play important roles in the regulation of various ion channels by interaction with receptors or functioning mainly as a blocker (Dingledine et al., 1999; Fleidervish et al., 2008; Lin and Veenstra, 2007; Stanfield and Sutcliffe, 2003). In addition, spermidine and spermine have been shown to protect cells from oxidative stress by direct scavenging of reactive oxygen species (ROS) and/or altering DNA structure, physically blocking DNA from interaction with assaulting agents (Feuerstein et al., 1989, 1990; Fujisawa and Kadoma, 2005; Warters et al., 1999).

Deregulated polyamine metabolism is linked to pathological processes and the pathway has been proposed as a promising target for the treatment and prevention of diverse diseases such as cancer and parasitic infection (Basuroy and Gerner, 2006; Casero and Marton, 2007; Heby et al., 2007; Shantz and Levin, 2007; Wallace and Fraser, 2004).

Structure, function and regulation of S-adenosylmethionine decarboxylase

S-adenosylmethionine decarboxylase (AdoMetDC) is a key enzyme in the biosynthesis of polyamines. It catalyzes the formation of decarboxylated *S*-adenosylmethionine (dcAdoMet) from S-adenosylmethionine (AdoMet). dcAdoMet serves as an aminopropyl donor in the synthesis of spermidine and spermine catalyzed by two aminopropyltransferases, spermidine synthase and spermine synthase, respectively. The aminopropyl acceptors are putrescine and spermidine, respectively. The by-product of the aminopropyl transfer reactions, 5′-methylthioadenosine (MTA), is rapidly degraded and removed from the cell (Pegg, 1986, 1988; Tabor and Tabor, 1984). The intracellular level of dcAdoMet is normally very low, and the activities of the aminopropyltransferases are largely controlled by the availability of this substrate. Thus, the conversion of putrescine to higher polyamines is controlled by the activity of AdoMetDC (Pegg, 1988, 2009a).

AdoMet, which is produced from the reaction of methionine with ATP catalyzed by the enzyme methionine adenosyltransferase (MAT, also known as SAM synthase), participates in many essential biochemical processes as a donor of methyl, methylene, amino, sulfur, ribosyl or aminopropyl group (Fontecave et al., 2004). These reactions are considered to be driven by the electrophilic character of the carbon centers that are

adjacent to the positively charged sulfur atom of AdoMet (Cantoni, 1975; Chiang et al., 1996). Most of the intracellular AdoMet molecules are used in various methyl transfer reactions catalyzed by methyltransferases. It is the major biological methyl donor in all living organisms. Nucleic acids, proteins and lipids are suitable methyl acceptors. Methylation of DNA is critical for the regulation of gene expression. Methylation of RNAs changes their metabolism. Methylation of proteins helps in regulating their activity and function (Cantoni, 1975; Loenen, 2006). Methylation of phospholipids keeps the membranes fluid and the receptors mobile (Vance and Vance, 2004). Only 2-5% of intracellular AdoMet is used in spermidine and spermine synthesis. AdoMet cannot directly act as an aminopropyl donor. In order to play a role in polyamine metabolism, AdoMet must be activated by AdoMetDC. Once decarboxylated, AdoMet is committed to polyamine biosynthesis and not available for methyl transfer or other possible metabolic reactions (Pegg, 1986, 1988, 2009b; Pegg et al., 1998).

Mammalian AdoMetDC is usually an α2ß2 heterotetramer (**Fig. 1-3**), each of the α subunits contains a covalently bound pyruvate that functions as a prosthetic group. The pyruvoyl residue will form a Schiff base with the AdoMet substrate to facilitate decarboxylation (Pegg, 1984, 2009b; Pegg et al., 1998). AdoMetDC enzyme is first synthesized as a 38 kDa proenzyme. The proenzyme then undergoes an autocatalytic process to produce two subunits (α: 30.6 kDa, ß: 7.7 kDa) of the mature enzyme. The pyruvate group is generated simultaneously from an internal serine residue (Ser68) at the N-terminus of the α-subunit (Tolbert et al., 2003). The proenzyme sequence around the serine is highly conserved in all eukaryotic AdoMetDCs (Hoyt et al., 2000; Muller et al., 2000; Roberts et al., 2002; Xiong et al., 1997). During the processing reaction, an internal

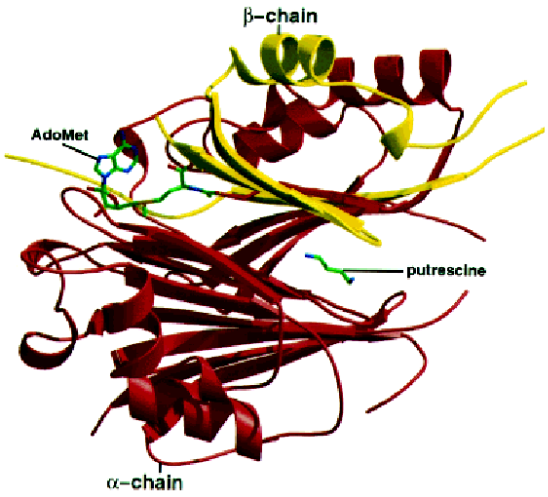

Fig. 1-3 S-Adenosylmethionine decarboxylase αß monomer (from: (Tolbert et al., 2001))

ester bond is formed from the hydroxyl oxygen of the serine. This ester bond is cleaved to produce a terminal dehydroalanine and this residue is then hydrolyzed to form the pyruvate (Ekstrom et al., 2001).

hAdoMetDC sequence has been identified, cloned, expressed and studied in detail. Its crystal structure is also solved. Studies by site-directed mutagenesis have identified the residues that are important for AdoMetDC activity and proenzyme processing, and these residues are conserved in different species (Pegg, 2009b; Pegg et al., 1998). Truncation mutant studies of the AdoMetDC proenzyme have found that removal of the C- terminal 8 residues from the human protein did not reduce the rate of processing or the activity of processed AdoMetDC in the presence of putrescine. Further truncation greatly reduced the rate of processing and activity. Since the C-terminal regions of the known eukaryotic AdoMetDCs are not conserved, the results suggest that the length of the polypeptide chain is critical for its autocatalytic processing (Xiong et al., 1997).

In accord with the critical role of AdoMetDC in the regulation of polyamine content, AdoMetDC is highly regulated at multiple levels including transcription, translation, proenzyme processing, catalytic activity and degradation (Pegg, 2009b; Pegg et al., 1998). Elevated AdoMetDC activities are observed in response to various internal and external stimuli including growth factors and polyamine depletion. It is also found using RIA or western blotting that the increased activity is due to the rise in the amount of enzyme protein (Shirahata and Pegg, 1985).

Regulation of AdoMetDC gene transcription: Growth factors like insulin or a decline in spermidine by pretreatment with polyamine biosynthesis inhibitors have been observed to increase the levels of AdoMetDC mRNA (Pajunen et al., 1988; Soininen et al., 1996).

Experiments with transfection of plasmid constructs containing portions of the AdoMetDC promoter region have shown that the reporter gene expression was altered by spermidine, but not by spermine, suggesting that there is a spermidine-responsive element in this promoter (Shantz et al., 1992). An insulin-responsive element was also identified in the rat AdoMetDC promoter (Soininen et al., 1996).

Regulation of AdoMetDC mRNA translation: Translational regulation plays an important role in controlling AdoMetDC content (Pegg, 2009b; Pegg et al., 1998; Shantz and Pegg, 1999). Increased mRNA transcription is insufficient to account for the increase in the AdoMetDC protein levels that is found in many cases. In fact, much of the regulation occurs at the translation level. Early studies have found that the 5'-untranslated region (5'-UTR) of AdoMetDC mRNA had a negative effect on AdoMetDC translation. Later, it was found that a highly conserved upstream open reading frame (uORF) of 5'-UTR functioned as a negative regulatory element by causing ribosome stalling and it also imparted cell-specific expression. AdoMetDC translation is negatively regulated by spermidine and spermine and a polyamine responsive element was identified in the 5'-UTR. The amino acid sequence that is encoded by the uORF is thought to be critical for polyamine regulation of AdoMetDC synthesis and polyamines may affect the synthesis by interacting with this hexapeptide MAGDIS. The mechanism of interaction is unclear.

Regulation of AdoMetDC proenzyme processing and catalytic activity: Both proenzyme processing and catalytic activity can both be stimulated by putrescine (Kameji and Pegg, 1987; Pegg, 2009b; Pegg et al., 1998). This is an important mechanism for polyamine regulation because it allows more dcAdoMet to be produced for the synthesis of spermidine when putrescine levels go up. Structural analysis shows that a putrescine

molecule binds to the proenzyme or processed hAdoMetDC through interactions with several negatively charged residues in a buried site. The interactions may cause conformational changes that can accelerate the proenzyme processing or decrease the Km of AdoMetDC for AdoMet although the mechanism is not totally understood (Ekstrom et al., 2001; Pegg, 2009b; Pegg et al., 1998).

Regulation of AdoMetDC degradation: AdoMetDC protein has a very rapid rate of turnover, less than 1 h in many cells. This characteristic enables it to respond quickly to internal and external stimuli by changing protein levels. $T_{1/2}$ of AdoMetDC is inversely related to the cellular content of spermidine and spermine. When the levels of higher polyamines go up, AdoMetDC undergoes more rapid turnover, resulting in less protein. This may be an important control mechanism in maintaining AdoMetDC and polyamine levels. Binding of inhibitors can block the rapid turnover of AdoMetDC. This effect may lead to a paradoxical increase in enzyme activity at some time range after administration of inhibitors (Pegg, 2009b; Pegg et al., 1998). The mechanisms for the AdoMetDC degradation and inactivation remain unknown and may involve a transamination from the product, dcAdoMet, and the pyruvoyl group generating an N-terminal alanine (Anton and Kutny, 1988; Pegg, 2009b; Pegg et al., 1998).

Spermidine synthase and spermine synthase

Spermidine synthase (SpdS, EC 2.5.1.16) and spermine synthase (SpmS, EC 2.5.1.22) are the two aminopropyltransferases in polyamine biosythesis. SpdS transfers an aminopropyl group from dcAdoMet to putrescine to produce spermidine and SpmS transfers an aminopropyl group from dcAdoMet to spermidine to produce spermine. The two enzymes are expressed constitutively with a half-life of several days; thus the levels

of the substrates dcAdoMet and putrescine, or dcAdoMet and spermidine, determine spermidine or spermine synthesis rates, respectively. A few studies suggest that the aminopropyltransferase levels may be inducible in certain physiological situations including mammary development and lactation during pregnancy (Forshell et al., 2010; Ikeguchi et al., 2006; Pegg, 2009a; Pegg et al., 2011a; Russell and McVicker, 1972).

Spermidine is essential for growth in lower eukaryotes (Chattopadhyay et al., 2008; Chattopadhyay et al., 2002; Ikeguchi et al., 2006)) since the production of active eukaryotic translation initiation factor 5A (eIF-5A) requires a post-translational spermidine-dependent hypusine modification (Park 2006; Park et al. 2010; Wolff et al. 2007), and, although mouse ES cells with targeted SpdS deletion have been produced (http://www.komp.org/geneinfo.php?geneid=80254), the attempted generation and characterization of SpdS knockout mice has not been reported.

However, the *in vivo* functions of spermine have been studied in several mouse models (Pegg and Wang, 2009). Male Gyro (Gy) mice with a large deletion on the X chromosome that includes most of the SpmS gene are viable despite a nearly complete absence of tissue spermine, yet they exhibit profound abnormalities such as deafness, inner ear abnormalities, circling behavior, sterility and a greatly reduced lifespan, which can all be prevented by transgenic expression of SpmS (Wang et al., 2004; Wang et al., 2009; Woodward et al., 1993). In humans, mutations in the *SMS* gene that abolish nearly all SpmS activity have been identified in the rare genetic disorder Snyder-Robinson syndrome, which is characterized by mild-to-moderate mental retardation, hypotonia, cerebellar circuitry dysfunction, facial asymmetry, thin habitus, osteoporosis and kyphoscoliosis (Becerra-Solano et al., 2009; Cason et al., 2003; de Alencastro et al.,

2008). Transgenic overexpression of SpmS in mice had little effect on spermine levels (Ikeguchi et al., 2004), but no *in vivo* studies have addressed the question of whether unregulated elevation of SpdS activity alters polyamine content.

Mouse skin chemical carcinogenesis model

The mouse skin chemical carcinogenesis model is a well characterized system (reviewed in (Abel et al., 2009)) and it has been widely utilized to study the role of polyamines in epithelial tumor development. Carcinogenesis in skin and other epithelia can be divided into three distinct stages: initiation, promotion and progression (malignant conversion). Initiation is the earliest stage and is induced by the administration of a single dose of a carcinogen such as 7,12-dimethylbenz[a]anthracene (DMBA), which causes a mutation in a critical gene, c-Ha-*ras*. This mutation occurs in a limited number of epidermal cells (called initiated cells), is irreversible and maintained for the lifetime of the animal. Following initiation, promotion is accomplished by several weeks of repetitive applications of a non-carcinogenic tumor promoter such as 12-O-tetradecanoyl -phorbol-13-acetate (TPA). Promoter treatment causes epigenetic changes in gene expression as well as enzyme activities, and produces a tissue environment that allows initiated cells to expand clonally to form macroscopic, usually benign, tumors termed papillomas. Progression is a process during which papillomas are converted to invasive carcinomas. It may occur spontaneously at a low frequency in most strain backgrounds, although the frequency can be greatly enhanced by exposure to mutagens.

Studies have shown that DMBA application induces mutations at nucleotides A (adenine)182 and A183 in the c-Ha-*ras* gene, and they occur with approximately equal frequency (Finch et al., 1996). However, tumors derived from the DMBA/TPA treatment

protocol predominantly (>90%) contain an activating mutation at codon 61 (A to T transversion at nucleotide 182) of the c-Ha-*ras* gene (Balmain et al., 1984; Quintanilla et al., 1986). Skin stems cells are believed to be the target cells of DMBA initiator. Those cells are primarily found in the bulge region of the hair follicle and at the basal layer of the interfollicular epidermis (Jones and Watt, 1993; Morris, 2004; Tani et al., 2000).

Although the causative alteration induced by tumor promoter application is not as well defined, promoter treatment is known to transiently induce a number of epigenetic changes. Studies have shown that TPA treatment induces a massive transient increase in ODC activity along with a more prolonged moderate increase in AdoMetDC activity (O'Brien et al., 1975a; O'Brien, 1976b; Yuspa et al., 1976). Also papillomas derived from DBMA/TPA skin carcinogenesis exhibit constitutively elevated ODC activity and polyamine content (Koza et al., 1991).

Susceptibility to two-stage skin carcinogenesis in mice is strongly influenced by genetic background and is controlled by multiple alleles (Angel and DiGiovanni, 1999). Studies also found that the difference in susceptibility is most likely due to the variation in the response to the promoter treatment, but not the initiator (Angel and DiGiovanni, 1999). Compared with SENCAR mice that are very sensitive, and C57BL/6 mice that are resistant, FVB mice are moderately sensitive to two-stage skin carcinogeneis (Hennings et al., 1993). This feature makes the FVB inbred mice a good strain to analyze unknown (increased or decreased) susceptibility on skin carcinogenesis resulting from transgene expression. In addition, FVB mice have a high proportion of papilloma progression to squamous cell carcinoma (Hennings et al., 1993), which is desirable for studies of tumor progression.

Polyamines and nonmelanoma skin cancer

Elevated levels of polyamines have long been associated with tumor development in many tissues including skin. Nonmelanoma skin cancer, including basal cell carcinoma (BCC) and squamous cell carcinoma (SCC), are the most common malignancies in the white populations worldwide. More than 1.0 million new cases are diagnosed each year in the United States and they represent a major public health concern (Bickers et al., 2006).

Polyamine metabolism is dysregulated in nonmelanoma skin cancers and both BCC and SCC of the skin show elevated levels of ODC and polyamines (Kagoura et al., 2000; Scalabrino and Ferioli, 1985). Studies have shown that induction of ODC play a critical role in tumor promotion (Hayes et al., 2006; O'Brien, 1976a; Pegg et al., 2003). However, clinical trials using ODC-targeting strategies with its specific and irreversible inhibitor α-difluoromethylornithine (DFMO) have not been successful mainly due to the compensatory up-regulation of polyamine metabolism and transport, though all the animal studies demonstrated DFMO as a promising anti-tumor agent (Meyskens and Gerner, 1999). Still, DFMO was found to be effective in tumor prevention (Tang et al., 2004; Tempero et al., 1989) and it is currently undergoing clinical trials as a chemopreventive agent for nonmelanoma skin cancer and colorectal cancer (Alberts et al., 2000; Bailey et al., 2010; Gerner and Meyskens, 2009; Meyskens et al., 2008).

Previous studies using transgenic mice which overexpress key enzymes in the polyamine biosynthetic pathway in specific skin cell populations by using keratin promoters found that a) Keratin 5 (K5)-ODC and K6-ODC mice develop skin tumors after treatment with initiating agent without the need for tumor promotion (O'Brien et al.,

1997; Peralta Soler et al., 1998); b) K5-AZ or K6-AZ mice have reduced skin tumor development (Feith et al., 2001; Feith et al., 2007); c) K6-SSAT mice, which have increased levels of putrescine and decreased levels of spermidine and spermine, exhibit increased incidence of skin papillomas and progression to carcinomas after a two-stage (initiation and promotion) chemical carcinogenesis protocol (Coleman et al., 2002). In addition, ODC inhibitor DFMO treatment has tumor prevention effect and can cause tumor regression (Fischer et al., 2003; Rebel et al., 2002; Takigawa et al., 1982; Weeks et al., 1982) . A simple and unifying explanation for those studies is that induction of ODC and increase in putrescine, but not spermidine or spermine, play a critical role in skin tumor development (**Fig. 1-4**). The effects of AZ, DFMO, SSAT are mediated via the changes they produce in ODC and putrescine levels. Moreover, in K6-SSAT mice, H_2O_2 and reactive aldehydes released from SSAT-stimulated polyamine catabolism could also enhance tumor development and may account for the increased progression to carcinomas in those mice (Pegg and Feith, 2007; Wang et al., 2007).

AdoMetDC is a rate-limiting enzyme in polyamine biosynthesis and the conversion of putrescine into spermidine and spermine is controlled by this enzyme. Therefore, elevated AdoMetDC activity may promote the synthesis of higher polyamines at the expense of putrescine, and decreased putrescine levels will lead to tumor suppression. To test this hypothesis, we generated transgenic mice with targeted overexpression of AdoMetDC in the skin and investigated the effect on susceptibility to skin chemical carcinogenesis.

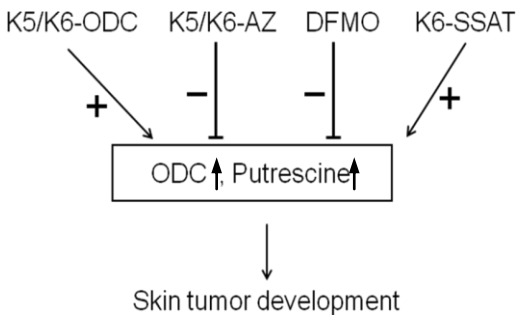

Fig. 1-4 Schematic diagram of polyamines and skin tumor development

Skin hair follicle morphogenesis and cycling

The production of mouse hair follicles and hair starts in late embryogenesis and finishes at around postnatal day 8 (Muller-Rover et al., 2001; Schmidt-Ullrich and Paus, 2005). Hair follicle morphogenesis has been divided into nine distinct developmental stages (0–8) and these stages can be differentiated mainly based on the length of the developing hair follicle as described in Paus et al. (1999). It is known that ODC mRNA is induced and detected at the leading edge of the hair follicle during morphogenesis (Nancarrow et al., 1999).

Mature mouse hair follicle growth undergoes cycles of growth (anagen), regression (catagen) and rest (telogen) throughout the life of the mouse (Paus et al., 1999; Schneider et al., 2009). ODC activity is induced in anagen follicles and polyamine levels are elevated, while little ODC activity is measured in telogen follicles (Probst and Krebs, 1975; Sundberg et al., 1994b).

Both ODC and SSAT overexpression in mouse skin cause hair follicle degeneration and lead to alopecia (Panteleyev et al., 2000; Pietila et al., 2001; Soler et al., 1996). Topical application of the stable polyamine analogue α-methylspermidine induces the growth of resting hair follicles in mice (Fashe et al., 2010). On the other hand, mice treated with DFMO exhibit hair loss (Takigawa et al., 1982) and topical DFMO cream (Vaniqa™) is now used to treat unwanted facial hair in women. Taken together, these studies indicate that proper hair follicle morphogenesis and function is impaired by either excess or restricted polyamine content.

For initiation-promotion two-stage skin chemical carcinogenesis experiments, usually 7 to 9–week old mice are initiated because most mice at this age are in

synchronized and lengthy telogen (resting phase of the hair cycle) (Abel et al., 2009; Muller-Rover et al., 2001). Mouse skin has increased susceptibility to tumor initiation during the early anagen (growth phase of the hair cycle) due to cell proliferation in the bulge region of the hair follicle (Miller et al., 1993).

Tet-Off system and generation of mice with tet-regulated AdoMetDC expression

Tetracycline-controlled transcriptional activator (tTA) (Tet-Off) system (Zhu et al., 2002) (**Fig. 1-5**) is utilized in our study to enable a tissue-specific and conditional expression of the AdoMetDC transgene.

In this system, two separate transgene constructs are required in order to get expression of the target gene. One is tTA trangene directed by a tissue- or cell type-specific promoter (P_{TS}), which expresses tTA protein, a fusion protein of the tetracycline repressor of *E. coli* (TetR) and the transcription activation domain of viral protein 16 of herpes simplex virus (VP16). The other trangene is the target gene driven by the tetracycline-resistance operon of *E. coli* transposon Tn10 (TetO) and minimum promoter from human cytomegalovirus (P_{cmv}). In the absence of the regulating agent doxycycline (Dox, a tetracycline analog), tTA protein binds the TetO responsive elements and activates the coupled Pcmv, thus turning on the expression of the downstream target gene. In the presence of Dox, tTA dissociates from TetO to bind Dox and the target gene expression is shut off. Moreover, the expression can be titrated by varying the amount of Dox (Zhu et al., 2002).

Using this system, our transgenic mouse model was derived by breeding K5-tTA FVB mice with uniform tTA expression in the skin (Diamond et al., 2000) with TetO-AdoMetDC mice. Mitotically active keratinocytes in the basal layer of the

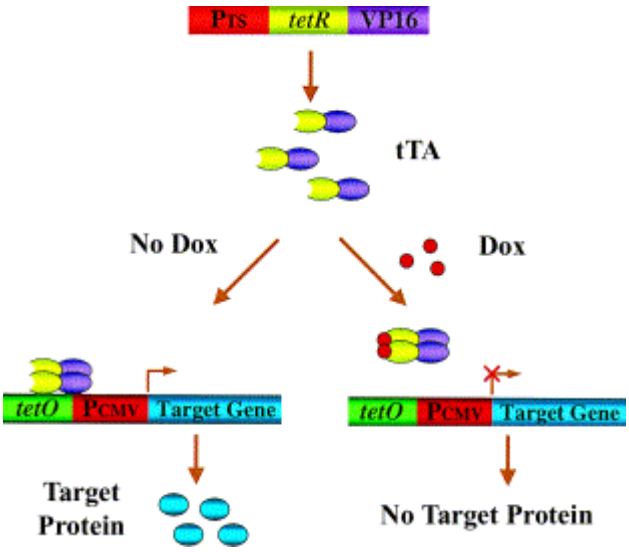

Fig. 1-5 Tetracycline-controlled transcriptional activator (tTA) system: "Tet-Off" (from (Zhu et al., 2002))

epidermis and the outer root sheath of the hair follicle are targeted by use of the K5 promoter. In AdoMetDC/tTA mice, the AdoMetDC transgene is constitutively expressed in the skin and expression can be repressed by exposure to Dox. This mouse model will allow us to study the effect of AdoMetDC overexpression on polyamine metabolism and test its influence on skin chemical carcinogenesis.

We chose to use the tet-regulated system based on the following reasons: a) this system allows us to turn on/off transgene expression at different phases of skin carcinogenesis; b) previous studies in our lab have shown that it is very difficult to overexpress AdoMetDC in cell culture due to unclear toxic effects; by using Tet system, we can regulate the levels of transgene expression to avoid potential toxicity in animal models; c) by giving Dox to shut off transgene expression during embryogenesis, this system may allow us to express AdoMetDC in previously lethal combination of AdoMetDC with other polyamine enzymes; d) TetO-AdoMetDC single trangenic mice can be crossed with other transgenic mouse lines with tissue-specific promoter driven tTA/rTA to study AdoMetDC function in other tissues like heart and mammary gland. We chose Tet-off over the Tet-on system (Zhu et al., 2002) because we want to achieve AdoMetDC overexpression without the need for Dox administration for a large period of time during the study process, also for the two mouse strains we have, the rTA transgene expression is relatively low and not as uniform in the skin as the tTA transgene. However, compared with Tet-On, the major disadvantage of Tet-Off system is that, if the transgene expression is not desired until later in development, the animal must be exposed (beginning at conception) to levels of Dox sufficient to silence transgene expression. This can be expensive and may lead to unknown side effects. Furthermore, the induction rate

of transgene expression later is limited by the clearance of Dox from the animal.

Work presented in the thesis and objectives

This thesis describes the creation and characterization of two novel transgenic mouse lines with altered polyamine metabolism, one with widespread overexpression of spermidine synthase (SpdS) and the other with regulated S-adenosylmethionine decarboxylase (AdoMetDC) expression in the skin. Experiments were designed to determine the impact of elevated SpdS activity on mouse development and physiology, and to elucidate the roles of AdoMetDC and polyamines in skin carcinogenesis.

CAG-SpdS mice: In Chapter II, we describe the generation and characterization of a transgenic mouse line that overexpresses human SpdS from the composite cytomegalovirus-immediate early gene enhancer/chicken β-actin (CAG) promoter. Studies were also done on mice that simultaneous overexpress SpdS and other polyamine biosynthetic enzymes by combining transgenic models.

AdoMetDC/tTA mice: We utilized the tet-regulated system to produce conditional expression of AdoMetDC in basal keratinocytes using the Keratin 5 promoter. In these mice, elevated AdoMetDC activity is expected to alter polyamine levels, especially putrescine levels, thus affecting skin tumor development. Our long-term goal is to elucidate the role that polyamines play in nonmelanoma skin cancer (epithelial cancer in general) in order to develop novel cancer prevention and treatment strategies.

Our hypothesis for this study is that targeted AdoMetDC overexpression in the skin of transgenic mice will reduce the level of putrescine and decrease the susceptibility to skin chemical carcinogenesis. The established specific aims are:

Aim 1 (Chapter III): Generate transgenic mice with tet-regulated expression of

AdoMetDC in the skin; examine phenotype and alterations in polyamine metabolism.

Aim 2 (Chapter IV): Test the impact of AdoMetDC overexpression on the enzyme induction and epidermal hyperplasic response following short term TPA treatment.

Aim 3 (Chapter V): Investigate the effect of AdoMetDC overexpression on skin chemical carcinogenesis.

Chapter II

Characterization of transgenic mice with overexpression of spermidine synthase

INTRODUCTION

Spermidine synthase (SpdS) and spermine synthase (SpmS) are the two aminopropyltransferases in polyamine biosynthesis. They are expressed constitutively with a half-life of several days. Transgenic overexpression of SpmS from the ubiquitous CAG promoter in mice had little effect on spermine levels and did not affect SpdS activity. CAG-SpmS mice had normal survival, fertility, behavior, and growth up to the age of 12 months. However, breeding of the mice with MHC-AdoMetDC mice that have a large increase in cardiac AdoMetDC activity was lethal (Ikeguchi et al., 2004). In order to determine the impact of elevated SpdS activity on polyamine metabolism, murine development and physiology, and to enable simultaneous overexpression of SpdS and other polyamine biosynthetic enzymes by combining transgenic models, we generated a transgenic mouse line that overexpresses human SpdS from the CAG promoter.

This chapter describes the generation and characterization of the transgenic mouse line. Biochemical measurements of SpdS transgene expression and alterations in SpmS activity and polyamine levels in different organs of CAG-SpdS mice are presented. The aminopropyl donor, dcAdoMet levels and AdoMetDC activities are also measured in selected organs. Aminopropyltransferase activities and polyamine content in different organs of CAG-SpdS/CAG-SpmS bitransgenic mice that simultaneously overexpress both aminopropyl-transferases are presented, followed by cardiac polyamine measurement in CAG-SpdS/MHC-AdoMetDC bitransgenic mice at the end.

MATERIALS AND METHODS

All chemicals, unless noted, were purchased from Sigma Chemical Company (St. Louis, MO). Restriction enzymes were purchased from New England Biolabs (Beverly, MA). Oligonucleotides used as primers were synthesized and purified in the Macromolecular Core Facility (Pennsylvania State University College of Medicine). [^{35}S]-dcAdoMet was synthesized from L-[^{35}S]methionine (PerkinElmer Life Sciences, Boston, MA) as described previously (Mackintosh and Pegg, 2000). *S*-adenosyl-L-[carboxyl-^{14}C]methionine (55 mCi/mmol) was obtained from American Radiolabeled Chemicals (St. Louis, MO).

Transgene construction and microinjection

The transgene for widespread expression of SpdS was constructed essentially as described previously for CAG-SpmS mice (Ikeguchi et al., 2004). Human SpdS cDNA was inserted in a vector containing a composite CMV-IE enhancer–β-actin (CAG) promoter to replace the enhanced green fluorescent protein coding sequence by *Eco*RI digestion of plasmid pCX-EGFP (Okabe et al., 1997; Sawicki et al., 1998) (**Fig. 2-1**). Human SpdS cDNA was amplified by PCR from plasmid pET28a-LIC-hSpdS (Wu et al., 2007) and was engineered to contain a nine amino acid amino-terminal hemagglutinin (HA) epitope coding sequence with sense primer 5'-GACGCATTAGGAATTCGCCAC CATGGGATACCCCTACGACGTCCCCGACTACGCCGCCCGGCCCCGACGG-3' and antisense primer 5'-GACGCATTAG*GAATTC*TCATCAGCTCACATCATTCAG GG-3' (*Eco*RI sites in italics and HA epitope coding sequence underlined). The PCR reaction was carried out in a 0.1 ml volume containing 2.5 units of *Pfu* polymerase (Stratagene, La Jolla, CA), 25 ng of template DNA and 25 pmol of each primer under the

following conditions: initial denaturation for 2 min at 94 °C, followed by 25 cycles of denaturation (94°C for 30 s), annealing (58°C for 30 s) and extension (72°C for 2 min), with a final extension at 72°C for 5 min. The entire SpdS cDNA insert was sequenced at the DNA Sequencing Core (Pennsylvania State University College of Medicine) to ensure the correct orientation and that no secondary mutations were introduced during the plasmid construction.

The plasmid pCAG-SpdS was digested with *Sal*I and *Bam*HI to remove prokaryotic vector sequences and liberate a 3.4 kb transgene fragment. The transgene was purified using the Perfectprep gel cleanup kit (Eppendorf, Hauppauge, NY) and Elutip-D-mini-columns (Schleicher & Schuell, Keene, NH) and then precipitated and resuspended in microinjection buffer (10 mM Tris/HCl, pH 7.4, and 0.1 mM EDTA). The transgene was microinjected into fertilized C57BL/6 oocytes using standard techniques in the Transgenic Mouse Facility (Pennsylvania State University, University Park) and transgenic founder animals were identified by PCR as described below.

Breeding and PCR identification of transgenic mice

All animal studies were reviewed and approved by the Institutional Animal Care and Use Committee of the Penn State University College of Medicine. Transgenic CAG-SpdS lines were established by breeding transgenic founders and their progeny to wild type C57BL/6J mice (The Jackson Laboratory, Bar Harbor, ME) to produce approximately equal numbers of transgenic mice and wild type littermate controls. Genomic DNA was extracted from tail biopsies from potential transgenic mice and subjected to PCR analysis using the REDExtract-N-Amp Tissue PCR Kit (Sigma, St. Louis, MO) to detect the transgene DNA. PCR analysis utilized one of two independent primer sets. For the first, a

sense primer (5'-TACGACGTCCCCGACTACG-3') binds within the HA epitope coding region and the antisense primer (5'-TCGATCTCACACTGGACCAC-3') binds within the hSpdS region (**Fig. 2-1A**) to amplify a 397 bp product only in genomic DNA samples from CAG-SpdS mice. Alternatively, the transgene was detected with a sense primer (5′-TTCGGCTTCTGGCGTGTGAC-3′) that binds in the β-actin promoter region and an antisense primer (5′-CTTACTGCGGAAGACGAGG-3′) that binds in the human SpdS coding region to amplify a 330 bp product. A second primer pair that yields a 520 bp product from the mouse antizyme 1 gene (*Oaz1*) was also included in the reaction, which provides a positive control for successful PCR amplification for each genomic DNA sample (Feith et al., 2007).

To generate and characterize CAG-SpdS/CAG-SpmS bitransgenic animals, heterozygous mice from two different transgenic lines were bred and offspring were genotyped for both transgenes by PCR. CAG-SpmS line 8, which had been backcrossed to the C57BL/6J inbred strain for >10 generations, were identified as described previously (Ikeguchi et al., 2004). The MHC-AdoMetDC transgene was maintained on a mixed B6D2 genetic background and transgenic animals were identified as described previously (Nisenberg et al., 2006). All experimental groups included both male and female mice and no sex-dependent differences were observed unless noted.

SpdS and SpmS enzymatic activity assays and SpdS western blotting

Mice were euthanized at the indicated age and tissues were harvested and flash frozen in liquid nitrogen. To determine aminopropyltransferase activity, each tissue sample was placed in ice-cold spermidine/spermine synthase harvesting buffer (50 mM sodium phosphate (pH 7.2), 0.3 mM EDTA, 10 mM 2-mercaptoethanol and 1x protease inhibitor

cocktail (Calbiochem, LaJolla, CA), homogenized on ice using a Polytron for 30 s with 15 s on/15 s off and centrifuged at 20000 x*g* for 30 min at 4°C. Epidermis was separated from dermis as described (Feith et al., 2001) and then processed on ice by sonication for 30 s with 10 s on/10 s off. Tissues and extracts were stored at −80°C before use. SpdS and SpmS activity were assayed by measuring the production of [^{35}S]methylthioadenosine from [^{35}S]-dcAdoMet in the presence of the appropriate aminopropyl acceptor as reported previously (Mackintosh and Pegg, 2000; Wiest and Pegg, 1998). Cytosolic proteins (50 µg) were fractionated by SDS-PAGE, transferred to PVDF membrane, and SpdS protein was detected by western blotting using a rabbit polyclonal antibody to human SpdS (anti-SRM, Sigma, St. Louis, MO) or to the HA epitope of transgene-derived SpdS protein (sc-805, Santa Cruz Biotechnology, Santa Cruz, CA). Signals were visualized with a chemiluminescence detection system (Cell Signaling Technology, Beverly, MA).

HPLC analysis of polyamine and AdoMet/dcAdoMet content

For polyamine quantification, tissue samples were homogenized in 10% trichloroacetic acid (Fisher Scientific, Pittsburgh, PA) and analyzed by HPLC using an ion-pair reverse-phase separation method with post-column derivatization using *o*-phthaldialdehyde as described previously (Pegg et al., 1989) and normalized to tissue wet weight. For AdoMet and dcAdoMet quantification, tissue extracts were reacted with chloroacetaldehyde to convert AdoMet and dcAdoMet to fluorescent 1,N^6-etheno derivatives, which were then separated and quantified by HPLC as described previously (Pegg et al., 2011a) and normalized to tissue wet weight.

AdoMetDC activity assay

Tissue samples were placed in ice-cold AdoMetDC harvesting buffer (50 mM sodium phosphate (pH 6.8), 2.5 mM putrescine, 2.5 mM dithiothreitol, 0.1 mM EDTA and 1× protease inhibitor cocktail (Calbiochem, LaJolla, CA)), homogenized on ice using a Polytron for 30 s with 15 s on/15 s off and centrifuged at 20000 x*g* for 30 min at 4°C. AdoMetDC activity was assayed by measuring the production of [^{14}C]-labeled CO_2 as described previously (Nisenberg et al., 2006).

Statistical analysis

All comparisons between wild type controls and transgenic mice utilized the two-tailed, unpaired Student's *t* test.

RESULTS

Generation and identification of CAG-SpdS transgenic mice

Our initial goal was to generate a transgenic mouse line with ubiquitous SpdS expression that is devoid of the normal regulatory elements that govern SpdS transcription and translation. To achieve this goal, we utilized the CAG promoter to drive expression of a human SpdS cDNA that was modified to add an HA epitope to the amino terminus to facilitate the detection of transgene-derived SpdS and differentiate this protein from the endogenous mouse SpdS protein (**Fig. 2-1A**). Genomic DNA screening (**Fig. 2-1B**) identified two transgenic founders (lines A and B) and both were found to transmit the transgene in a Mendelian fashion. Transgenic mice were produced and maintained on a C57BL/6J background and no obvious phenotypic abnormalities were observed in any of the founder mice or their progeny up to 1.5 years of age.

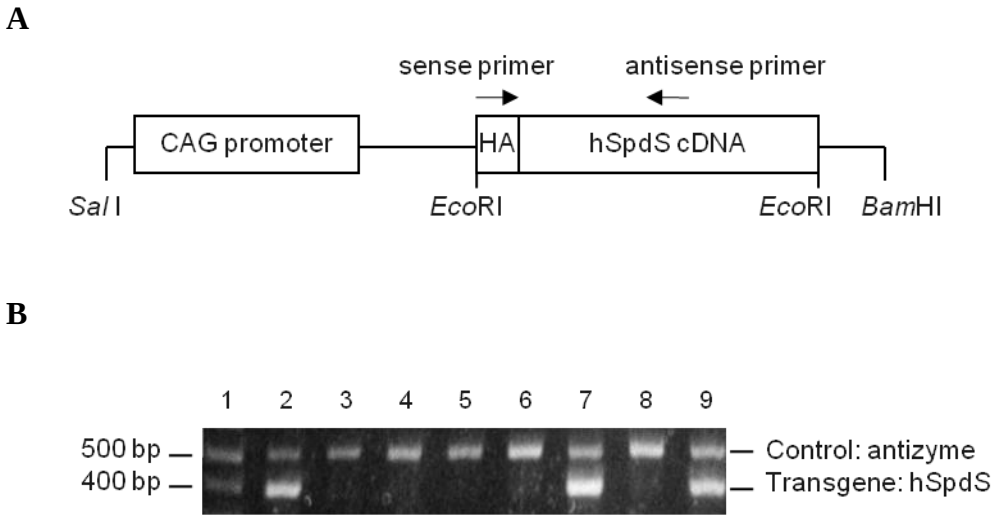

Fig. 2-1 Transgene construct and PCR identification of transgenic mice

A, The human SpdS cDNA was placed under the control of composite cytomegalovirus-immediate early gene enhancer/chicken β-actin (CAG) promoter elements to generate the transgene expression construct. An HA epitope was added to the amino terminus of the hSpdS to enable detection of transgene-derived SpdS protein. Arrows indicate the positions of primers used for PCR identification of transgenic mice. ***B***, A representative analytic gel of tail DNA extracts from eight potential transgenic mice (lanes 2 to 9) and a DNA standard (lane 1). Genotyping by PCR yielded a 397 bp product from the genomic DNA from transgenic animals (lanes 2, 7 and 9). Primers that amplify a 520 bp product from the mouse antizyme gene were included in all reactions as a positive control.

Aminopropyltransferase activity in CAG-SpdS transgenic mice

To evaluate transgene expression in CAG-SpdS mice, SpdS activity and protein levels were determined in several tissues from 7-week-old mice from the two founder lines. Transgenic mice from line B exhibited elevated SpdS activity relative to wild type controls in most tissues examined (**Table 2-1**). Heart and skeletal muscle showed the greatest fold increase (6.0 and 8.9, respectively) in SpdS activity, liver had a moderate 2.6-fold increase, skin tissues (epidermis and dermis) had an approximately 1.5-fold increase, while brain and kidney showed no statistically significant increase in SpdS activity. The higher expression in heart and skeletal muscle is likely related to the β-actin promoter and a similar effect was seen previously in CAG-SpmS mice (Ikeguchi et al., 2004). Tissues of transgenic mice from line A failed to show any evidence of increased SpdS activity or alterations in polyamine content (data not shown). Subsequent studies utilized progeny of CAG-SpdS line B unless noted.

Tissue extracts were also subjected to Western blot analysis using anti-hSpdS and anti-HA antibodies (**Fig. 2-2**). Significant amounts of SpdS protein were detected in skeletal muscle, heart and liver from transgenic mice of line B. Transgene-derived SpdS was detected to a lesser extent in epidermis and dermis but not in brain and kidney of mice from line B (**Fig. 2-3**), which is in agreement with the SpdS activity data in **Table 2-1**. SpdS protein was below the limit of detection in all tissues from wild type and CAG-SpdS mice of line A. Given that SpdS activity is quite high in some wild type mouse tissues such as brain and liver (**Table 2-1**), this result indicates that the anti-hSpdS antibody does not efficiently recognize the mouse SpdS protein.

	Spermidine synthase (pmol/mg/h)		Spermine synthase (pmol/mg/h)	
Tissue	Control	CAG-SpdS	Control	CAG-SpdS
Heart	272 ± 23	1630 ± 211**	20	19
Muscle	169 ± 61	1506 ± 428**	119	114
Liver	1928 ± 452	4974 ± 1032**	11	9
Kidney	731 ± 128	814 ± 95	57	61
Brain	5052 ± 1246	5050 ± 1213	102	98
Epidermis	1953 ± 374	2856 ± 479*		
Dermis	2908 ± 406	3977 ± 710*		

Table 2-1 Aminopropyltransferase activity in control and CAG-SpdS mice

All measurements were done in CAG-SpdS mice from founder line B. Spermidine synthase activity (mean ± S.D., n=4) was measured in 7-week-old mice. Spermine synthase activity (average of 2 mice) was measured in mice at the same age. *$p<0.05$, **$p<0.005$ vs. wild type controls.

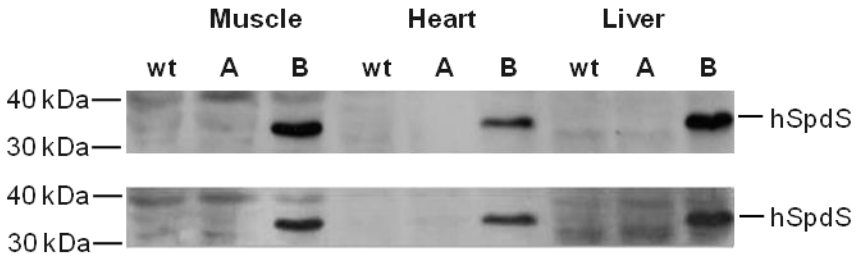

Fig. 2-2 Detection of SpdS protein in tissues extracts from CAG-SpdS mice

Tissues extracts of skeletal muscle, heart and liver from wild type (wt) control and transgenic mice from each founder line (A and B) were blotted for SpdS protein using anti-hSpdS antibody (top) or anti-HA antibody (bottom). Each lane contains 50 μg of cytosolic proteins.

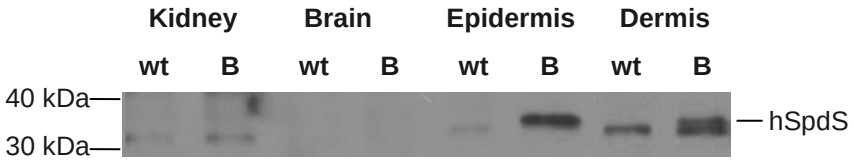

Fig. 2-3 Detection of SpdS protein in tissues extracts from CAG-SpdS mice

Tissues extracts of kidney, brain, epidermis and dermis from wild type (wt) control and transgenic mice from line B were blotted for SpdS protein using anti-hSpdS antibody. Each lane contains 50 μg of cytosolic proteins.

Next we assessed whether increased expression of SpdS led to an increase or decrease in SpmS activity. Elevated SpdS activity did not result in a compensatory alteration of SpmS activity in any of the five tissues examined (**Table 2-1**). Similarly, dramatic elevation of SpmS activity failed to influence SpdS activity in CAG-SpmS mice (Ikeguchi et al., 2004).

Polyamine, AdoMet and dcAdoMet content in tissues from CAG-SpdS mice

The impact of SpdS overexpression on tissue polyamine levels and AdoMet/dcAdoMet content was measured in tissues of CAG-SpdS mice and controls at 7 weeks of age. Spermidine levels increased significantly and the Spm:Spd ratio decreased significantly in heart, skeletal muscle and liver (**Table 2-2)**, which are the tissues with the greatest increase in SpdS activity (**Table 2-1**). The elevations in spermidine were relatively small given the fold increase in SpdS activity in those tissues. There was no significant alteration in putrescine or spermine content associated with SpdS overexpression, except for a modest 13.6% reduction in liver spermine levels.

The synthesis of spermidine from putrescine is not only dependent on SpdS activity but also on the levels of the aminopropyl donor, dcAdoMet (Pegg, 2009a). Therefore, AdoMet and dcAdoMet levels were determined in heart and skeletal muscle (**Table 2-3**) since these tissues exhibited the greatest increase in SpdS activity. Heart AdoMet and dcAdoMet levels were not altered by SpdS overexpression even though increased SpdS activity is expected to consume dcAdoMet for spermidine synthesis. The stable dcAdoMet pool may be maintained by a compensatory change in AdoMetDC activity, which was increased nearly 2-fold in the heart of CAG-SpdS mice. AdoMet, dcAdoMet and AdoMetDC measurements in muscle extracts revealed clear differences between

male and female mice regardless of genotype, and there was a nominal decrease in dcAdoMet content associated with SpdS overexpression in this tissue.

Tissue	Group	Polyamine content (pmol/mg tissue)			Spm:Spd ratio
		Putrescine	Spermidine	Spermine	
Heart	Control	8.0 ± 0.4	183 ± 18	328 ± 23	1.8 ± 0.2
	CAG-SpdS	6.3 ± 1.3	278 ± 39**	345 ± 82	1.2 ± 0.2*
Muscle	Control	9.6 ± 3.0	113 ± 23	179 ± 17	1.6 ± 0.4
	CAG-SpdS	8.4 ± 2.7	222 ± 69*	161 ± 26	0.8 ± 0.4*
Liver	Control	16 ± 4	693 ± 86	693 ± 64	1.0 ± 0.1
	CAG-SpdS	19 ± 5	832 ± 31*	599 ± 21*	0.7 ± 0.0**
Kidney	Control	64 ± 17	383 ± 49	644 ± 39	1.7 ± 0.1
	CAG-SpdS	51 ± 26	410 ± 7	631 ± 33	1.5 ± 0.1
Brain	Control	9.6 ± 1.4	317 ± 33	268 ± 18	0.9 ± 0.1
	CAG-SpdS	9.8 ± 2.3	257 ± 58	306 ± 15*	1.2 ± 0.3*

Table 2-2 Polyamine content in control and CAG-SpdS mice

Polyamine content (mean ± S.D.) was determined in 7-week-old mice (n=4 per genotype). *$p<0.05$, **$p<0.005$ vs. wild type controls.

Tissue	Group	Sex	AdoMet (pmol/mg tissue)	dcAdoMet (pmol/mg tissue)	AdoMetDC activity (pmol CO_2/min/mg protein)
Heart	Control	M and F	36.5 ± 6.2	0.24 ± 0.04	3.4 ± 0.3
	CAG-SpdS	M and F	33.2 ± 2.9	0.26 ± 0.09	6.1 ± 0.3**
Muscle	Control	F	14.2, 17.2	0.23, 0.23	37, 37
		M	10.9, 9.0	1.53, 1.50	191, 161
	CAG-SpdS	F	17.7, 25.3	0.14, 0.13	34, 31
		M	11.5, 12.1	0.78, 0.25	450, 205

Table 2-3 AdoMet and dcAdoMet content and AdoMetDC activity in control and CAG-SpdS mice

AdoMet and dcAdoMet content and AdoMetDC enzymatic activity were determined in 7-week-old mice (n=4 per genotype). Heart values represent mean ± S.D. of 2 male and 2 female mice. Muscle values differed between male and female mice so individual values are presented for each of 2 male and 2 female mice. **$p<0.005$ vs. wild type controls.

Simultaneous overexpression of SpdS and SpmS in bitransgenic mice

CAG-SpmS mice with ubiquitous overexpression of SpmS using the same CAG promoter have been reported previously (Ikeguchi et al., 2004). In those mice, up to 2000-fold increases in SpmS activity led to only small changes in spermine and spermidine levels and SpdS activity was unaltered. Therefore we bred CAG-SpdS and CAG-SpmS mice to determine whether simultaneous overexpression of both aminopropyltransferases would affect tissue polyamine profiles. CAG-SpdS/CAG-SpmS mice were generated at the expected frequency (9 of 34 offspring, 26.5%) and did not exhibit any obvious phenotypic abnormalities. In heart and liver from 5-week-old bitransgenic mice we demonstrated that both aminopropyltransferase activities were elevated to levels that are comparable to values from single transgenic animals (**Tables 2-1 and 2-4**) and to those observed in previous studies of CAG-SpmS mice (Ikeguchi et al., 2004). Next, polyamine content was measured in heart, skeletal muscle, liver, kidney and brain (**Table 2-5**). In agreement with previous results (**Table 2-2** and (Ikeguchi et al., 2004)), CAG-SpdS mice exhibited increased spermidine levels and decreased Spm:Spd ratios while CAG-SpmS mice exhibited increased spermine levels, decreased spermidine levels and increased Spm:Spd ratios. In bitransgenic mice, spermidine and spermine levels as well as Spm:Spd ratios were intermediate between the values obtained in individual single transgenic mice in all tissues except brain, which lacks transgene-derived SpdS activity (**Table 2-1**). Putrescine levels did not appear to be depleted in response to SpdS or SpmS overexpression. These results clearly show that overexpression of SpdS, SpmS or both aminopropyltransferases is not sufficient to yield considerable increases in the higher polyamines spermidine and spermine.

Tissue	Group	Spermidine synthase (pmol/mg/h)	Spermine synthase (pmol/mg/h)
Heart	Control	574 ± 69	59 ± 2
	CAG-SpdS	2908 ± 433**	51 ± 8
	CAG-SpmS	432 ± 41*	16030 ± 801**
	CAG-SpdS/CAG-SpmS	2064 ± 179**	15517 ± 357**
Liver	Control	4330 ± 312	11 ± 1
	CAG-SpdS	11952 ± 861**	7 ± 2
	CAG-SpmS	3742 ± 501	9240 ± 940**
	CAG-SpdS/CAG-SpmS	9069 ± 1676*	9575 ± 1125**

Table 2-4 Aminopropyltransferase activity in control, CAG-SpdS, CAG-SpmS and CAG-SpdS/CAG-SpmS mice

Spermidine and spermine synthase activity (mean ± S.D.) was assayed in tissues from 5-week-old mice (n=4 per genotype). *$p<0.05$, **$p<0.005$ vs. wild type controls.

Tissue	Group	Polyamine content (pmol/mg tissue)			Spm:Spd ratio
		Putrescine	Spermidine	Spermine	
Heart	Control	32 ± 5	219 ± 15	383 ± 14	1.8 ± 0.1
	CAG-SpdS	25 ± 1*	322 ± 28**	330 ± 24**	1.0 ± 0.1**
	CAG-SpmS	46 ± 9*	128 ± 18**	477 ± 28**	3.8 ± 0.6**
	CAG-SpdS/CAG-SpmS	44 ± 6*	165 ± 12**	430 ± 24**	2.6 ± 0.2**
Muscle	Control	36 ± 5	172 ± 54	286 ± 89	1.8 ± 0.7
	CAG-SpdS	24 ± 3**	323 ± 15**	212 ± 29	0.7 ± 0.1*
	CAG-SpmS	47 ± 9*	75 ± 24**	309 ± 33	4.4 ± 1.4**
	CAG-SpdS/CAG-SpmS	36 ± 11	151 ± 50	278 ± 68	2.0 ± 0.6
Liver	Control	32 ± 6	879 ± 61	814 ± 62	0.9 ± 0.1
	CAG-SpdS	26 ± 1	1009 ± 142*	486 ± 71**	0.5 ± 0.1**
	CAG-SpmS	58 ± 18*	527 ± 112**	1252 ± 140**	2.4 ± 0.4**
	CAG-SpdS/CAG-SpmS	58 ± 22*	539 ± 51**	1040 ± 79**	1.9 ± 0.1**
Kidney	Control	41 ± 5	397 ± 40	821 ± 30	2.1 ± 0.2
	CAG-SpdS	38 ± 9	474 ± 35*	773 ± 40	1.6 ± 0.1*
	CAG-SpmS	67 ± 13**	232 ± 34**	964 ± 61**	4.2 ± 1.0**
	CAG-SpdS/CAG-SpmS	61 ± 13**	250 ± 22**	920 ± 81*	3.7 ± 0.5**
Brain	Control	21 ± 3	270 ± 71	322 ± 29	1.3 ± 0.3
	CAG-SpdS	25 ± 4	275 ± 51	333 ± 22	1.2 ± 0.3
	CAG-SpmS	29 ± 3**	208 ± 22	405 ± 58*	2.0 ± 0.1**
	CAG-SpdS/CAG-SpmS	35 ± 7**	206 ± 22*	398 ± 94	1.9 ± 0.4**

Table 2-5 Polyamine content in control, CAG-SpdS, CAG-SpmS and CAG-SpdS /CAG-SpmS mice

Polyamine content (mean ± S.D.) was measured in tissues from 5-week-old control (n=6), CAG-SpdS (n=4), CAG-SpmS (n=5) and CAG-SpdS/CAG-SpmS (n=8) mice. *$p<0.05$, **$p<0.005$ vs. wild type controls.

Combined overexpression of SpdS and AdoMetDC in the mouse heart

In order to test whether insufficient dcAdoMet content was limiting the ability of SpdS to mediate a greater increase in spermidine and spermine levels, we bred CAG-SpdS mice with MHC-AdoMetDC mice in which AdoMetDC expression is driven by the cardiac-specific αMHC promoter (Nisenberg et al., 2006). These mice exhibit a >100-fold increase in cardiac AdoMetDC activity and a >400-fold increase in cardiac dcAdoMet content (Pegg et al., 2011a). Bitransgenic CAG-SpdS/MHC-AdoMetDC animals were generated at the expected frequency (7 of 30 offspring, 23.3%). Therefore, overexpression of both AdoMetDC and SpdS in the heart is compatible with the production of viable bitransgenic mice, whereas crosses of CAG-SpmS and MHC-AdoMetDC mice did not yield any viable bitransgenic offspring at 3 weeks of age (Ikeguchi et al., 2004). CAG-SpdS/MHC-AdoMetDC mice exhibited cardiac polyamine levels that were nearly identical to MHC-AdoMetDC littermates (**Table 2-6**). This result demonstrates that factors other than SpdS and AdoMetDC activity control cardiac spermidine and spermine accumulation.

Group	Polyamine content (pmol/mg tissue)			
	Putrescine	Spermidine	Spermine	Spm:Spd ratio
Control	15 ± 4	187 ± 14	332 ± 47	1.8 ± 0.2
CAG-SpdS	10 ± 2*	217 ± 22*	287 ± 36	1.3 ± 0.0**
MHC-AdoMetDC	9 ± 3*	109 ± 19**	354 ± 7	3.3 ± 0.6*
CAG-SpdS/MHC-AdoMetDC	9 ± 1*	104 ± 9**	355 ± 24	3.4 ± 0.4**

Table 2-6 Cardiac polyamine content in control, CAG-SpdS, MHC-AdoMetDC and CAG-SpdS/ MHC-AdoMetDC mice

Polyamine content (mean ± S.D.) was measured in tissues from 5-week-old control (n=6), CAG-SpsS (n=6), MHC-AdoMetDC (n=4) and CAG-SpdS/MHC-AdoMetDC (n=6) mice. *$p<0.05$, **$p<0.005$ vs. wild type controls.

DISCUSSION

The CAG enhancer/promoter element was chosen to drive overexpression of a human SpdS cDNA in the mouse without the endogenous regulatory controls that govern SpdS transcription and translation. Although this promoter was chosen to enable ubiquitous overexpression (Okabe et al., 1997), the greatest increase in activity was detected in heart and muscle as seen previously with CAG-SpmS mice (Ikeguchi et al., 2004). It is unclear whether the lesser activity in other tissues of SpdS mice is due to tissue-specific regulatory factors or, more likely, positional effects related to transgene integration site. The increase in SpdS activity in CAG-SpdS tissues (**Table 2-1**) was modest relative to the 2000-fold increase in SpmS activity that was achieved in some tissues of CAG-SpmS mice. However, there is a much higher constitutive level of SpdS activity compared to SpmS activity in most tissues and it is readily apparent from both the enzymatic assays and the western blots that a significant amount of additional SpdS enzyme was produced. The increased SpdS activity led to a 1.5 to 2-fold reduction in the Spm:Spd ratio (**Table 2-2**) as compared to the 2 to 4-fold increase in Spm:Spd ratio in tissues of CAG-SpmS mice. There was little or no compensatory change detected in either SpdS or SpmS in response to transgenic overexpression of the other synthase (**Tables 2-1 and 2-4** and (Ikeguchi et al., 2004)); therefore, we conclude that the activity of these enzymes is not responsive to cellular Spm:Spd ratios *in vivo*.

The decarboxylation of AdoMet irreversibly commits it to polyamine biosynthesis rather than cellular methylation reactions and dcAdoMet levels are typically less than 5% of AdoMet (Hibasami et al., 1980; Pegg, 1984). dcAdoMet levels are elevated in mice or humans lacking SpmS activity and widespread overexpression of SpmS slightly depletes

tissue dcAdoMet, thus there is an inverse relationship between dcAdoMet content and SpmS activity (Pegg et al., 2011a). However, there was no reduction in cardiac dcAdoMet levels in CAG-SpdS mice, possibly due to a concurrent increase in AdoMetDC activity (**Table 2-3**). Conversely, cardiac dcAdoMet levels were reduced in CAG-SpmS mice that also exhibited decreased cardiac AdoMetDC activity (Pegg et al., 2011a). These opposing results may be related to the differing cellular Spm:Spd ratios in CAG-SpdS and CAG-SpmS mice and the fact that spermine is a stronger repressor of AdoMetDC than spermidine (Pegg, 2009b). Interestingly, measurements of muscle AdoMet, dcAdoMet and AdoMetDC showed clear differences between male and female mice regardless of genotype. In both sexes, CAG-SpdS mice exhibit decreased dcAdoMet content that correlates with a lack of AdoMetDC induction in samples from female animals and modest AdoMetDC induction in males. The greatly elevated AdoMetDC activity in males relative to females requires further investigation and may be related to continued increases in muscle mass in young adult males (age 7 weeks old) but not females.

Substantial increases in SpdS or SpmS activity altered the Spm:Spd ratio in transgenic tissues and this was normalized somewhat by the combined overexpression of both aminopropyltransferases (**Table 2-5**). Overexpression of SpdS, SpmS or both enzymes failed to yield a dramatic elevation in spermidine and spermine content, which indicates that either low capacity or compensatory alterations in ODC and AdoMetDC limit polyamine synthesis. CAG-SpdS and MHC-AdoMetDC mice were bred to determine if elevated dcAdoMet would enable a greater cardiac spermidine accumulation but polyamine levels in bitransgenic animals did not support this hypothesis. In fact, the

data indicate that increased dcAdoMet availability in CAG-SpdS mice facilitates spermine accumulation rather than spermidine (**Table 2-6**), which reinforces the concept that SpmS and its access to dcAdoMet are limiting for cardiac spermine accumulation (Ikeguchi et al., 2004; Pegg et al., 2011a). Previous studies demonstrated that the combined overexpression of SpmS and AdoMetDC in the heart is lethal because this limiting step is removed and presumably putrescine and spermidine are rapidly converted to spermine (Ikeguchi et al., 2004). Conversely, our results suggest that endogenous cardiac SpmS levels are compatible with normal development even in the face of seemingly unlimited dcAdoMet and spermidine availability in CAG-SpdS/MHC-AdoMetDC mice. The cardiac overexpression of both ODC and AdoMetDC is also lethal (Nisenberg et al., 2006), again demonstrating that the decarboxylases provide the regulatory steps that limit toxic polyamine accumulation. We did not attempt to generate tri-transgenic CAG-SpdS/MHC-AdoMetDC/MHC-ODC mice. Studies of cardiac physiology in these animals, and the combined overexpression of all four polyamine biosynthetic enzymes, will require more advanced models with conditional transgene expression.

We studied two founder animals identified out of 53 pups that resulted from microinjection of fertilized oocytes with the transgene, one of which failed to exhibit any increase in SpdS activity. The failure to detect any evidence of increased SpdS in CAG-SpdS line A mice is almost certainly due to the integration of transgene DNA in a transcriptionally silent region of the genome but we did not pursue this supposition. The CAG-SpdS line B mice reported here are viable and phenotypically normal, which may argue against a causative role for high spermidine levels in the abnormalities of Gy mice

or Snyder-Robinson syndrome patients. However, it remains a formal possibility that additional founders with ubiquitous and extreme SpdS expression were not generated due to adverse consequences from very high levels of SpdS activity. The increased SpdS activity in CAG-SpdS mice was not uniform in all tissues and was not sufficient to cause elevations in spermidine of the same magnitude as observed in Gy mice (up to 5-fold (Wang et al., 2004)), but there was robust SpdS expression in the heart of CAG-SpdS animals and the sudden death in Gy mice is likely due to arrhythmias related to polyamine modulation of cardiac ion channels (Pegg and Wang, 2009). Future studies to evaluate the consequences of SpdS overexpression in the Gy background may provide additional evidence of a role for increased spermidine in the Gy phenotype. One thing needs to be considered in the experimental design is that since Gy mice do not survive on a C57BL/6 background, SpdS mice need to be moved to a mixed B6C3H background, which the Gy mice are only viable and maintained on (Pegg and Wang, 2009; Wang and Pegg, 2011). CAG-SpdS/Gy mice expressing the human SpdS would also address the provocative question of whether spermine is detected in cells from Snyder-Robinson syndrome patients, but not Gy mice, because the human SpdS enzyme displays less substrate specificity than the mouse enzyme (Ikeguchi et al., 2006).

Chapter III
Generation and characterization of transgenic mice with tissue specific and regulated AdoMetDC expression in the skin

INTRODUCTION

Previous studies have indicated that the induction of ODC and subsequent increase in polyamine levels, especially putrescine, play a critical role in skin tumor development (Gilmour, 2007; Pegg and Feith, 2007; Peralta Soler et al., 1998). *S*-adenosylmethionine decarboxylase (AdoMetDC) catalyzes the decarboxylation reaction to produce the aminopropyl donor dcAdoMet and its activity is rate limiting for the synthesis of the higher polyamines from putrescine (Pegg, 2009b; Shantz et al., 1992). Although AdoMetDC activity is closely related to the levels of intracellular putrescine and also known to be induced by the tumor promoter TPA (O'Brien et al., 1975b), the function of AdoMetDC in skin carcinogenesis is poorly understood. To evaluate the role of AdoMetDC and altered polyamine levels in mouse skin carcinogenesis, transgenic mouse lines with AdoMetDC overexpressed in skin keratinocytes are required.

We have chosen to use the tetracycline-regulated system to produce targeted and regulated expression of AdoMetDC in specific mouse skin cell populations based on the reasons described in Chapter I. Using this system, AdoMetDC expression is directed to mitotically active keratinocytes in the basal layer of the interfollicular epidermis (IFE) and hair follicle outer root sheath (ORS) by the Keratin 5 (K5) promoter and regulation is accomplished by giving mice the tetracycline analogue doxycycline (Dox) in their chow. Luciferase reporter protein is also expressed from the transgene construct in target cells and will be used as a surrogate marker of AdoMetDC expression.

This chapter will describe the development of the bitransgenic mouse model with regulated AdoMetDC expression in the skin (AdoMetDC/tTA mice) and the screening process to utilize luciferase reporter expression to identify the best line for further experiments. Following that, biochemical measurements of AdoMetDC transgene expression, alterations in polyamine metabolism as well as skin phenotype studies will be presented.

We are the first to generate a transgenic mouse model with targeted AdoMetDC expression in the skin and this mouse model will provide a unique system to evaluate the effects of AdoMetDC overexpression on susceptibility to mouse skin chemical carcinogenesis.

MATERIALS AND METHODS

All chemicals, unless noted, were purchased from Sigma Chemical Company (St. Louis, MO). Restriction enzymes were purchased from New England Biolabs (Beverly, MA). Oligonucleotides used as primers were synthesized and purified in the Macromolecular Core Facility (Pennsylvania State University College of Medicine). [^{35}S]-dcAdoMet was synthesized from L-[^{35}S]methionine (PerkinElmer Life Sciences, Boston, MA) as described previously (Mackintosh and Pegg, 2000). *S*-adenosyl-L-[carboxyl-^{14}C]-methionine (54 mCi/mmol) was obtained from Amersham Pharmacia Biotech (Piscataway, NJ).

Plasmid construction

To make the plasmid for the TetO-AdoMetDC single transgenic mice, human AdoMetDC cDNA was inserted into the *Sal*I and *Spe*I sites of the inducible vector TMILA (provided by Dr. Lewis Chodosh, University of Pennsylvania, Philadelphia, PA) that contains an

internal ribosome entry site (IRES)-firefly luciferase cassette downstream of the tet operon repeat sequences (**Fig. 3-1A**). Human AdoMetDC cDNA was amplified by PCR from plasmid αMHC-AdoMetDC (Nisenberg et al., 2006) and was modified to add specific restriction sites and to replace the carboxyl-terminal 6 residues with a nine amino acid hemagglutinin (HA) epitope with sense primer 5'-GACGCATTAG*GTCGAC*GTTT AATTTAGTTGATTTTCTGTGG-3' (*Sal*I site in italics) and antisense primer 5'-GACG CATTAG*ACTAGT*TCATCAAGCGTAGTCTGGGACGTCGTATGGGTACTTCTTAGA AAACTGGTAAAAAC-3' (*Spe*I site in italics and HA epitope coding sequence underlined). The PCR reaction was carried out in a 0.1 ml volume containing 2.5 units of *Pfu* polymerase (Stratagene, La Jolla, CA), 25 ng of template DNA and 25 pmol of each primer under the following conditions: initial denaturation for 2 min at 94°C, followed by 25 cycles of denaturation (94°C for 30 s), annealing (52°C for 30 s) and extension (72°C for 2 min), with a final extension at 72°C for 5 min. The entire AdoMetDC cDNA insert in plasmid pTetO-AdoMetDC was sequenced at the DNA Sequencing Core (Pennsylvania State University College of Medicine) to ensure that no secondary mutations were introduced during the plasmid construction.

A 5.6kb transgene fragment released by *Not*I digestion of the plasmid pTetO-AdoMetDC to remove prokaryotic vector sequences was used for microinjection. The transgene was purified using the Perfectprep gel cleanup kit (Eppendorf, Hauppauge, NY) and Elutip-D-mini-columns (Schleicher & Schuell, Keene, NH) and then precipitated and resuspended in microinjection buffer (10 mM Tris/HCl, pH 7.4, and 0.1 mM EDTA). The integrity and concentration of the DNA was documented using the Agilent Bioanalyzer at the Functional Genomics Core (Pennsylvania State University

College of Medicine). The transgene construct (at 4 ng/µl) was microinjected into fertilized FVB/NJ oocytes using standard techniques in the Transgenic Mouse Facility (Pennsylvania State University, University Park) and transgenic founder animals were identified by PCR as described below.

Founder line identification and propagation

All animal studies were reviewed and approved by the Institutional Animal Care and Use Committee of the Pennsylvania State University College of Medicine. Genomic DNA was isolated from tails of potential transgenic founders and subjected to PCR analysis using the REDExtract-N-Amp Tissue PCR Kit (Sigma, St. Louis, MO) to detect the transgene DNA. A sense primer (5'-GAGCTCGTTTAGTGAACCGTCAG-3') binds in the TetO/CMV enhancer/promoter region and the antisense primer (5'-GTATGTCCCACT CAGATCTTGGG-3') binds in the human AdoMetDC coding region (**Fig. 3-1B**) to amplify a 330 bp product only in genomic DNA samples from mice bearing the transgene. A second primer pair that yields a 520 bp product from the mouse antizyme 1 gene (*Oaz1*) was also included in the reaction, which provides a positive control for successful PCR amplification for each genomic DNA sample (Feith et al., 2007).

Bitransgenic TetO-AdoMetDC/tTA mice were derived by breeding hemizygous TetO-AdoMetDC transgenic founders or their TetO-AdoMetDC progeny to hemizygous K5/tTA mice on an inbred FVB/NJ genetic background (Diamond et al., 2000) (provided by Dr. Adam Glick, Pennsylvania State University, University Park) to produce approximately equal numbers of bitransgenic, TetO-AdoMetDC single transgenic, K5-tTA single transgenic and wild type littermate controls. 3-week- old offspring were genotyped for both transgenes by PCR. The K5-tTA transgene was identified with sense

primer (5'-CGCCCAGAAGCTAGGTGTAG-3') and antisense primer (5'-GCTCCAT CGCGATGACTTAG-3') that hybridize with sequences in the tet transactivator coding region (Diamond et al., 2000) and yield a 200bp product. The primer pair that amplifies the 520 bp product from the mouse antizyme 1 gene stated above was also included in the PCR reaction as a positive control (Feith et al., 2007).

Mice were housed and maintained at the Penn State University College of Medicine animal research farm. Animals were provided Teklad Rodent Diet (Harland-Teklad, Madison, WI) and chlorinated tap water *ad libitum*. All experimental groups included both male and female mice and no sex-dependent differences were observed.

***In vivo* bioluminescence imaging**

In vivo bioluminescence imaging was conducted on Xenogen IVIS 50 Imaging System (Caliper Life Sciences, Alameda, CA) to monitor the luciferase reporter expression. The system detects the light emitted from luciferase-expressing cells within the animal body and transmitted through the tissue after mice are injected with luciferase substrate luciferin and calculates the light strength over a defined period of time with the coupled Living Image software (Caliper Life Sciences). Mice were anaesthetized with ketamine/xylazine (100mg/kg and 10mg/kg, respectively, i.p.), and luciferin (135 mg/kg i.p.) (Prolume Ltd., Beverly Hills, CA) was injected 10 minutes prior to imaging. An acquisition time of 20 seconds was used for luminescent image acquisition and the resulting light emission was quantified as the sum of all detected photon counts within the whole dorsal body area. Values were reported as photons/second.

Initial screening for luciferase expression: 6-week-old bitrangenic, TetO-AdoMetDC single transgenic, and wild type littermate controls from each founder line were analyzed

with the *in vivo* imaging system and compared for luciferase expression (**Fig. 3-2A and 2B**).

Dox regulated transgene expression: 5-week-old bitransgenic mice and wild type controls were put on a diet containing 2g/kg Dox (Bio-Serv, Frenchtown, NJ) for 7 days, then switched to normal chow and *in vivo* imaging was done at different time points to monitor the repression and reactivation of luciferase expression upon Dox removal.

Skin sample processing

Mice were sacrificed at 7 weeks of age by CO_2 asphyxiation and skin tissues were prepared (Feith, 2001) for enzyme activity assays and polyamine, AdoMet/dcAdoMet analysis. Skin was excised from the mouse, exposed to 55 ºC dH_2O for 20 s and then the epidermis was scraped from the dermis. Both epidermis and dermis were divided into equal-sized portions for different measurements (dermis was minced thoroughly with scissors) and were flash frozen in liquid nitrogen and stored at −80°C.

Luciferase activity assay

10 µl tissue supernatant processed in AdoMetDC harvesting buffer (described below) was diluted in 40 µl Passive Lysis Buffer (Promega). 20 µl of this solution was injected with 100 µl Luciferase Assay Substrate (Promega) in duplicate and luciferase activity was read in a Monolight 2010 luminometer (Analytical Luminescence Laboratory, Ann Arbor, MI) according to manufacturer's instructions. Luciferase activity values were normalized to total protein levels determined using the Bio-Rad dye reagent (Bio-Rad Laboratories, Hercules, CA) with BSA as a standard.

Screening for luciferase activity: one week after imaging at 6 weeks of age, bitransgenic, TetO-AdoMetDC single transgenic, and wild type littermate controls from

different lines were sacrificed and epidermis and dermis were harvested and processed for luciferase activity assay to compared levels of transgene expression between different lines.

Tissue specific and regulated transgene expression: 7-week-old untreated bitransgenic, TetO-AdoMetDC single transgenic, and wild type littermate controls were sacrificed. Tissues that are expected to exhibit K5-driven transgene expression (epidermis, dermis, tongue, thymus, forestomach, mammary gland) (Bol et al., 1998; Byrne and Fuchs, 1993; Ramirez et al., 1994) and random tissues (liver, brain, kidney, lung, heart, skeletal muscle) were harvested and processed for luciferase activity assay. Also K5-expressing tissues from 7-week-old mice treated with Dox from the day of birth by placing the nursing dams on Dox (Liu et al., 2001) were assayed for luciferase activity to check if Dox treatment could silence the transgene expression.

AdoMetDC activity assay and AdoMetDC western blotting

To determine AdoMetDC activity, epidermal and dermal tissues were thawed on ice and then resuspended in ice-cold AdoMetDC harvesting buffer (50 mM sodium phosphate (pH 6.8), 2.5 mM putrescine, 2.5 mM dithiothreitol, 0.1 mM EDTA and 1x protease inhibitor cocktail (Calbiochem, La Jolla, CA)). Epidermis was lysed on ice by sonication for 30 s with 10 s on/10 s off and centrifuged at 20000 x *g* for 30 min at 4°C. Dermis was homogenized on ice using a Polytron for 30 s with 15 s on/15 s off and centrifuged the same way. The resulting supernatant was transferred to a new tube and stored at −80°C before use. AdoMetDC activity was assayed in duplicate for each sample by measuring the production of [^{14}C]-labeled CO_2 as described previously (Nisenberg et al., 2006). Protein concentration in the supernatant was determined using the Bio-Rad dye reagent

(Bio-Rad Laboratories, Hercules, CA) with BSA as a standard. Cytosolic proteins (50 µg) were fractionated by 15% SDS-PAGE, transferred to PVDF membrane, and AdoMetDC protein was detected by western blotting using a rabbit polyclonal antibody to the HA epitope (sc-805, Santa Cruz Biotechnology, Santa Cruz, CA). Signals were visualized with a chemiluminescence detection system (Cell Signaling Technology, Beverly, MA).

HPLC analysis of polyamine and AdoMet/dcAdoMet content

For polyamine quantification, epidermal and dermal tissues were homogenized in 10% trichloroacetic acid (0.1 N HCl, then add 20% TCA) (Fisher Scientific, Pittsburgh, PA) and analyzed by HPLC using an ion-pair reverse-phase separation method with post-column derivatization using *o*-phthaldialdehyde as described previously (Pegg et al., 1989) and normalized to tissue wet weight or protein content. For AdoMet and dcAdoMet quantification, tissue extracts were reacted with chloroacetaldehyde to convert AdoMet and dcAdoMet to fluorescent 1,N^6-etheno derivatives, which were then separated and quantified by HPLC as described previously (Pegg et al., 2011a) and normalized to tissue wet weight.

Skin histological analysis

1-day-old pups and 7-week-old mice treated with or without Dox were studied for skin histology for bitrangenic mice, single transgenic controls and wild type littermate controls to examine if transgene expression has any effect on skin structure and hair follicle growth. Mice were euthanized and skin was isolated and fixed overnight in 10% neutral buffered formalin, embedded in paraffin, and 5 µm serial sections were obtained and stained with hematoxylin and eosin. Numbers of hair follicles at different morphogenesis stages were counted and also hair follicle cycle stages were determined

by established criteria (Hardy, 1992; Muller-Rover et al., 2001).

Statistical analysis

All comparisons between wild type controls and transgenic mice utilized the two-tailed, unpaired Student's *t* test.

RESULTS

Generation and identification of AdoMetDC/tTA transgenic mice

In order to generate mice with targeted and regulated AdoMetDC expression, we utilized the tet system that relies on the combination of two independent transgenic lines. The TetO-AdoMetDC single transgenic mice were produced on an FVB background, and then were crossed with the K5-tTA single transgenic mouse line already made on the same background that has tTA overexpression in the skin. The human AdoMetDC cDNA insert derived from plasmid αMHC-AdoMetDC has a greatly abbreviated 5'-UTR and 3'-UTR (52 bp of 5'-UTR and 66 bp of 3'-UTR) to abrogate translational regulation by polyamines in order to enable high level transgene activity (Nisenberg et al., 2006). The cDNA was also modified to replace the carboxyl-terminal six residues with a nine amino acid HA epitope to facilitate the detection of transgene-derived AdoMetDC and differentiate this protein from the endogenous mouse AdoMetDC protein (**Fig. 3-1A**). This modification is based on truncation mutant studies that show removal of the carboxyl-terminal eight residues did not affect the rate of processing or the activity of processed human AdoMetDC protein in the presence of putrescine (Xiong et al., 1997). Genomic DNA screening (**Fig.3-1B**) identified eight potential founder mice (designated A to H), but only six founders transmitted the transgene to their offspring upon breeding. No abnormalities were observed in any of the founder mice or their TetO-AdoMetDC

single transgenic progeny. However, bitransgenic mice from two founder lines (line A and B) started to show a thin fur phenotype at a young age (**Fig.3-6A**). For line A, bitransgenic mice were produced at a slightly lower frequency than expected (120 out of 617, 19.4%) when breeding TetO-AdoMetDC with K5-tTA single transgenic mice. They also had slightly squinted eyes. No other obvious phenotypic abnormalities were observed in bitransgenic mice from this line for up to 2 years of age.

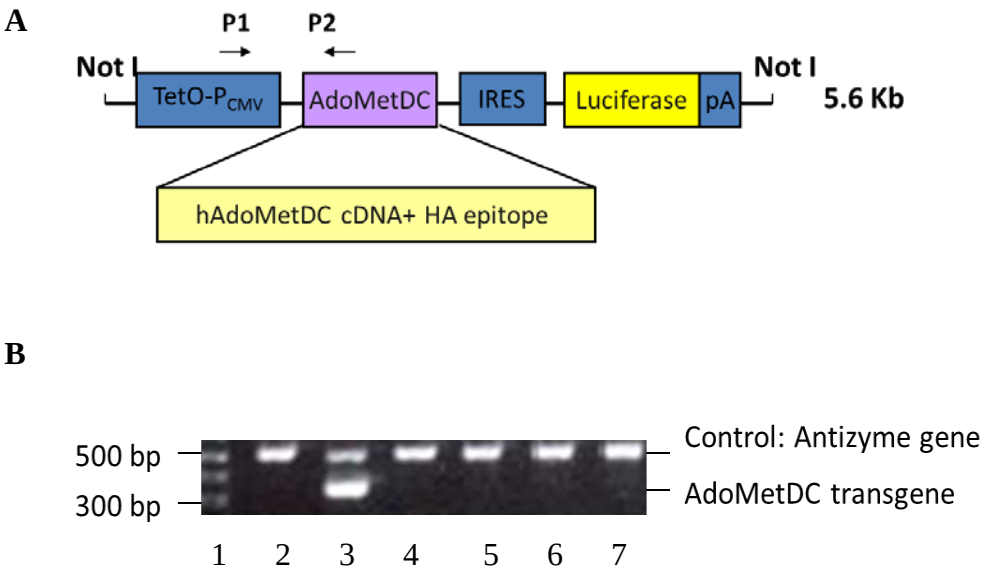

Fig. 3-1 Diagram of the TetO-AdoMetDC construct used for microinjection and PCR detection of transgenic mice.

A, Human AdoMetDC cDNA with greatly abbreviated 5' and 3'-UTR was modified by PCR to add specific restriction sites and to replace the C-terminal 6 residues with an HA epitope. The modified cDNA was then digested and ligated into TetO vector (TMILA) containing an IRES-luciferase cassette. A 5.6 Kb fragment released by Not I digestion was purified and used for microinjection. ***B***, Genotyping by PCR yielded a 330-bp product only from the tail DNA of transgenic animals (lane 3). Lanes 2- 7 were the tail DNA extracts from each potential transgenic mouse. Primers that amplify a 520 bp product from the mouse antizyme gene were included in all reactions as a positive control. TetO, seven repeats of the tetracycline operator; P_{CMV}, minimal cytomegalovirus enhancer/promoter; P1, sense primer; P2, antisense primer.

Initial screening for transgene expression in founder lines

Since the transgene construct also contains an IRES-luciferase cassette, luciferase reporter protein is translated from the same mRNA as AdoMetDC in bitransgenic mice. The luciferase activity can be measured *in vivo* using non-invasive bioluminescence imaging and by *in vitro* luciferase activity assay conveniently and more accurately. Bitransgenic mice from all the six founder lines were initially screened at 6 weeks of age for luciferase expression to identify 2-3 lines for further characterization. *In vivo* imaging results show that luciferase signal was detected in bitransgenic mice from all lines. Line A and line B had the strongest luciferase signal, line E had moderate level of signal, and the other three lines had poor luciferase signal (**Fig. 3-2 A and B**). No luciferase signal was detected in wild type or single transgenic TetO-AdoMetDC mice. *In vitro* luciferase activity assay showed generally the same conclusion (**Fig. 3-2 C**). From the results, lines A, B and E were chosen for further screening.

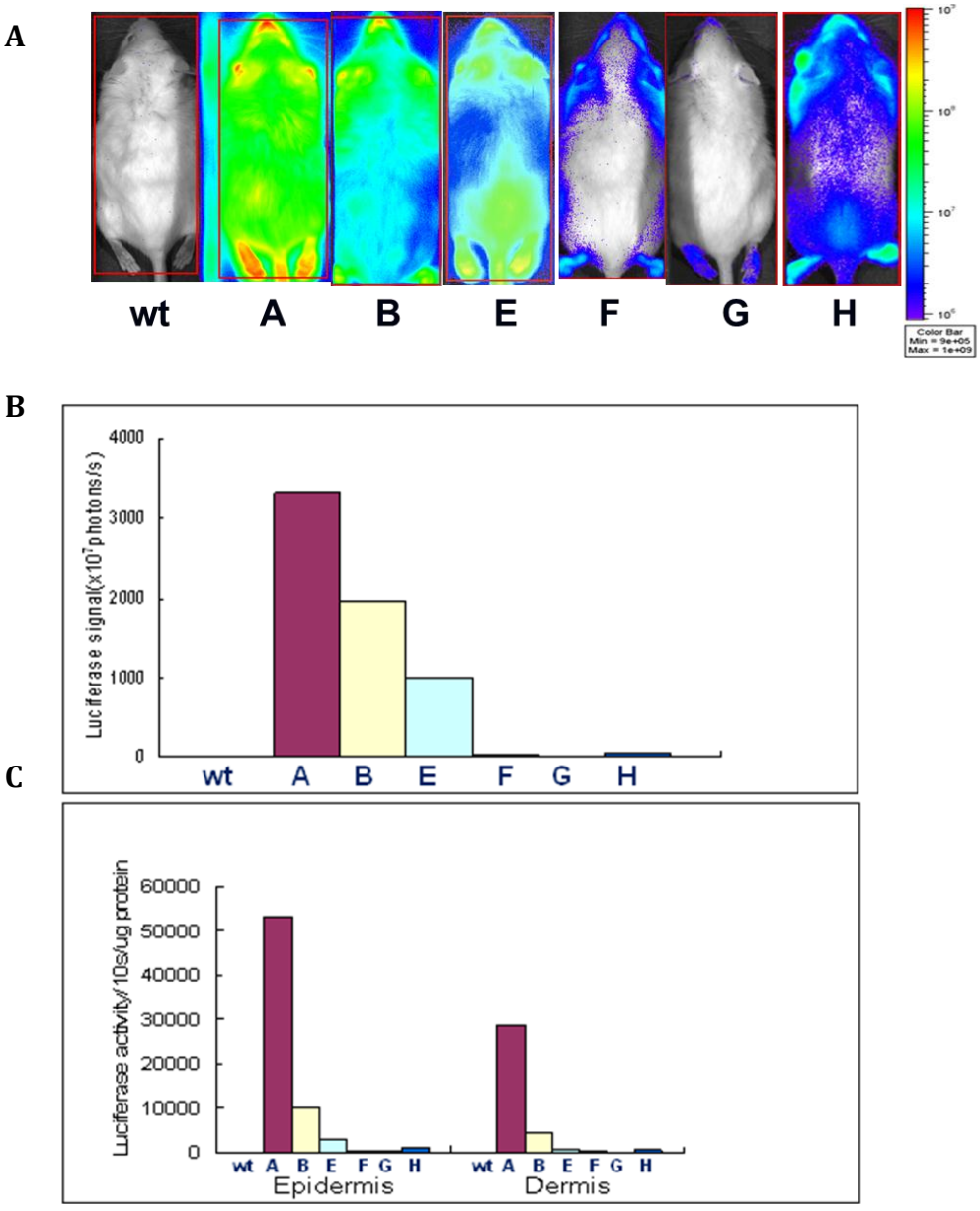

Fig. 3-2 Relative luciferase activity in the skin of AdoMetDC/tTA bitransgenic mice from different founder lines.

A, Images of wt and representative bitransgenic mice from each of 6 founder TetO-AdoMetDC lines (A,B,E,F,G,H). Luciferase expression was analyzed by *in vivo* imaging at 6 weeks of age in the absence of Dox. Mice were anesthetized, luciferin was injected i.p. and *in vivo* light production was analyzed using the Xenogen IVIS 50 and LivingImage software. ***B***, *In vivo* luciferase signal intensity average from 2-3 bitransgenic mice from each founder line. ***C***, *In vitro* luciferase activity. One week after imaging, mice were sacrificed and epidermis and dermis were harvested and processed for luciferase activity assay.

AdoMetDC activity and protein in the skin of AdoMetDC/tTA mice

To evaluate and compare AdoMetDC transgene expression between lines A, B and E, AdoMetDC activity was measured in epidermis and dermis of 7-week-old mice from the three lines (**Table 3-1**). Bitransgenic mice from line A exhibited a 7.2-fold increase in AdoMetDC activity in epidermis and a 7.8-fold increase in dermis. Mice from line B had a lesser increase in AdoMetDC activity. Mice from Line E displayed the least increase (approximately 1.3-fold in epidermis and dermis, data not shown).

Epidermal and dermal extracts were also subjected to Western blot analysis using anti-HA antibodies. Significant amounts of transgene-derived AdoMetDC protein (α subunit, 31 kDa) were detected in dermis (**Fig. 3-3**) from bitransgenic mice of line A, and AdoMetDC was detected to a lesser extent in line B, which is in agreement with the AdoMetDC activity data in Table 3-1. Western blot for epidermal extracts showed the same results (data not shown). Very little AdoMetDC protein was detected in epidermis and dermis of mice from line E (data not shown). The 38 kDa proenzyme was undetectable because it is usually rapidly processed (Xiong et al., 1997). Based on these results, line A and line B were chosen for further characterization.

Tissue	wt (n=5)	tTA (n=3)	AdoMetDC(A) (n=3)	AdoMetDC (A)/tTA (n=8)	AdoMetDC (B)/tTA (n=3)
Epidermis	2.4 ± 0.5	3.1 ± 1.1	2.9 ± 0.8	17.2 ± 3.3**	6.4 ± 1.7**
Dermis	2.5 ± 0.4	3.6 ± 2.0	2.6 ± 0.1	19.4 ± 4.9**	4.6 ± 1.6 *

Table 3-1 AdoMetDC activity in the skin of AdoMetDC/tTA mice.

Epidermis and dermis were harvested from 7-week-old wt, K5-tTA (tTA), TetO-AdoMetDC (AdoMetDC) single transgenic and AdoMetDC/tTA bitransgenic mice from lines A and B. AdoMetDC activity (mean ± S.D., pmol/mg protein per 30 min) was measured using a standard assay. Group sizes are indicated in parenthesis. *P<0.05, ** P<0.005 vs. wild type controls.

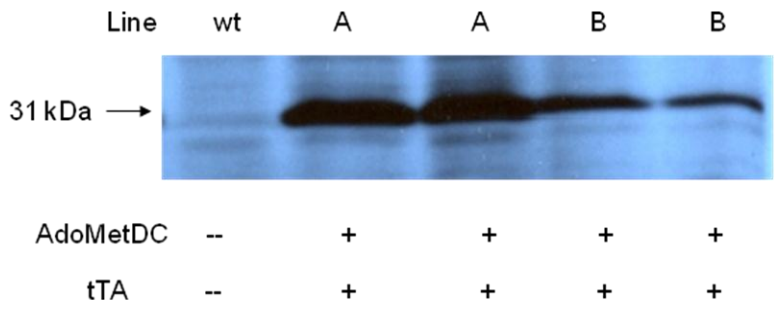

Fig. 3-3 AdoMetDC protein in the skin of AdoMetDC/tTA mice.

50 µg of dermal protein extract were analyzed by Western blotting using an antibody recognizing the HA epitope of transgene derived AdoMetDC protein (31 kDa).

Tissue specificity and regulation of transgene expression

The tet-regulated system is expected to provide tissue-specific and regulated transgene expression. To evaluate tissue specificity, luciferase activity in tissues where the K5 promoter is active (K5 tissues, including epidermis, dermis, tongue, thymus, forestomach, mammary gland) and non-K5 tissues (liver, brain, kidney, lung, heart, skeletal muscle) was measured in 7-week-old mice from line A (**Fig. 3-4**). Luciferase was expressed abundantly (> 10^5 relative luciferase units (RLU)/μg protein)) in all the K5 tissues, while minimally (< 300 RLU/μg protein) expressed in non-K5 tissues in bitransgenic mice and single transgenic TetO-AdoMetDC mice**.** K5 tissues of mice from line B were also assayed for luciferase activity and similar results were obtained with less luciferase activities in bitrangenic mice (**Fig. 3-5**).

To analyze Dox regulation of transgene expression, a time course of luciferase suppression by Dox administration and reactivation with Dox withdrawal was done by *in vivo* imaging on two bitransgenic mice from line A (**Fig. 3-6**). Upon Dox treatment, a rapid decrease in luciferase signal was observed and there was little signal after one week of treatment. Switching back to normal chow led to a quick recovery of luciferase signal in the first week and then a slow increase afterwards. Regulation by Dox was also studied in 7-week-old mice that were put on Dox from the day after birth. Epidermal and dermal luciferase activity was minimal (≤ 50 RLU/μg protein) in those Dox-treated bitrangenic mice (**Table 3-2**), also they did not show thin fur as observed in untreated bitrangenic mice (will be discussed more later in this part), which indicate that the thin fur phenotype is caused by transgene expression in the skin and Dox treatment can shut down the expression and eliminate the phenotype.

Our results demonstrate that in bitransgenic mice from line A, transgene expression is tissue specific, and silenced by Dox treatment promptly and reactivated by removing Dox. Along with previous results that line A had the highest levels of transgene expression and minimal leakiness in AdoMetDC single transgenic mice, line A was considered the optimal line and all subsequent studies utilized progeny of line A unless noted.

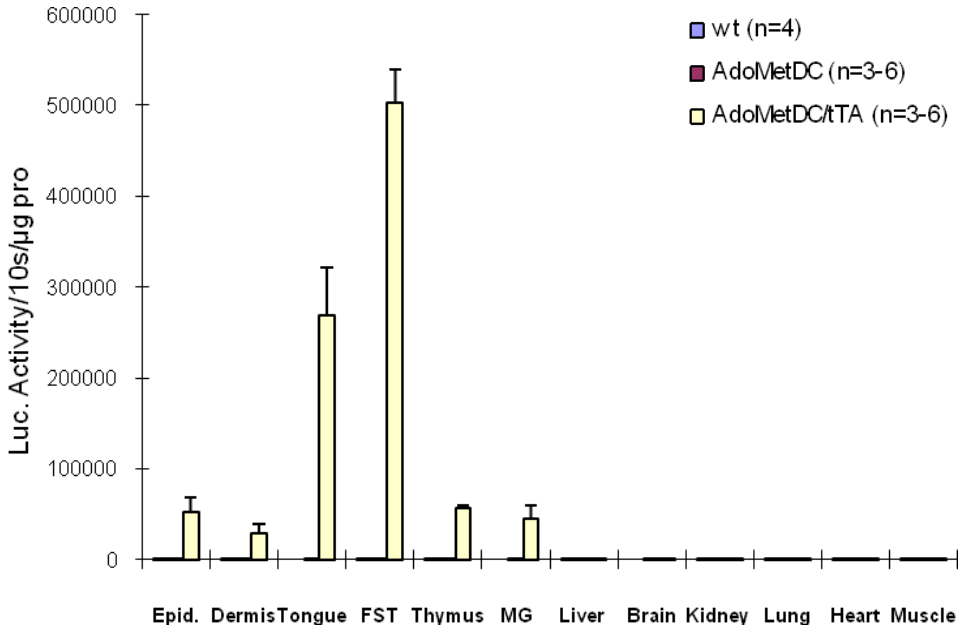

Fig. 3-4 Luciferase activity in K5 and non-K5 tissues of AdoMetDC/tTA mice (line A).

Tissue extract from 7-week-old wt, AdoMetDC single transgenic and AdoMetDC/tTA bitransgenic mice from line A were assayed for *in vitro* luciferase activity. Group sizes are indicated in parenthesis. Epid., epidermis; FST, forestomach; MG, mammary gland.

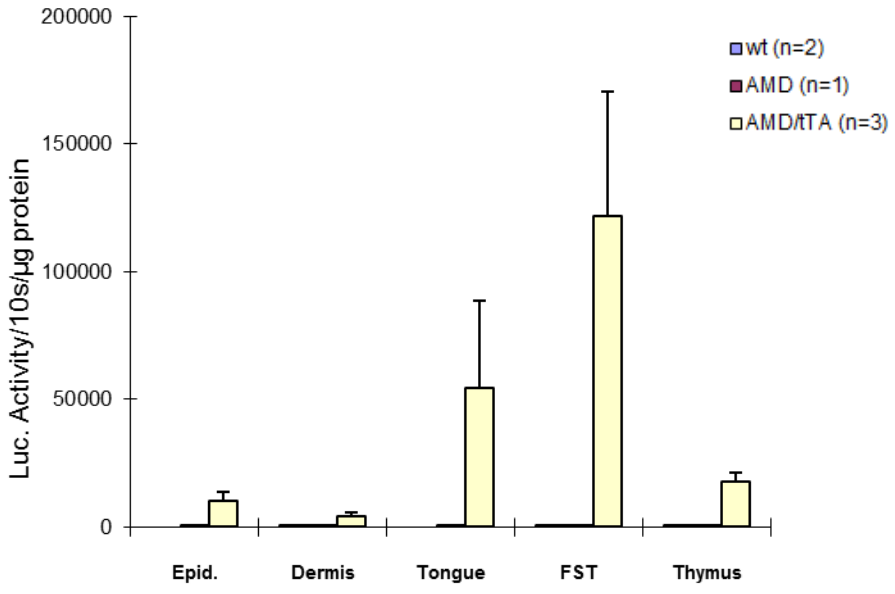

Fig. 3-5 Luciferase activity in K5 tissues of AdoMetDC/tTA mice (line B).

Tissue extract from 7-week-old wt, AdoMetDC single transgenic and AdoMetDC/tTA bitransgenic mice from line B were assayed for *in vitro* luciferase activity. Group sizes are indicated in parenthesis. Epid., epidermis; FST, forestomach.

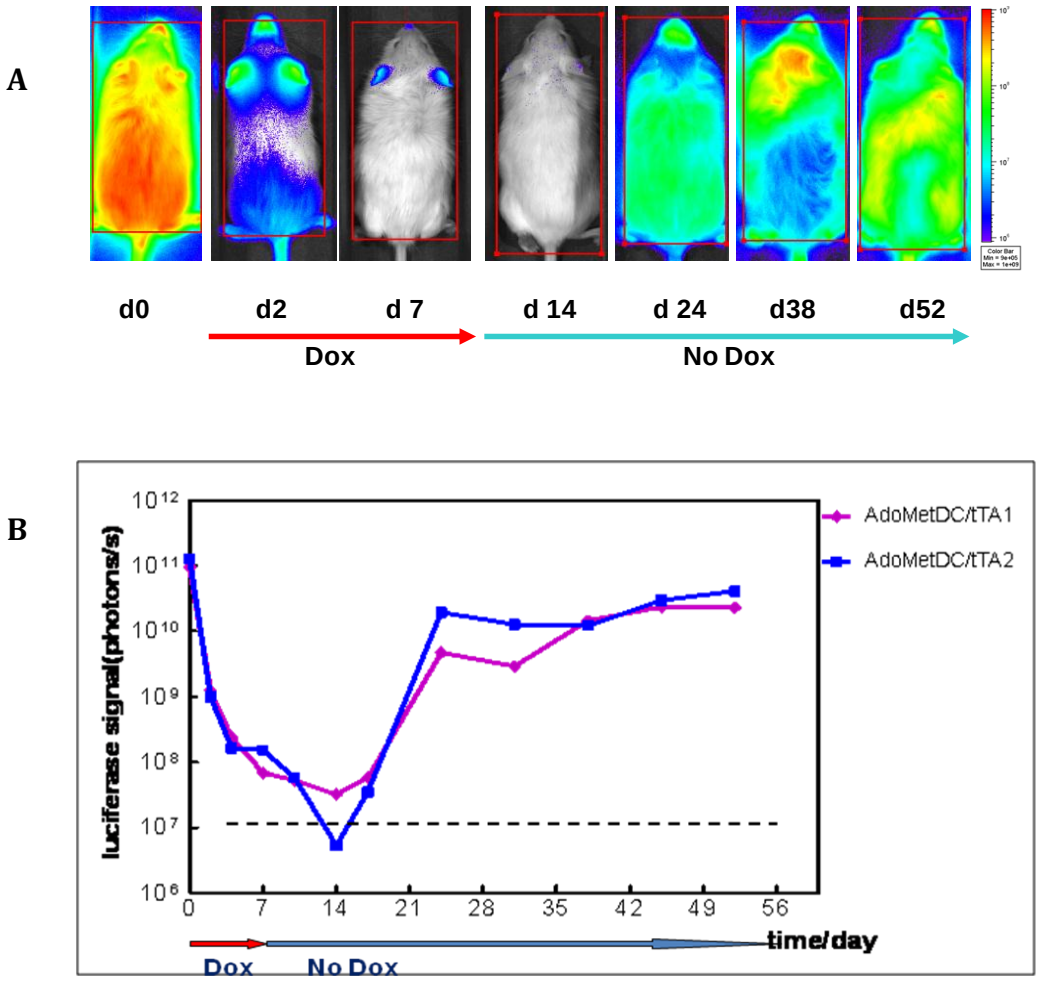

Fig. 3-6 Dox regulation of transgene expression in AdoMetDC/tTA mice.

5-week-old AdoMetDC/tTA mice from line A were put on a diet containing 2g/kg Dox for 7 days and *in vivo* imaging was done at d0 to d7. Mice were then switched to normal chow and images were taken at d10 to d52**.** ***A***, *In vivo* imaging pictures of a bitransgenic mouse at different time points. Boxes indicate the region that was quantified and plotted in **B.** ***B***, Quantification of *in vivo* luciferase signal. Each line represents an individual bitransgenic mouse. The gray dashed line indicates the background signal level of wt mice.

Tissue	wt (n=3)	tTA (n=4)	AdoMetDC (n=3)	AdoMetDC/tTA (n=4)
Epidermis	4 ± 5	3 ± 5	2 ± 1	31 ± 19
Dermis	1 ± 1	0 ± 0	2 ± 2	12 ± 7

Table 3-2 Luciferase activity in skin extracts of Dox-treated AdoMetDC/tTA mice.

Epidermis and dermis were harvested from 7-week-old wt, K5-tTA (tTA), TetO-AdoMetDC (AdoMetDC) single transgenic and AdoMetDC/tTA bitransgenic mice from lines A that were put on a diet containing 2g/kg Dox from the day after birth. Luciferase activity (mean ± S.D., RLU/μg protein) was measured. Group sizes are indicated in parenthesis.

Alterations in AdoMet/dcAdoMet levels

The decarboxylation reaction catalyzed by AdoMetDC forms the aminopropyl donor dcAdoMet from AdoMet. Therefore, the impact of AdoMetDC overexpression on skin AdoMet/dcAdoMet content was measured in dermis of AdoMetDC/tTA mice and controls at 7 weeks of age (this was not done in epidermis because there was not enough tissue for the measurement). As shown in Table 3-3, dcAdoMet levels rose by 8-fold, which is similar to the fold increase (7.8-fold) in AdoMetDC activity in dermis (**Table 3-1**). AdoMet level was also increased by 2.4-fold in the dermis of bitransgenic mice.

	wt (n=4)	tTA (n=4)	AdoMetDC (n=3)	AdoMetDC /tTA (n=4-6)
AdoMet	2.79 ± 0.79	3.93 ± 1.17	2.57 ± 0.26	6.67 ± 1.49**
dcAdoMet	0.024 ± 0.008	0.028 ± 0.015	0.043 ± 0.015	0.193 ± 0.079*

Table 3-3 AdoMet and dcAdoMet content in AdoMetDC/tTA mice.

7-week-old wt, tTA, AdoMetDC single transgenic and AdoMetDC/tTA bitransgenic mice from line A were sacrificed, and AdoMet and dcAdoMet content (mean ± S.D., pmol/mg tissue) was measured in dermal extracts using high performance liquid chromatography (HPLC). Group sizes are indicated in parenthesis. *P<0.05, * * P<0.005 vs. wild type controls.

Characterization of thin fur phenotype in AdoMetDC/tTA mice

It was mentioned earlier that the AdoMetDC/tTA bitransgenic mice from lines A and B exhibited a thin fur phenotype. This could be detected as soon as mice began to develop fur and retained for at least 2 years (**Fig. 3-7A**). When newborn pups were treated with Dox from the day of birth, the thin fur phenotype was not apparent through 7 weeks of age (**Fig. 3-7B**), which indicated that the thin fur phenotype was due to transgene overexpression in the skin.

To further investigate this phenotype, we conducted histological analysis of hair follicle morphogenesis in 1 day old pups and hair follicle cycling on adult mice treated with or without Dox.

We scored hair follicle morphogenesis stage by established criteria (Paus et al., 1999), and our result shows there was no difference between any of the four genotype groups for scores of hair follicle morphogenesis stage in 1 day old mouse skin (**Fig. 3-8**). So the thin fur phenotype is not caused by altered morphogenesis. We also measured polyamine content in whole skin extract of these newborn pups and saw a decrease in putrescine ($p<0.05$), a trend of increase in spermine levels, and increased Spm/Spd ratio ($p<0.05$) in AdoMetDC/tTA mice compared to control groups (**Table 3-4**).

We then analyzed hair follicle cycling in a number of 7-9 week old mice without Dox treatment. While all the wt and AdoMetDC single transgenic mice were in a resting phase (telogen) of hair follicle growth, all the AdoMetDC/tTA mice and more than half of the tTA mice were in the growth phase (anagen) (**Fig. 3-9**). It is known that anagen hair follicles have high ODC activity and elevated polyamine levels (Probst and Krebs, 1975; Sundberg et al., 1994a). This observation could explain the elevated polyamine content

we measured in dermis of 7-week-old mice (**Table 3-5**). AdoMetDC/tTA mice had a large increase in all of the three polyamine levels. Two of the four tTA mice also showed highly increased polyamine levels compared to wt and single AdoMetDC controls, which accounted for the large variability in the tTA group. So it is very likely that the increase in polyamines is caused by anagen hair follicles rather than being caused directly by transgene expression. When mice were treated with Dox since the day after birth, some of the AdoMetDC/tTA mice and tTA mice (7-week-old) still had anagen hair follicles. From the above, we concluded that the altered hair follicle cycling is caused by both tTA transgene and AdoMetDC overexpression. It is not so surprising to us that tTA single transgenic mice did not behave like wt mice, because during our course of studies, another group who used the same tTA mouse line found that those mice were more resistant to skin chemical carcinogenesis than wt mice and Dox treatment did not affect tumor counts over time (Rozenberg et al., 2009).

A

B

Fig. 3-7 Thin fur phenotype exhibited by AdoMetDC/tTA mice.

A, Bitransgenic mice (indicated by arrow) exhibit thinner fur than their wild type (wt) and single transgenic littermates. Left, 10 day old pups without Dox treatment; Right, 6 month old mice without Dox treatment. ***B***, A nursing female was put on a diet containing 2g/kg Dox on the day of delivery. The pups shown were 10 days old as in ***A***. Two bitransgenic mice (identified by PCR at weaning) in this litter are indistinguishable from wt and single transgenic littermates.

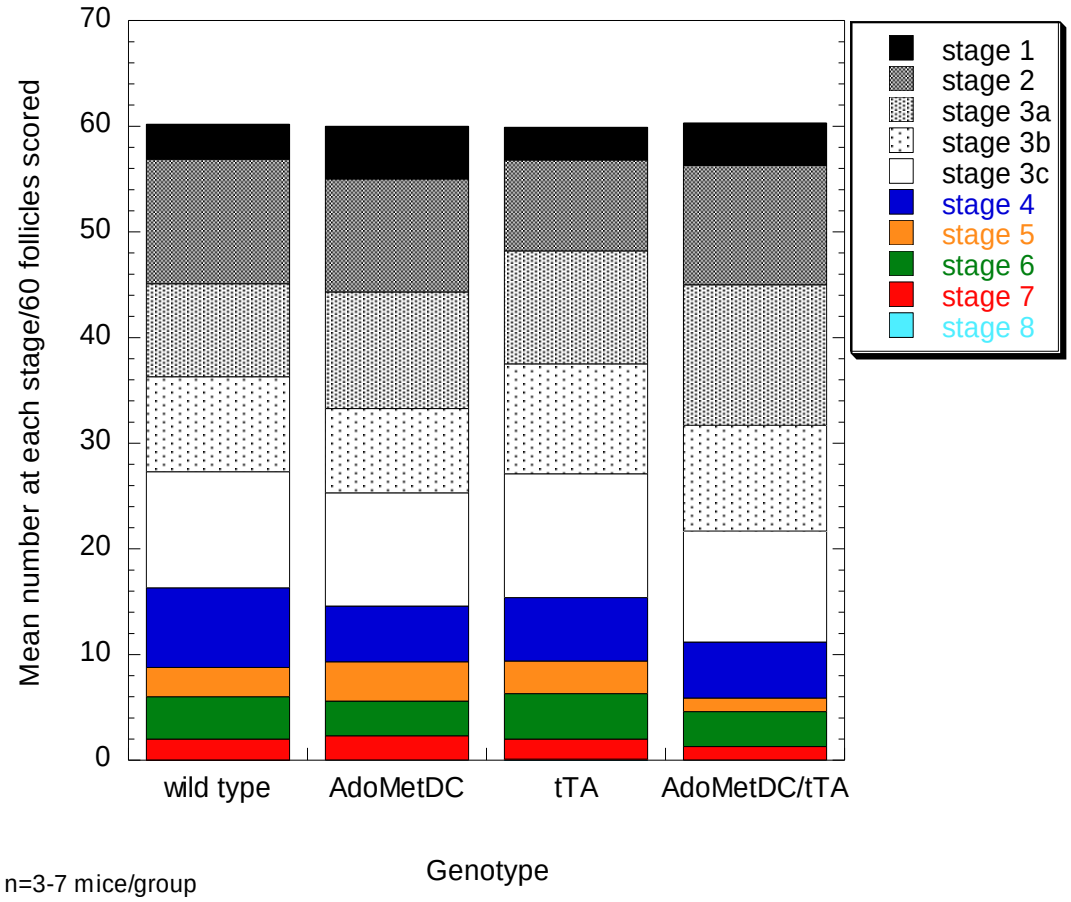

Fig. 3-8 Hair follicle morphogenesis stages in 1-day-old mice.

Histological sections of dorsal skin from 1-day-old wt, tTA, AdoMetDC single transgenic and AdoMetDC/tTA bitransgenic mice were assessed for morphogenesis stages by established criteria (Paus et al., 1999). Totally 60 follicles were counted for each mouse in each group (n=3-7 mice/group). The height of the bars represents the average number of hair follicles per mouse at each of the stages for all four genotypes.

A **B**

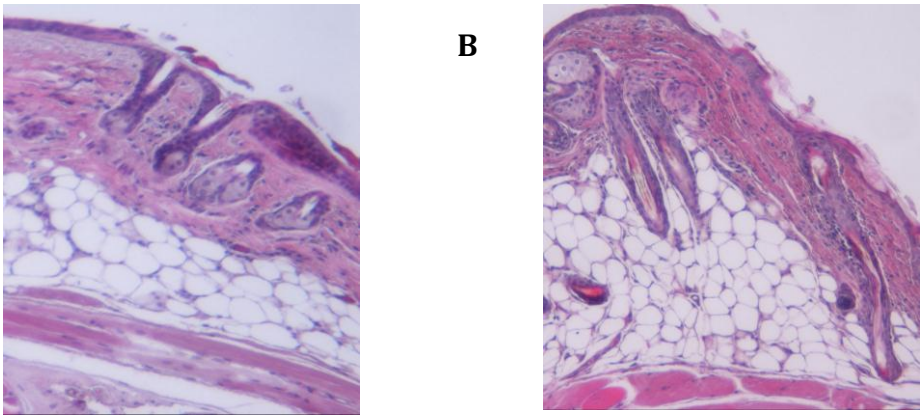

Fig. 3-9 Hair follicle histology in wt and AdoMetDC/tTA mice

A, Skin histology with H & E staining. 7- week-old wt mice are in a resting phase (telogen) of hair follicle growth. ***B***, Skin histology with H & E staining. 7-week-old AdoMetDC/tTA mice are in growth phase (anagen) of hair follicle growth.

Group	Polyamine content (nmol/mg protein)			
	Putrescine	Spermidine	Spermine	Spm:Spd ratio
wt (n=3)	6.7 ± 0.4	22.4 ± 2.2	7.4 ± 0.7	0.33 ± 0.01
AdoMetDC(n=3)	7.7 ± 0.7	26.8 ± 0.6	8.6 ± 0.3	0.32 ± 0.01
tTA(n=5)	5.7 ± 0.8	22.4 ± 2.5	7.5 ± 1.1	0.34 ± 0.01
AdoMetDC/tTA (n=4)	3.4 ± 0.9 **	23.8 ± 7.3	11.3 ± 3.2	0.47 ± 0.02**

Table 3-4 Polyamine content in 1-day-old AdoMetDC/tTA mice.

Polyamine content (mean ± S.D.) was determined in whole skin of 1-day-old mice (number of animals in parentheses) and normalized to tissue protein content. **$p<0.005$ vs. wild type and tTA controls.

Group	Polyamine content (pmol/mg tissue)			
	Putrescine	Spermidine	Spermine	Spm:Spd
wt (n=4)	19 ± 12	194 ± 65	149 ± 62	0.8 ± 0.1
AdoMetDC(n=3)	28 ± 2	208 ± 3	177 ± 4	0.8 ± 0.0
tTA(n=4)	172 ± 141	460 ± 172	272 ± 51*	0.7 ± 0.2
AdoMetDC/tTA (n=9)	171 ± 76 **	614 ± 178**	375 ± 128*	0.6 ± 0.1*

Table 3-5 Polyamine content in 7-week-old AdoMetDC/tTA mice.

Polyamine content (mean ± S.D.) was determined in dermis of 7-week-old mice (number of animals in parentheses). *$p<0.05$, **$p<0.005$ vs. wild type controls.

DISCUSSION

We have established a novel transgenic mouse model with tissue-specific and Dox-regulated expression of AdoMetDC enzyme from the combination of a K5-tTA founder line and a TetO-AdoMetDC founder line. Transgene expression is targeted to skin basal keratinocytes of the interfollicular epidermis (IFE) and hair follicle outer root sheath (ORS) as well as other stratified epithelia where the K5 promoter is active (Ramirez et al., 1994). The two regions within the skin are where the interfollicular stem cell niche and follicular stem cell niche reside. Both of the niches are considered to be the origins of initiated cells in skin carcinogenesis (Box et al., 2010; Fuchs, 2009; Gerdes and Yuspa, 2005).

In our mouse model, AdoMetDC is constitutively expressed in the skin and expression can be repressed by exposure to Dox. Untreated AdoMetDC/tTA mice generated from one founder line display a massive increase in *in vivo* and *in vitro* luciferase activity, a 7 to 8-fold increase in AdoMetDC activity in epidermis and dermis at 7 weeks of age, and a corresponding increase in the enzymatic product dcAdoMet levels. Minimal transgene expression is detected in either single transgenic AdoMetDC or Dox-treated bitransgenic mice. AdoMetDC/tTA mice also exhibited a thin fur phenotype that could be eliminated by Dox treatment.

Since the transgene is only expressed in a small portion of skin cell populations, and the biochemical measurements of AdoMetDC transgene expression and the enzymatic product dcAdoMet levels were performed in epidermal and/or dermal tissue extracts, the results could not truly reflect the changes within targeted cells. Intracellular AdoMetDC activity, protein and dcAdoMet levels might be much higher in targeted cells.

In AdoMetDC/tTA mice, AdoMetDC expression can be repressed rapidly and completely by exposure to Dox. However, it is worthy to note that transgene reactivation took a relatively longer time after Dox withdrawal and this might be due to the slow elimination of Dox. Besides the thin fur phenotype caused by transgene overexpression in the skin, AdoMetDC/tTA mice also had slightly squinted eyes, and this might be due to the fact that the transgene was also expressed in corneal epithelium. We do not observe any adverse effects on mouse development caused by this eye phenotype and we do not believe it affects our assay results or our future skin carcinogenesis study.

It is our hypothesis that AdoMetDC overexpression in the skin of transgenic mice will reduce the level of putrescine. We saw highly increased levels of all three polyamines in dermis of 7-week-old AdoMetDC/tTA mice and some tTA mice. However, these changes may be due to the anagen hair follicle rather than direct effect of AdoMetDC overexpression. Polyamine content in whole skin extract of 1-day-old AdoMetDC/tTA pups showed a decrease in putrescine level, and an increase in Spm/Spd ratio, which is in agreement with our hypothesis.

7 to 9-week old mice are typically used for skin carcinogenesis study since their hair follicles are usually in the telogen phase at this age. In our AdoMetDC/tTA mice and some tTA mice hair follicles were at anagen phase between 7 to 9 weeks of age, and Dox treatment could not correct the alteration in hair follicle cycling caused by tTA transgene. This effect of tTA may be caused by tTA transgene integration or may be secondary to tTA protein expression. It is known that anagen hair follicles are more sensitive to carcinogen initiation than telogen hair follicles (Miller et al., 1993). Based on these findings, we decided to initiate 1-day-old pups which showed no difference in hair

follicle morphogenesis between each genotype for our skin chemical carcinogenesis study (Chapter V). This is feasible since the genetic changes caused by DMBA initiation persist throughout the life span of the animal (Stenback et al., 1981).

This unique mouse model will allow us to evaluate the ability of AdoMetDC to control polyamine levels *in vivo* and further elucidate the role of polyamines in skin carcinogenesis. The tet-regulated system will enable temporal manipulation of polyamine content in specific keratinocyte populations and permit the study of polyamine functions at different stages of skin carcinogenesis.

Chapter IV

Evaluation of the effects of AdoMetDC overexpression on mouse skin response to short term TPA treatment

INTRODUCTION

In the DMBA/TPA mouse skin carcinogenesis model, repeated topical TPA applications lead to morphological changes characterized by sustained epidermal hyperplasia, which eventually allows the initiated stem cells to undergo selective clonal expansion to form benign papillomas. Short-term histological changes of tumor promotion include increased epidermal thickness, proliferation of basal keratinocytes and dermal inflammation. Those changes caused by TPA are believed to result from epigenetic mechanisms involving activation of protein kinase C (reviewed in (Abel et al., 2009; Angel and DiGiovanni, 1999; DiGiovanni, 1992; Yuspa, 1994, 1998)).

It has been well established that TPA treatment highly induces ODC activity and causes polyamine accumulation, which are essential for tumor promotion ((O'Brien et al., 1975b; Peralta Soler et al., 1998); reviewed in (Gerner and Meyskens, 2004; Pegg et al., 2003)). Besides ODC induction, TPA treatment also induces AdoMetDC activity, but to a lesser extent and in a more prolonged manner (O'Brien, 1976a; O'Brien et al., 1975b; Yuspa et al., 1976). So far, the molecular mechanism by which polyamines promote skin tumor development is unclear.

In our TetO-AdoMetDC/tTA mice, AdoMetDC overexpression in specific skin cell populations might alter the response to TPA promotion. To investigate the effects, we conducted a set of studies with single or multiple applications of TPA. This chapter details these studies on TPA-mediated ODC and AdoMetDC induction, skin cellular

proliferation, epidermal hyperplasia and alterations in polyamine levels in AdoMetDC/tTA mice.

MATERIALS AND METHODS

Maintenance, expansion and identification of transgenic mice

Transgenic mice were housed together with normal littermates under conditions as described in Chapter III. The transgenic line was expanded by breeding AdoMetDC mice with tTA mice identified in the progeny to produce equal numbers of AdoMetDC/tTA bitransgenic, AdoMetDC single transgenic, tTA single transgenic and wild type littermate controls for experiments. Mice were genotyped for both transgenes by PCR as described in Chapter III. The number and age of the mice are indicated in the figure legend for each experiment. All the numbers represent a group including both male and female mice and no sex-dependent differences were observed.

TPA treatment and skin sample collection

An area of posterior dorsal skin (approx. 2.5 x 2.5 cm) was shaved at 7-8 weeks of age with surgical clippers, and 6.8 nmol of TPA (Calbiochem-Novabiochem Corp., La Jolla, CA) in 200 µl of acetone was applied 16–24 h later. For multiple applications of TPA, mice were treated twice weekly for two weeks with 3 to 4-day intervals. Control groups were treated in the same manner with an equal volume of acetone. Mice with obvious wounds or abrasions in the shaved area were not treated and were eliminated from the experiment. Mice were sacrificed at the indicated time after TPA/acetone application, and treated skin was separated into epidermal and dermal fractions as described in Chapter

III, flash frozen in liquid nitrogen and stored at −80°C for biochemical analysis to measure enzyme activity and/or polyamine levels.

ODC, AdoMetDC enzymatic activity assays and polyamine measurement

To measure ODC activity, epidermal and dermal tissues were thawed on ice and then resuspended in ice-cold ODC harvesting buffer (25 mM Tris-HCl (pH 7.5), 2.5 mM dithiothreitol, 0.1 mM EDTA, 1x protease inhibitor cocktail (Calbiochem, La Jolla, CA), and 0.01% Tween 80). Epidermis was lysed by sonication, dermis was homogenized using a Polytron and tissue protein extracts were prepared in the same way as described for AdoMetDC activity assay in Chapter III. ODC activity was assayed in duplicate for each sample by measuring the release of $^{14}CO_2$ from L-[1-^{14}C] Ornithine (57.1 mCi/mmol; NEN Life Science Products, Boston, MA) as described previously (Coleman and Pegg, 1998). Protein concentration was determined using the Bio-Rad dye reagent (Bio-Rad Laboratories, Hercules, CA) with BSA as a standard. AdoMetDC activity in epidermal and dermal tissues was assayed as described in Chapter III. For polyamine measurement, epidermal and dermal tissues were collected one day (for 4x TPA treatment) after the final TPA application, extracted in 10% trichloroacetic acid and analyzed by reverse phase HPLC analysis as described in Chapter III with results normalized to tissue wet weight.

ODC western blotting

Cytosolic proteins (50 µg) in ODC buffer were fractionated by 15% SDS-PAGE, transferred to PVDF membrane, and ODC protein was detected by western blotting using a purified rabbit polyclonal antibody against mouse ODC (Shantz and Pegg, 1998).

Signals were visualized with a chemiluminescence detection system (Cell Signaling Technology, Beverly, MA).

Histological analysis and immunohistochemistry

Dorsal skin samples were collected 17 hours (for 1x TPA) or 1 day (for 4x TPA) after TPA application, fixed 4 hours in 10% neutral buffered formalin, and embedded in paraffin. 5 μm serial sections were cut and one section was stained with H&E.

To evaluate cell proliferation rate, mice were injected with 5-bromo-2'-deoxyuridine (BrdU, i.p. 100 μg/g body weight in 0.9% NaCl) (Sigma, St. Louis, MO) 1h before sacrifice. Immunohistochemistry for BrdU was performed as described previously (Feith et al., 2006) using the peroxidase-conjugated mouse monoclonal anti-BrdU Fab fragments (Roche, Indianapolis, IN) and BrdU staining was visualized with DAB and hematoxylin counterstain. Labeling index for BrdU was calculated by dividing labeled nuclei by the total number of interfollicular epidermal basal cells counted in the section. Approximately 1000 total cells were counted in three random regions for each skin section with 3-4 mice per genotype group. For analysis of epidermal hyperplasia, epidermal thickness from the basal layer to the stratum corneum was measured at twelve random interfollicular sites for each H&E skin section with 3-4 mice per genotype group using a Nikon light microscope DS-L1 (Japan) equipped with an ocular micrometer. For each individual site, four vertical epidermal measurements were made and averaged.

Statistical analysis

All differences between wild type controls and transgenic mice were evaluated using the two-tailed, unpaired Student's *t* test.

RESULTS

Time course of TPA-stimulated ODC and AdoMetDC induction in wt mouse skin

Tumor promoter TPA treatment is known to highly induce ODC activity for a short period of time and also induce AdoMetDC activity in a more moderate and prolonged manner (O'Brien et al., 1975b). Prior to determination of TPA-stimulated ODC and AdoMetDC induction in transgenic mice, a pilot experiment was done to determine the peak time of enzyme induction in wild type FVB mice after a single TPA application. A dose 6.8 nmol of TPA that is known to induce a robust tumor response in FVB mice (Abel et al., 2009) was used. Following TPA treatment, ODC protein (ODC activity assay failed due to a reagent problem) and AdoMetDC activity was measured in epidermal extracts over a time course (ODC: 0h, 4h, 6h, 12h, 24 h; AdoMetDC: 0h, 6h, 12 h, 24 h, 48 h). The results are shown in **Fig. 4-1** and **Fig. 4-2**. There was a massive increase in ODC protein at 4 h and it was much less by 12 h after treatment. The AdoMetDC activity also increased after TPA treatment, reaching a peak (about 5-fold over that of control) at 12 h after treatment and slowly declining. Treatment with the acetone vehicle did not result in an induction of either ODC or AdoMetDC. Previous studies also showed that increases in dermal ODC and AdoMetDC activity follow the same time course as in epidermis but are of a lesser magnitude. For our study purpose, the time course of enzyme induction in dermis was left unmeasured. From this experiment, 4 h and 12 h after TPA treatment was considered the peak time of induction for ODC and AdoMetDC, respectively in wt FVB mice. These time points were chosen for the following experiments in transgenic animals.

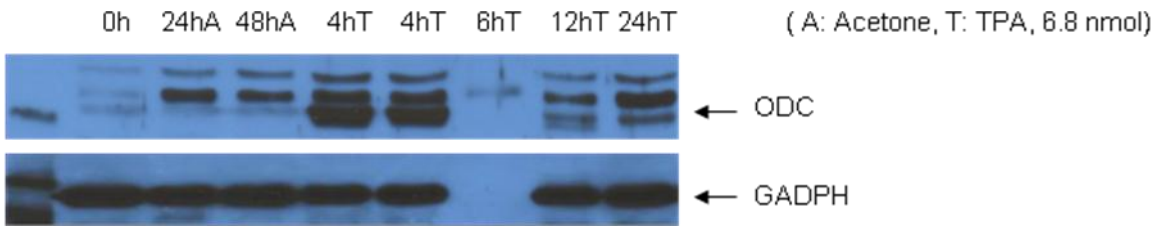

Fig. 4-1 Epidermal ODC protein in wt mice after a single application of TPA.

7 to 8 weeks old FVB mice were treated with a single dose of TPA (6.8 nmol) or acetone vehicle at time 0h and sacrificed at indicated time points after treatment (n=4 for each time point). ODC protein (51 kDa) was detected by Western blotting in representative epidermal samples with an ODC antibody as described in the Materials and Methods section. Blots were then re-probed for GAPDH as a loading control. *Note: The sample for 6h TPA was misloaded.*

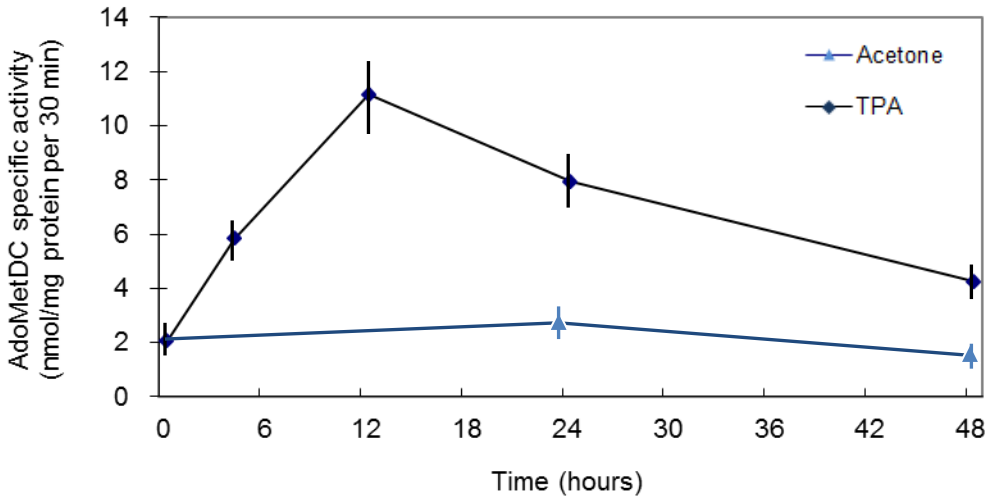

Fig. 4-2 Epidermal AdoMetDC activity in wt mice after a single application of TPA.

7 to 8 weeks old FVB mice were treated with a single dose of TPA (6.8 nmol) or acetone vehicle and sacrificed at indicated time points (0, 24, 48h for acetone, 0, 4, 12, 24, 48h for TPA) after treatment. AdoMetDC activity (mean ± SD, n=4) was assayed.

TPA induction of ODC and AdoMetDC activity in transgenic mouse skin

In the AdoMetDC/tTA transgenic mice, the K5 promoter directs AdoMetDC expression in the basal cell layer of the interfollicular epidermis and the outer root sheath of the hair follicle of the dermis in the absence of Dox. To evaluate the effects of AdoMetDC expression on TPA-stimulated enzyme induction in the skin, ODC and AdoMetDC activity were measured in transgenic mice and controls after a single acetone or TPA application. Skin tissues were isolated 4 h after TPA for ODC assay and 12 h after for AdoMetDC assay and the results are shown in **Fig. 4-3** and **Fig. 4-4**. The basal level of ODC activity (acetone-treated) was very low for each genotype group though it was slightly elevated in tTA and bitransgenic mice due to anagen hair follicles (confirmed by H&E). TPA applications caused a dramatic increase in the epidermal ODC activity at 4 h in wt and AdoMetDC single transgenic mice. Surprisingly, the increase was suppressed by more than 50% ($p<0.05$, **Fig. 4-3**) in epidermis of tTA single transgenic and AdoMetDC/tTA bitransgenic mice. As expected, dermal ODC activity was increased to a lesser extent for each group after TPA, but tTA and AdoMetDC/tTA mice still showed decreased ODC induction ($p<0.05$, **Fig. 4-3**) relative to wt and AdoMetDC mice. There was no difference in the levels of ODC induction in epidermis or dermis between tTA and AdoMetDC/tTA mice, so it is very likely that the reduced activity is related to the tTA transgene.

As for AdoMetDC activity, AdoMetDC/tTA mice exhibited the highest levels ($p<0.05$, **Fig. 4-4**) of basal AdoMetDC activity in the skin due to transgene expression. 12h after TPA treatment, though AdoMetDC activity was induced to a greater extent in wt, AdoMetDC and tTA groups than in AdoMetDC/tTA group, AdoMetDC/tTA mice still

had the highest levels of AdoMetDC activity ($p<0.05$, **Fig. 4-4**). Therefore, AdoMetDC activity in AdoMetDC/tTA mouse skin is constitutively elevated within a physiological range similar to the level induced transiently by TPA in wild type mouse skin.

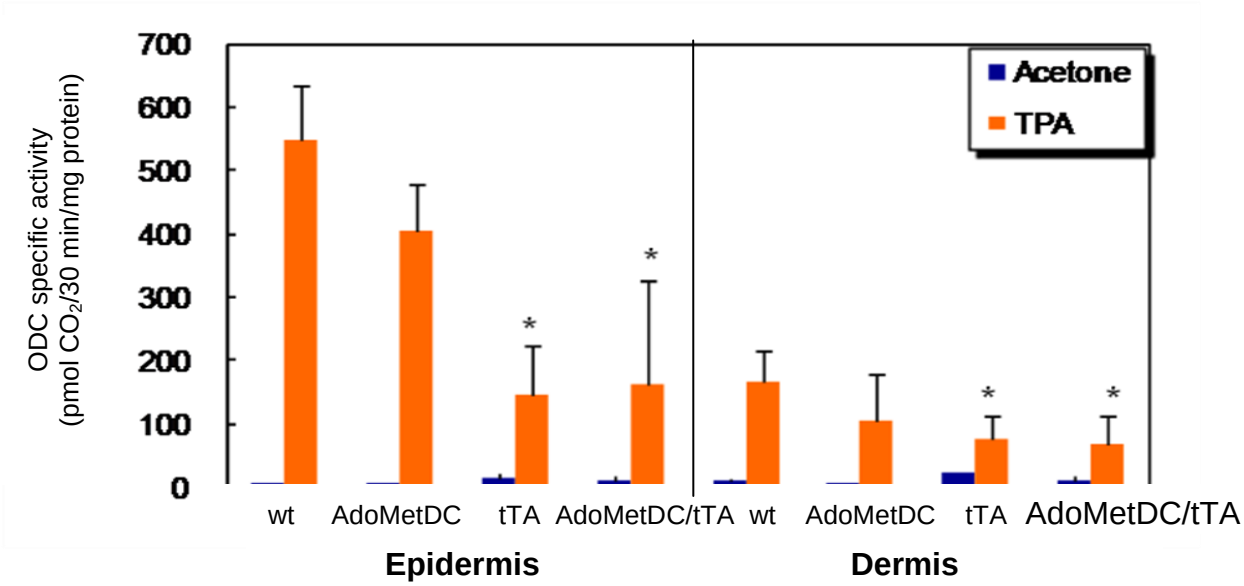

Fig. 4-3 Basal and TPA-induced ODC activity in epidermis and dermis of transgenic mice and controls.

7 to 8 weeks old mice were treated with a single dose of TPA (6.8 nmol) or acetone vehicle and sacrificed 4h later. ODC activity (mean ± SD, n=4) was measured in epidermal and dermal protein extracts. * $p<0.05$ vs TPA-treated wt.

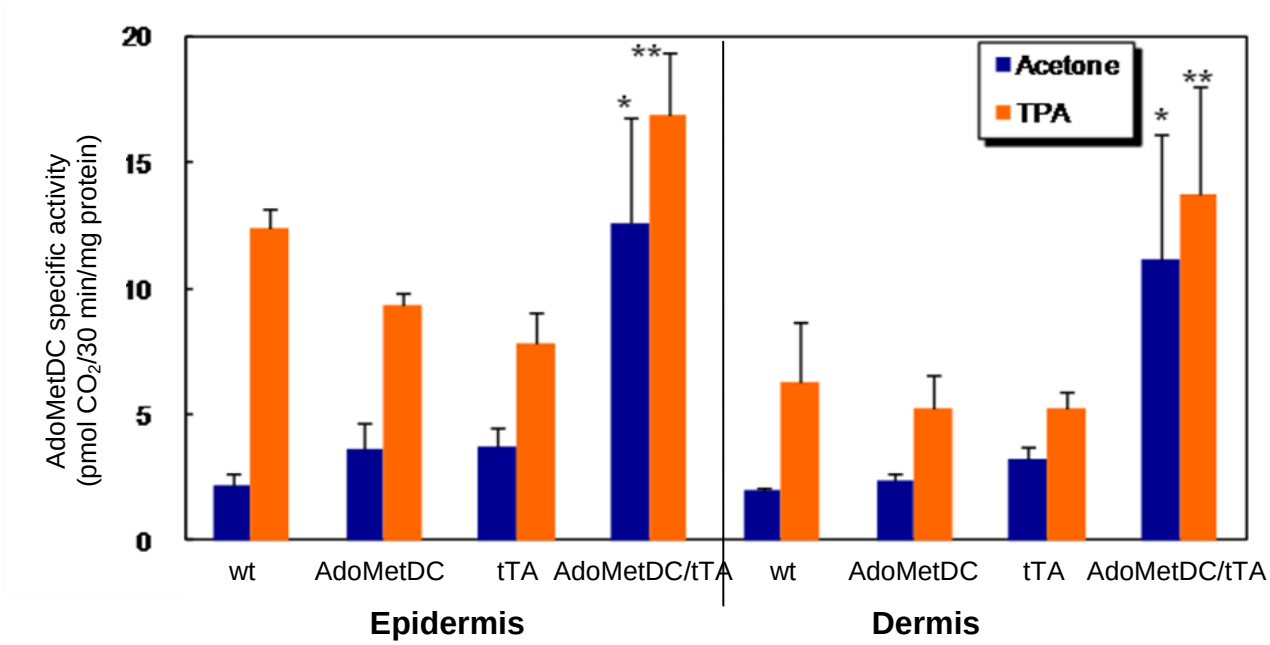

Fig. 4-4 Basal and TPA-induced AdoMetDC activity in epidermis and dermis of transgenic mice and controls.

7 to 8 weeks old mice were treated with a single dose of TPA (6.8 nmol) or acetone vehicle and sacrificed 12h later. AdoMetDC activity (mean ± SD, n=4) was measured in epidermal and dermal protein extracts. * $p<0.05$ vs acetone treated wt and tTA, ** $p<0.05$ vs TPA treated wt and tTA.

TPA-induced cell proliferation and epidermal hyperplasia in transgenic mice

To determine whether AdoMetDC expression would affect TPA-induced basal cell proliferation, skin sections were analyzed for BrdU incorporation after a single or multiple TPA (6.8 nmol) applications. Mice were injected with BrdU to label cells that were undergoing DNA synthesis (S phase), and the labeling index of the interfollicular epidermal basal cells was quantitated for each genotype. 17 h is the first peak of BrdU labeling after a single application of TPA (Chan et al., 2008). BrdU labeling index was similar in epidermis from wt (31.9% ± 12.0%) and AdoMetDC mice (31.7% ± 4.7%), and slightly reduced in AdoMetDC/tTA mice (26.8% ± 3.5%) and tTA mice (29.6% ± 3.1%), though the reduction was not statistically significant (**Fig. 4-5**). BrdU labeling index after 4x TPA applications (twice weekly for 2 weeks) in epidermis from AdoMetDC/tTA mice (18.4% ± 3.6%) was not significantly lower than in wt mice (20.8% ± 3.2%) either. The results indicate that AdoMetDC expression does not significantly alter skin basal cell proliferation rate after a single or multiple TPA treatments.

The effect of AdoMetDC expression on TPA-induced epidermal hyperplasia was analyzed by measuring epidermal thickness 24 h after 4x TPA applications (a single TPA application is not enough to induce a significant increase in epidermal thickness). Visual inspection of these sections revealed that AdoMetDC/tTA and tTA mice displayed reduced epidermal thickness compared with wt and AdoMetDC mice. Quantitative analysis of epidermal thickness for each genotype is shown in **Fig. 4-6B**. AdoMetDC/tTA and tTA mice exhibited statistically significant reductions (approximately 40% thinner) in epidermal thickness after 4x TPA compared to controls. There was no difference

between those two groups. Thus, the skins of AdoMetDC/tTA and tTA mice are hyposensitive to TPA-induced epidermal hyperplasia.

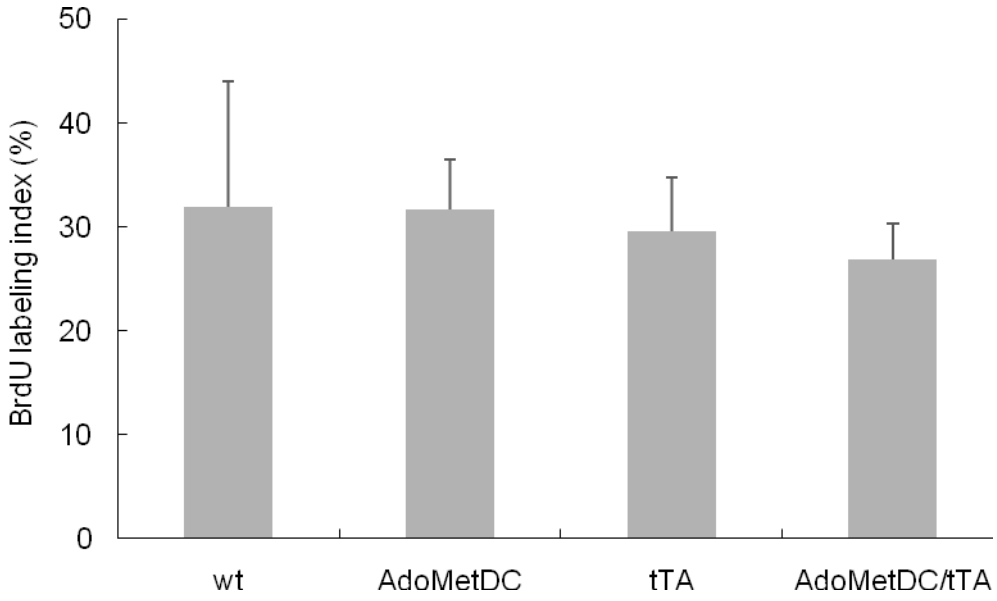

Fig. 4-5 TPA-induced basal cell proliferation in transgenic mice and controls after 1x TPA.

7 to 8 weeks old mice (n=3-4 /genotype group) were treated with a single dose of TPA (6.8 nmol) and sacrificed 17h later. Mice were injected with BrdU 1h prior to sacrifice, and skin sections were stained with an anti-BrdU antibody and analyzed for BrdU labeling index (mean ± SD) as described in the Materials and Methods section.

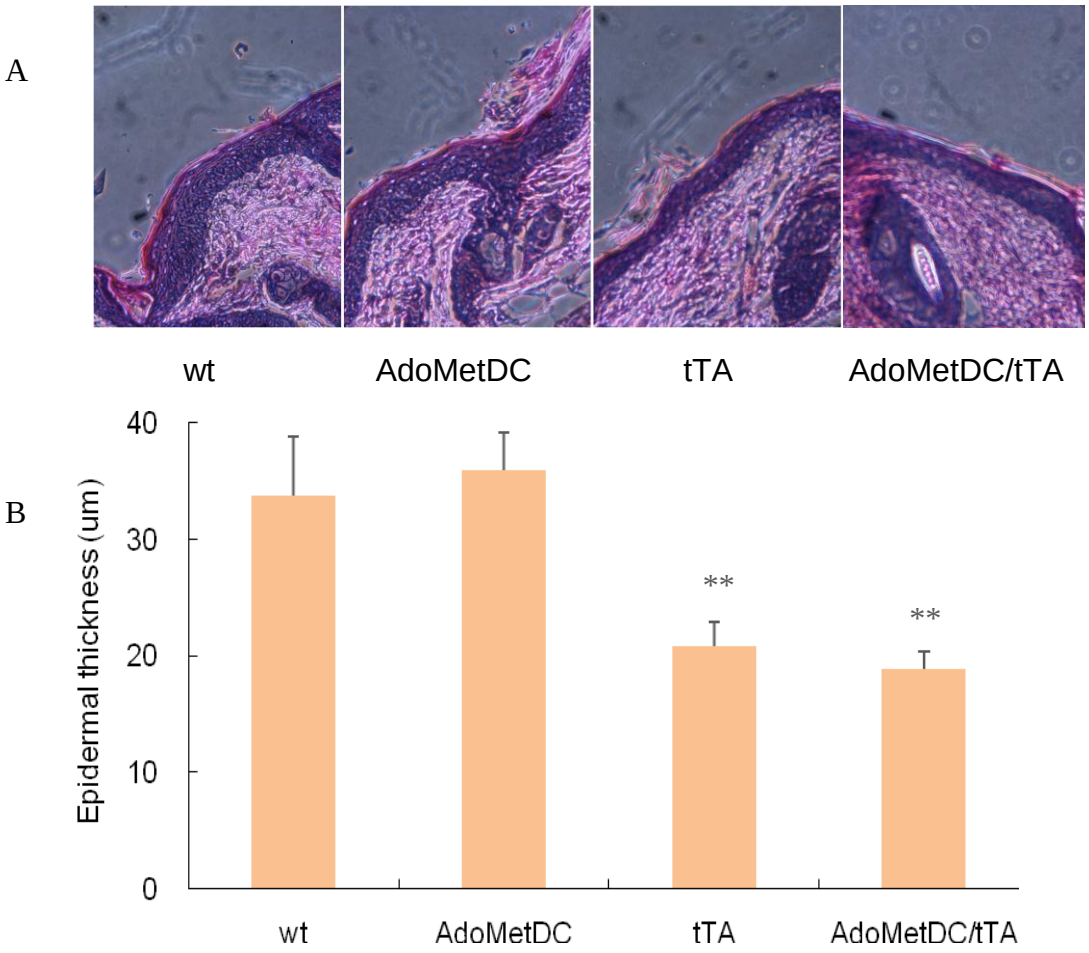

Fig. 4-6 Epidermal thickness in transgenic mice and controls after 4 x TPA.

7 to 8 weeks old mice (n=3-4 /genotype group) were treated with TPA (6.8 nmol) twice weekly for 2 weeks and sacrificed 24h after the last treatment. ***A***, Representative H&E-stained skin section from each genotype; ***B***, Quantification of epidermal thickness. Epidermal hyperplasia was analyzed by measuring epidermal thickness (mean ± SD) as described in the Materials and Methods section. **p<0.005 vs. wt controls.

Alterations in polyamine levels after 4x TPA in transgenic mice

TPA treatment induces the two decarboxylase activities in the skin and leads to polyamine accumulation. AdoMetDC transgene expression, along with altered enzyme induction by TPA as shown in **Figs. 4-3** and **4-4**, would cause alterations in polyamine levels. Mice treated with 4x TPA were analyzed 24h after the last treatment for polyamine content in epidermis and dermis. Compared with wt controls, epidermal putrescine levels in AdoMetDC/tTA mice were reduced by 67% ($p=0.06$) (**Fig. 4-7**). Although the reduction was not statistically significant, it agrees with our hypothesis that AdoMetDC expression in the skin decreases putrescine levels. There was also a slight decrease in spermidine and increase in spermine levels in AdoMetDC/tTA mice, and the Spm/Spd ratio was significantly increased ($p<0.05$) in the epidermis of AdoMetDC/tTA mice compared with wt controls. Dermal polyamine content in tTA and AdoMetDC mice is more difficult to interpret because it is affected by anagen (growth phase) hair follicles (hair follicle growth does not affect epidermal polyamine measurement) in addition to the TPA effect. The content of putrescine, spermidine, and spermine in the dermis of tTA mice was increased (by 36%, 27%, and 6%, respectively) relative to wt controls, however, only the increase in spermidine content was statistically significant. While spermidine and spermine levels in the dermis of AdoMetDC/tTA were increased (by 16% and 48%, respectively), putrescine levels were decreased (by 21%) compared with wt controls, which is different from untreated AdoMetDC/tTA mice that had large increases in all three polyamines in the dermis as shown in Chapter III Table 3-3. Taken together, these results suggest that AdoMetDC overexpression in the skin leads to a reduction in putrescine levels.

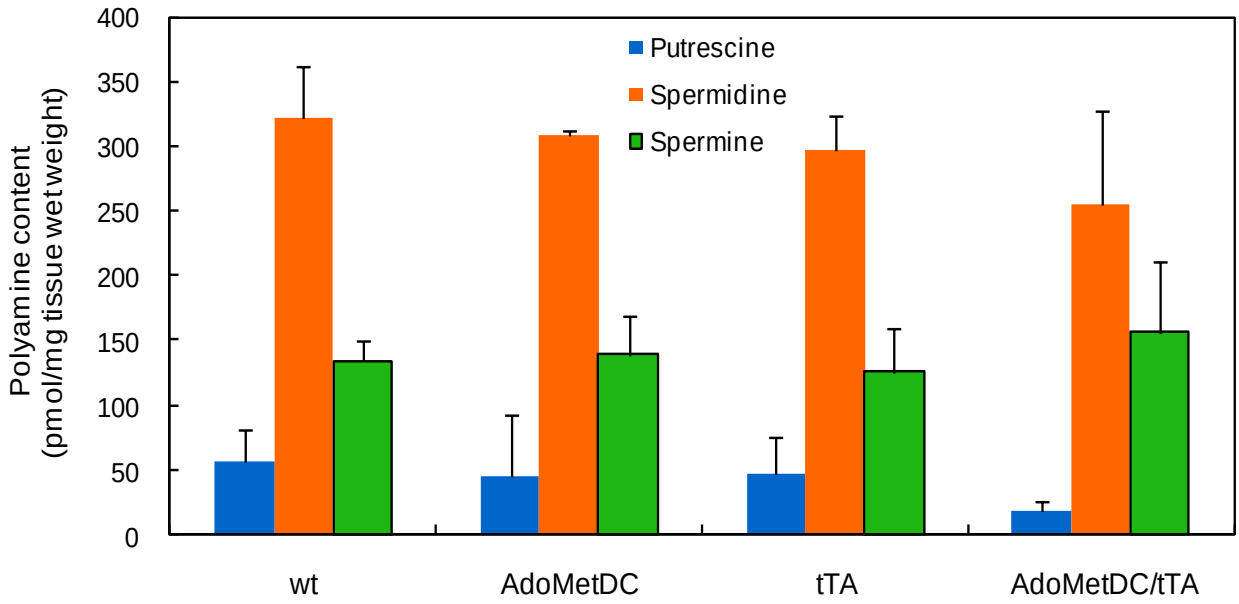

Fig. 4-7 Epidermal polyamine content 24 h after 4x TPA in transgenic mice and controls.

7 to 8 weeks old mice (n=3-4 /genotype group) were treated with TPA (6.8 nmol) twice weekly for 2 weeks and sacrificed 24h after the last treatment. Polyamine content (mean ± SD) was determined in the epidermis of transgenic mice and controls.

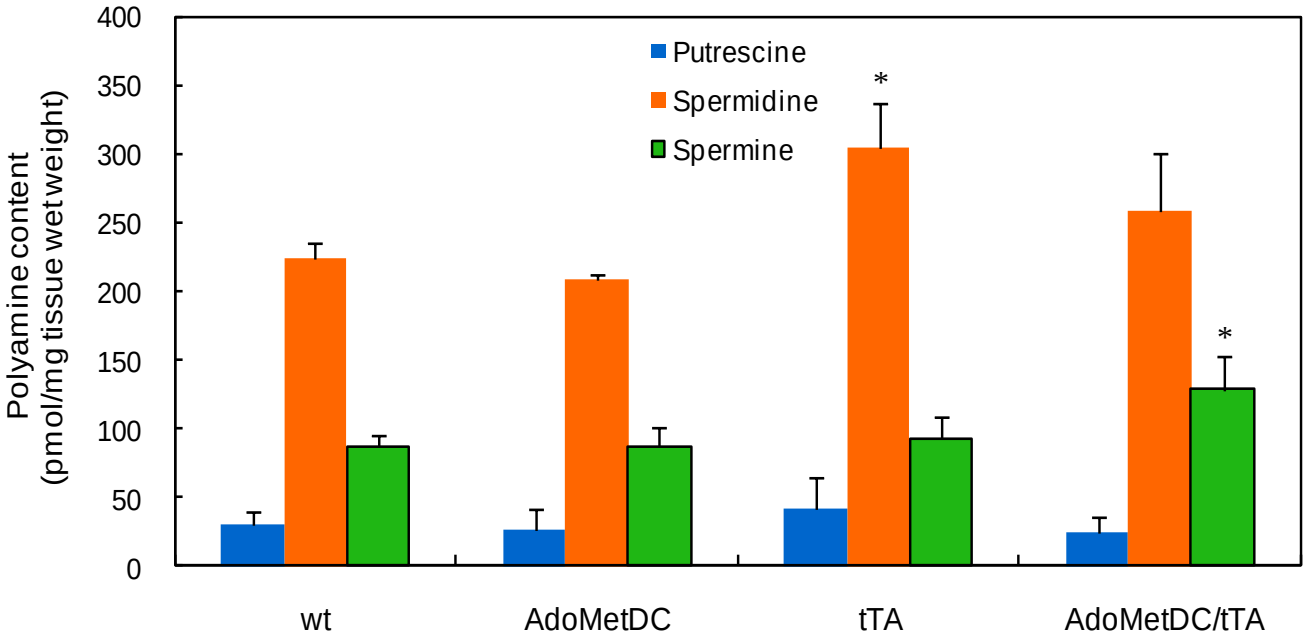

Fig. 4-8 Dermal polyamine content 24 h after 4x TPA in transgenic mice and controls.

7 to 8 weeks old mice (n=3-4 /genotype group) were treated with TPA (6.8 nmol) twice weekly for 2 weeks and sacrificed 24h after the last treatment. Polyamine content (mean ± SD) was determined in the dermis of transgenic mice and controls. *$p<0.05$ vs. wt controls.

DISCUSSION

The studies presented in this Chapter were designed to examine the effect of AdoMetDC overexpression on biochemical and histological changes caused by short-term TPA exposure that are closely related to tumor promotion. The results from these studies will provide information for the design of future DMBA/TPA carcinogenesis studies and predict whether and how AdoMetDC overexpression in transgenic mice affects the susceptibility to skin carcinogenesis. The changes we studied include the induction of the two polyamine biosynthetic enzymes ODC and AdoMetDC, polyamine accumulation and epidermal hyperplastic response following a single or multiple TPA applications.

ODC induction is considered to be essential in tumor promotion (Hayes et al., 2006; O'Brien, 1976a; Pegg et al., 2003). Numerous studies using a variety of transgenic (Feith et al., 2001; Feith et al., 2007) and pharmacologic (Takigawa et al. 1982) approaches have shown that inhibition of ODC induction by TPA is associated with reduced susceptibility to skin carcinogenesis. In our AdoMetDC/tTA mice, the induction of ODC activity 4 h after a single TPA (6.8 nmol) application was attenuated in both the epidermis and dermis compared with wt and single transgenic AdoMetDC mice. tTA mice also exhibited the same levels of reduction in TPA-induced ODC activity in both tissues (**Fig. 4-3**). Combined with what we have found and described in Chapter III that tTA mice showed altered hair follicle cycling that did not respond to Dox treatment (which indicates that the effect was not caused by tTA protein binding to DNA), we believe this effect on ODC induction is also caused by tTA transgene that is independent of AdoMetDC transgene expression. With decreased ODC induction, tTA mice would have decreased tumor susceptibility to DMBA/TPA skin carcinogenesis than wt controls,

which has been found in previous studies during the course of our studies (Rozenberg et al., 2009). The difference between AdoMetDC/tTA and tTA mice would be the effect caused by AdoMetDC transgene expression. In other words, tTA mice are the appropriate control for AdoMetDC/tTA mice in our studies to evaluate the effects of AdoMetDC expression on skin carcinogenesis in Chapter V.

As for TPA-stimulated AdoMetDC induction, we found that AdoMetDC/tTA mice exhibited elevated epidermal and dermal AdoMetDC activity 12 h after a single TPA treatment compared with control groups ($p<0.05$, **Fig. 4-4**). Since untreated (or acetone treated) AdoMetDC/tTA mice have higher levels of AdoMetDC activity in the epidermis and dermis due to transgene expression, AdoMetDC/tTA mouse skin therefore has constitutively elevated AdoMetDC activity within a physiological range similar to the level induced transiently by TPA in control mouse skin (O'Brien et al., 1975b).

Increased levels of polyamines, especially putrescine that result from ODC induction, are the real players in skin tumor promotion. We measured epidermal and dermal polyamine content 24 h after the last treatment of 4x TPA in AdoMetDC/tTA mice and control groups. The polyamine profile in epidermis of AdoMetDC/tTA mice did not show statistically significant alteration in any of the three polyamines. However, putrescine levels in the AdoMetDC/tTA mice did show more than 60% decrease relative to wt mice (**Fig. 4-7**), and a significant increase in Spm/Spd ratio, indicating that high AdoMetDC activity in the skin may act to lower putrescine levels to promote higher polyamine synthesis. ODC activity and polyamine synthesis are known to be up-regulated in anagen (growth phase) hair follicles and down-regulated in telogen (resting phase) hair follicles (Probst and Krebs, 1975; Sundberg et al., 1994b). All of the

AdoMetDC/tTA mice and more than half of the tTA mice used in this experiment had anagen hair follicles, and since the hair follicles are located mostly in dermis, the overall increased dermal polyamine content in AdoMetDC/tTA and tTA mice could be explained by those growing hair follicles.

It is worthwhile to point out again that AdoMetDC transgene is expressed only in very limited cell populations within the skin that include the target stem cells initiated and promoted by chemical carcinogenesis (Box et al., 2010; Fuchs, 2009; Gerdes and Yuspa, 2005). ODC activity and induction, AdoMetDC transgene expression and the resulting polyamine levels, especially putrescine, within these cells are likely to be the critical determinants of sensitivity to tumor promotion. However, the enzyme activity assays and polyamine measurements were performed on extracts from epidermis and dermis, which could not reflect the *in vivo* situation within the target cells. High levels of AdoMetDC expression and a large decrease in putrescine levels within these cells may not be detected in the *in vitro* assays. Moreover, the complex network regulation of polyamine metabolism (see Chapter I) makes it even more difficult to detect any changes in polyamine levels within small skin cell populations. To overcome the mixed-cell-types problem, we can use *in vitro* primary keratinocyte cultures isolated from newborn AdoMetDC/tTA mice and controls to directly analyze transgene expression and the impact on polyamine content specifically within the keratinocytes that are expressing AdoMetDC transgene. The results will provide an important mechanistic basis for our *in vivo* observations.

The basal cell proliferation index calculated from BrdU staining was slightly, but not significantly, reduced in the interfollicular epidermis of AdoMetDC/tTA mice following

a single or 4 x TPA applications. The cell proliferation index was not analysed in hair follicles because cell proliferation in that region would be affected by growing hair follicle in AdoMetDC/tTA and tTA mice. In addition to BrdU labeling to assess the S-phase cells, phospho-histone H3 immunohistochemistry can be done to measure the number of mitotic cells, which would provide information about whether transgene expression affects G2 transit time between S-phase and mitosis. Also epidermal cell apoptosis can be examined by TUNEL assay or cleaved caspase 3 staining.

The typically pronounced epidermal thickening induced by 4x TPA was decreased by approximately 40% in both AdoMetDC/tTA mice and tTA mice (**Fig. 4-6**), and again, we believe that was due to an unknown tTA trangene insertion effect. Also from the result, we predict that AdoMetDC/tTA and tTA mice would be resistant to DMBA/TPA-induced tumor development. Previous studies with different mouse models and pharmacologic treatments have shown that even mice without any appreciable changes in cell proliferation rate or epidermal thickening, alterations in skin tumor development can be detected (Feith, et al. 2007; Jansen AP et al. 2005; Rodriguez-Puebla et al. 2002; Trempus et al; 2000; Takigawa et al. 1982), which agrees with the concept that short-term TPA-induced hyperplastic response is not equal to tumor promotion targeting at the initiated cells in the skin. Therefore, AdoMetDC/tTA mice may still exhibit different susceptibility to DMBA/TPA skin carcinogenesis than tTA mice and wild type controls.

In conclusion, we found that AdoMetDC/tTA mice exhibit constitutively elevated AdoMetDC activity with or without TPA treatment, and the high levels of AdoMetDC activity tend to decrease putrescine content, which predicts a reduction in skin tumor development in a DMBA/TPA skin carcinogenesis experiment. Although AdoMetDC/tTA

and tTA mice showed decreased ODC induction and epidermal hyperplasia compared to wild type mice upon TPA treatment, it was very likely to be caused by tTA transgene insertion effect that is common to these two groups. Therefore, we can evaluate the effect of AdoMetDC expression on skin carcinogenesis by comparing these two groups.

Chapter V

Investigation of the effect of AdoMetDC overexpression on susceptibility to skin chemical carcinogenesis

INTRODUCTION

As described in Chapter III, we have created and characterized a transgenic mouse model, AdoMetDC/tTA mice, with tissue-specific and Dox-dependent expression of AdoMetDC. AdoMetDC is targeted to specific cell populations in the epidermis and dermis by using the K5 promoter. In Chapter IV we examined the impact of AdoMetDC overexpression on short-term TPA induced skin responses. In this chapter we will evaluate the effect of AdoMetDC overexpression on skin tumor development using the mouse skin chemical carcinogenesis model.

The mouse skin chemical carcinogenesis model is a well characterized system and is widely utilized to study the impacts of genetic, molecular and biochemical perturbations on epithelial tumor initiation, promotion and progression (reviewed in (Abel et al., 2009; Angel and DiGiovanni, 1999; DiGiovanni, 1992; Yuspa, 1994)). It is classically performed by administering a single, sub-carcinogenic dose of mutagenic tumor initiator DMBA, followed by repeated application of tumor promoter TPA to induce the formation of benign papillomas on mouse skin. Using this model, previous studies on mice with altered polyamine metabolism have shown that ODC overexpression is sufficient to promote tumor development from initiated skin cell populations (O'Brien et al., 1997; Peralta Soler et al., 1998; Smith et al., 1998). Additionally, inhibition of ODC

by antizyme or DFMO treatment can reduce skin tumor formation (Feith et al., 2001; Feith et al., 2007; Takigawa et al., 1982; Weeks et al., 1982), suggesting that ODC induction and polyamine accumulation following TPA treatment is required for tumor promotion and maintenance. Overexpession of the polyamine catabolic enzyme SSAT in mouse skin results in increased putrescine levels derived from spermidine and spermine, and hypersensitivity to the DMBA/TPA carcinogenesis protocol with increased incidence of progression to carcinomas (Coleman et al., 2002). Taken together, these studies suggest that increased ODC activity and the subsequent increase in putrescine levels play an essential role in skin tumor development. H_2O_2 and reactive aldehydes released from SSAT-stimulated polyamine catabolism could also enhance tumor development and may account for the increased progression to carcinomas in the SSAT mice (Pegg and Feith, 2007; Wang et al., 2007).

In order to further evaluate the role of polyamines in epithelial carcinogenesis, our novel AdoMetDC/tTA model was subjected to the DMBA/TPA carcinogenesis protocol. AdoMetDC activity provides the aminopropyl groups that are necessary for synthesis of the higher polyamines spermidine and spermine from putrescine. Therefore, in AdoMetDC/tTA mice, transgene overexpression may deplete putrescine through enhanced utilization, but promote spermidine and spermine production. The transgene effect on skin carcinogenesis will provide important evidence to the issue of which polyamine species is critical in tumor development.

METHODS

Maintenance, expansion and identification of transgenic mice

Transgenic mice were housed together with normal littermates in the Central Animal Quarters of the Pennsylvania State University College of Medicine. The transgenic line was expanded by breeding AdoMetDC mice to tTA mice identified in the progeny to produce equal numbers of AdoMetDC/tTA bitransgenic, AdoMetDC single transgenic, tTA single transgenic and wild type littermate controls for experiments. Mice were genotyped for both transgenes by PCR as described in Chapter III. All experimental groups utilized approximately equal numbers of male and female mice of the same age from multiple litters and no sex-dependent differences were observed.

DMBA/TPA skin chemical carcinogenesis

Approximately 40 newborn pups (1 day old) for each genotype were initiated with 200 nmol DMBA (Kodak Laboratory Chemicals, Rochester, NY) in 20 µl acetone topically to their lower back under yellow light, and the animals were not exposed to light for an additional 12 hours. Tumor promotion began at 8 weeks of age with twice weekly topical application of 6.8 nmol TPA (Calbiochem-Novabiochem Corp., La Jolla, CA) in 200 µl acetone. For each genotype the treatment groups were assigned as follows: 10 mice received DMBA alone and were monitored for 40 weeks for tumor development before sacrifice; approximately 30 mice received both DMBA and TPA and were monitored for 25 weeks for tumor development; after that, about half of the mice from each genotype were switched to a diet containing 2g/kg Dox (Bio-Serv, Frenchtown, NJ) and tumors were monitored for an additional 10 weeks while TPA promotion was continued. Tumors larger than 2 mm in diameter were counted weekly, and data are expressed as the

percentage of mice with one or more tumors (tumor incidence) and the mean number of tumors per animal in each group (tumor multiplicity). Tumor size (length x width) was measured at the endpoints of 25 weeks (before Dox) as well as 35 weeks (after Dox) of tumor promotion, and tumor volume was calculated as follows: mm^3=length x width x width x 0.52 (Tomayko and Reynolds, 1989). Mice that developed squamous cell carcinomas were euthanized for humane reasons. All animal protocols were approved by the Animal Care and Use Committee of the Pennsylvania State University College of Medicine.

Tumor processing

Mice were sacrificed 1 week after the final TPA application. Tumors and adjacent normal skin were excised immediately and either flash frozen in liquid nitrogen for biochemical analysis to measure luciferase, AdoMetDC, ODC activity and polyamine levels or fixed overnight in 10% neutral buffered formalin. Multiple tumors from a single mouse were combined. The fixed tumors were embedded in paraffin and 5 μm sections were obtained and stained with hematoxylin and eosin for histological analysis. Suspected carcinomas were also excised, fixed and processed in the same way for histological confirmation.

Biochemical assays and Western blots

Excised frozen tumor and adjacent normal skin samples were divided into different parts, then each part was minced with a scalpel and homogenized in corresponding ice-cold assay buffer to measure AdoMetDC, ODC and lucifease activity, or homogenized in 10% TCA for polyamine analysis using HPLC. All the methods were the same as described in Chapters III and IV.

Statistical analysis

For DMBA/TPA carcinogenesis studies, statistical comparisons between the genotype groups were performed with Mann-Whitney U test for tumor multiplicity and log-rank test of the Kaplan-Meier tumor-free survival curves for tumor incidence (the SAS system, SAS Institute Inc., Cary, NC). The change in tumor multiplicity for each experimental group was compared between before Dox (25 weeks of promotion) and after Dox (35 weeks of promotion) treatment using paired t-tests. AdoMetDC, ODC activity and polyamine levels in skin and tumors were compared between the groups using the two-tailed, unpaired Student's *t* test.

RESULTS

Tumor formation in AdoMetDC/tTA mice

To determine the effect of targeted AdoMetDC overexpression on tumor susceptibility, wild-type, AdoMetDC, tTA and AdoMetDC/tTA mice were subjected to DMBA/TPA treatment. Newborn mice were initiated with DMBA (200 nmol) in this study due to altered timing of the telogen phase in AdoMetDC/tTA and tTA mouse skin as described in Chapter III, and subsequent TPA promotion (6.8 nmol) began at 8 weeks of age.

AdoMetDC/tTA and tTA mice developed significantly fewer tumors per animal than wild-type and AdoMetDC mice over the course of 25 weeks of tumor promotion (**Fig. 5-1**; $P < 0.0001$). The average number of tumors per animal in AdoMetDC/tTA mice (1.5 tumors per mouse), was 46% lower than that for tTA mice (2.7 tumors per mouse) (**Fig. 5-1;** $P<0.0001$). The percent of mice with tumors was over 90% for wild-type and AdoMetDC groups, but only 74% for tTA group and 59% for AdoMetDC/tTA group.

Compared with tTA mice, tumor incidence was lower, but not significantly reduced in the AdoMetDC/tTA mice (**Fig. 5-2;** p=0.06). In addition to developing fewer tumors per mouse, the tumors from tTA and AdoMetDC mice were much smaller than those from wild-type and AdoMetDC mice (**Table 5-1**). This is very likely due to the tTA transgene since there was no size difference between the two groups. There was no histological difference in the papillomas or carcinomas for these experimental groups (data not shown). Very few papillomas (about 5%) developed into malignant carcinomas at a later stage of tumor promotion in each group.

AdoMetDC/tTA mice (n=10) treated with DMBA alone did not develop any tumors through 40 weeks of observation. Therefore, unlike ODC (O'Brien et al., 1997), elevated AdoMetDC activity is not sufficient for tumor promotion; it actually suppresses tumor promotion since AdoMetDC/tTA mice developed significantly fewer tumors than tTA controls. The tTA transgene itself also causes resistance to DMBA/TPA carcinogenesis, so the tTA group is the proper control group for our study.

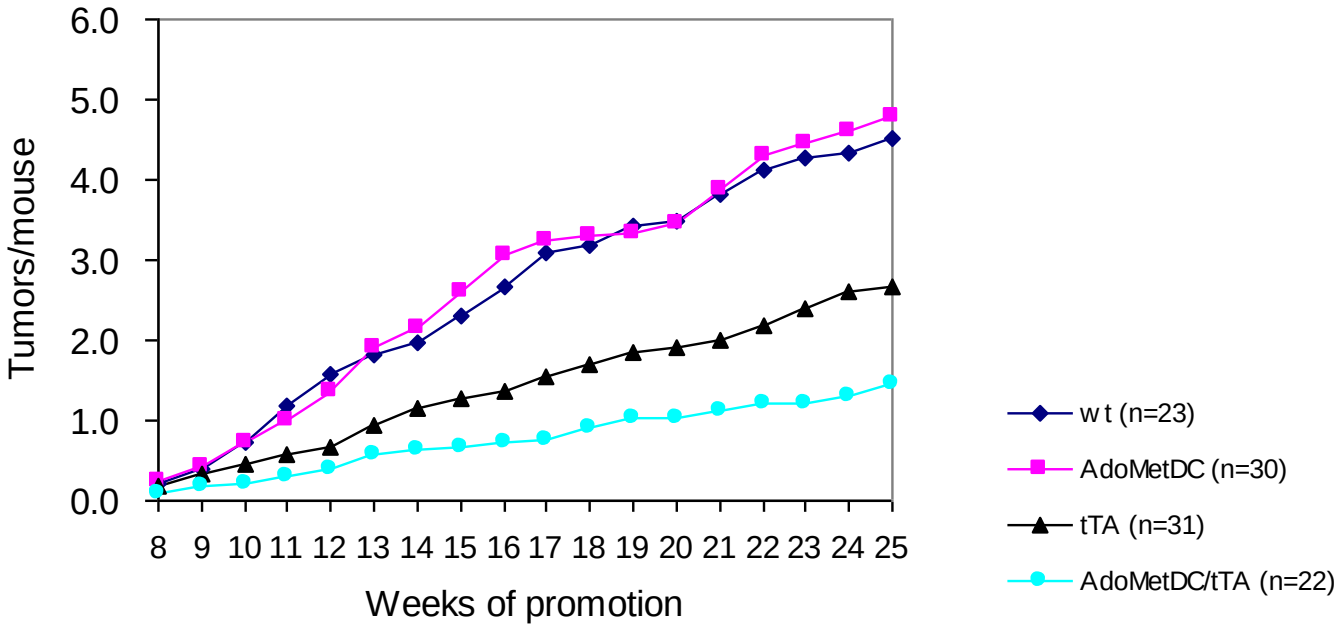

Fig. 5-1 Tumor multiplicity in response to DMBA/TPA carcinogenesis.

Mice were initiated at 1-day of age with 200 nmol of DMBA and twice weekly treatments of 6.8 nmol of TPA started 8 weeks later, and continued for 25 weeks. Tumors larger than 2 mm were counted weekly. Tumor multiplicity is presented as the mean for each genotype group, error bars are not included in order to improve the clarity of the graph. Group sizes are indicated in the figure. $p<0.0001$ for AdoMetDC/tTA mice vs. wild type controls and tTA controls, and $p<0.0001$ for tTA mice vs. wild type controls, as determined by Mann-Whitney U test.

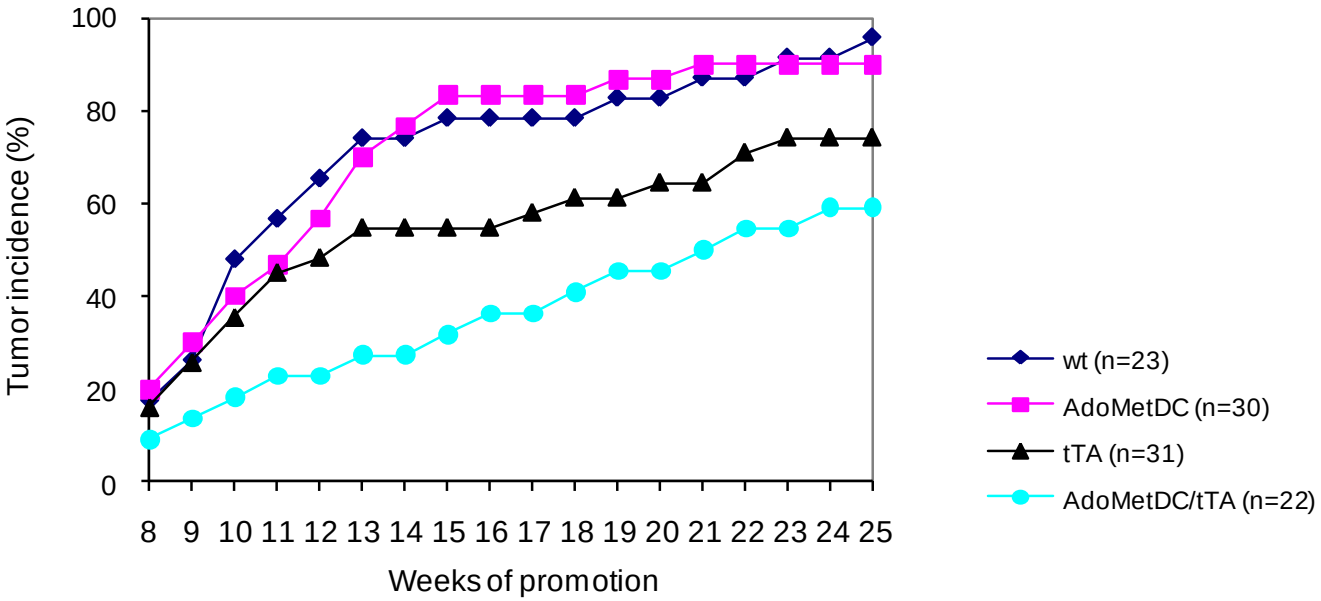

Fig. 5-2 Tumor incidence in response to DMBA/TPA carcinogenesis.

Mice were initiated at 1-day of age with 200 nmol of DMBA and twice weekly treatments of 6.8 nmol of TPA started 8 weeks later, and continued for 25 weeks. Tumors larger than 2 mm were counted weekly. Tumor incidence is presented as the percentage of mice in each group containing at least one tumor. Group sizes are indicated in the figure. P=0.001 for AdoMetDC/tTA mice vs. wild type controls; p=0.06 for AdoMetDC/tTA mice vs. tTA controls; p>0.1 for tTA mice vs. wild type controls as determined by log-rank test of the Kaplan-Meier tumor-free survival curves.

Group	Ave. tumor/mouse	Ave. volume/tumor	2-5 mm	6-10 mm	11-15mm
Wt (n=23)	4.52	149.42	47%	46%	8%
AdoMetDC (n=30)	4.80	168.57	35%	57%	8%
tTA (n=31)	2.68	31.24	89%	11%	0%
AdoMetDC/tTA (n=22)	1.45	33.51	97%	3%	0%

Table 5-1 Size of tumors in response to DMBA/TPA carcinogenesis.

Mice were initiated at 1-day of age with 200 nmol of DMBA and twice weekly treatments of 6.8 nmol of TPA started 8 weeks later, and continued for 25 weeks. The number of animals for each genotype group is shown in parenthesis. Tumor size (length x width) was measured at the termination of 25 weeks of tumor promotion, and tumor volume was calculated as mm^3=length x width x width x 0.52. The percentage of the tumors with indicated size range (mm in length) is shown for each group.

Effects of silencing transgene expression on tumor growth

We then examined whether the lower tumor multiplicity in AdoMetDC/tTA mice was because the initiated cells were eliminated through apoptosis or other irreversible mechanisms induced by elevated levels of AdoMetDC, or they were inhibited from developing into macroscopic tumors but still persist in a viable state in the skin. Transgene expression in a cohort of AdoMetDC/tTA mice and controls was silenced after 25 weeks of tumor promotion by transfering to the Dox diet (**Fig. 3-5**). TPA promotion was continued and tumor growth and appearance were monitored for an additional 10 weeks to detect the emergence of latent initiated cells as macroscopic papillomas. Tumor counts in Dox-treated AdoMetDC/tTA mice increased by 213% ($p<0.005$) to nearly equal the tumor multiplicity in the tTA control group, which increased by only 24% ($p=0.252$) (**Fig. 5-3**). Tumor multiplicity in wild-type and AdoMetDC groups were also increased by similar levels (26%, and 28% respectively) over the 10-week time course (data not shown). Tumors on tTA and AdoMetDC/tTA mice continued to grow more slowly, were similar in size and much smaller than tumors from the other two groups (data not shown).

At the end of the 25 weeks and 35 weeks, mice were sacrificed and luciferase activity was measured in the skin and tumor extracts of AdoMetDC/tTA mice. Extremely low luciferase activity was detected in Dox-treated animals (**Fig. 5-4**), which clearly shows that transgene expression was silenced. Our result indicates that the growth of initiated cells in AdoMetDC/tTA mice was blocked at a microscopic state that is still viable and capable of developing into a macroscopic papilloma upon silencing of AdoMetDC transgene expression.

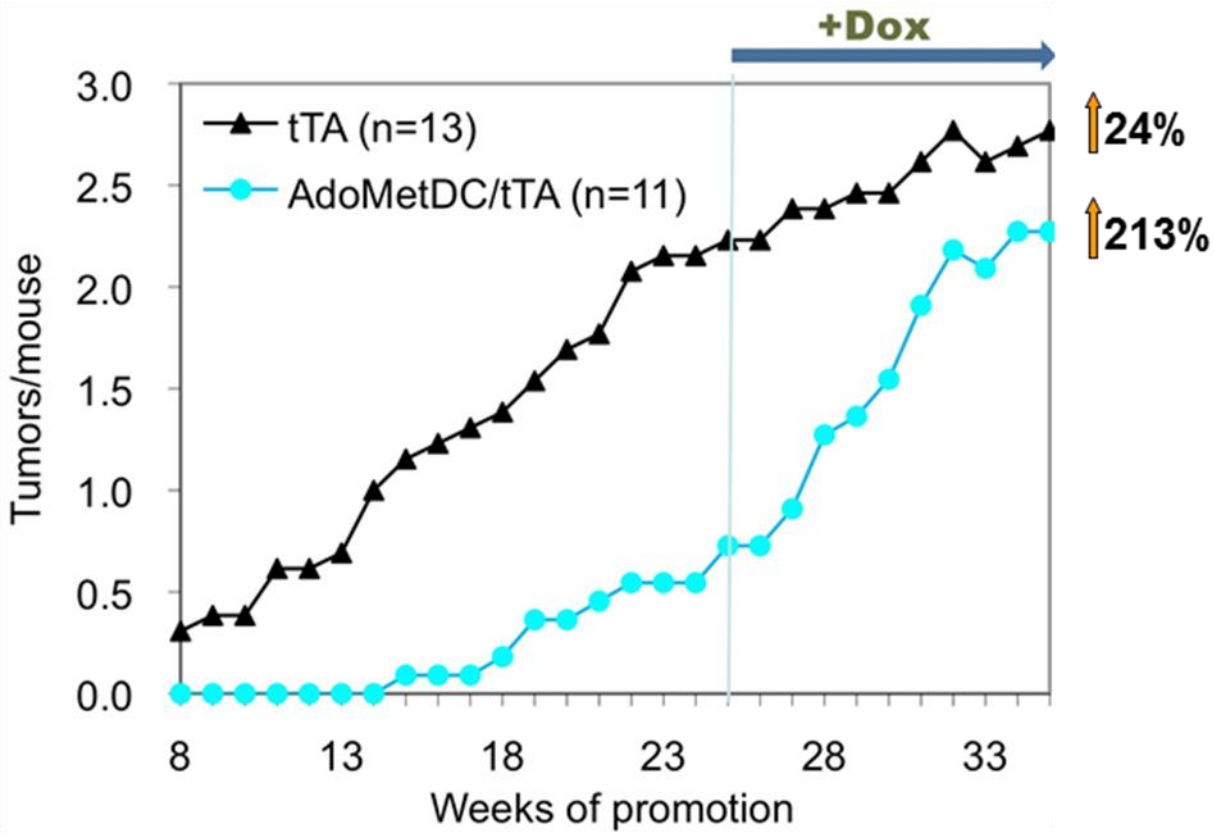

Fig. 5-3 Tumor multiplicity upon silencing of transgene expression.

Following 25 weeks of tumor promotion, a cohort of the mice was then switched to Dox-containing diet (2 g/kg) to silence transgene expression and tumor growth was monitored for an additional 10 weeks while TPA promotion was continued. Group sizes are indicated in the figure legend. Tumor multiplicity is presented as the mean for each genotype group. Over the 10-week experiment period, tumor counts in Dox-treated tTA control group increased by 24% ($p=0.252$), and the AdoMetDC/tTA group increased by 213% ($p<0.005$).

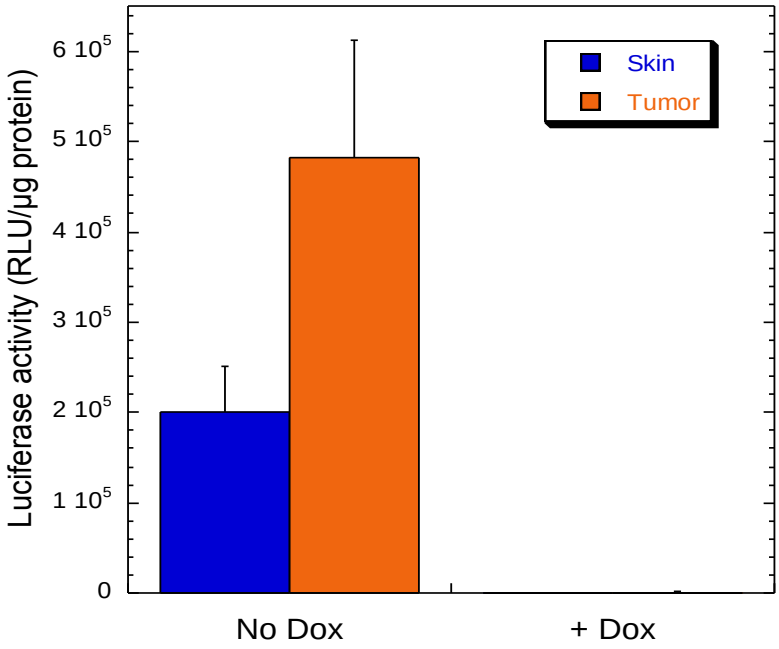

Fig. 5-4 Luciferase activity in skin and tumors of untreated and Dox-treated AdoMetDC/tTA mice.

AdoMetDC/tTA mice with or without Dox treatment were sacrificed one week after 25 weeks or 35 weeks of tumor promotion, and luciferase activity was measured in tumor and adjacent normal skin tissue extracts to evaluate the levels of transgene expression. The result is shown as Mean ± SEM (n=8).

Analysis of tumors and skin for ODC, AdoMetDC activity and polyamine levels

ODC activity is known to be constitutively elevated in DMBA/TPA-induced tumors (Koza et al., 1991; O'Brien et al., 1975a). To examine AdoMetDC activity levels and determine whether AdoMetDC expression altered ODC upregulation, tumor and adjacent whole skin tissues were collected 1 week after the final TPA application of 25-weeks tumor promotion. Tissues were analyzed to determine enzyme activity and polyamine content in wild-type, AdoMetDC, tTA and AdoMetDC/tTA mice. AdoMetDC/tTA mice showed significantly higher AdoMetDC activity in both skin and tumors (**Fig. 5-6**). ODC activity was highly increased in tumors relative to adjacent skin tissues. In tumors from AdoMetDC/tTA mice, there was a tendency of increase in ODC activity compared to tumors from other groups (**Fig. 5-7**). Polyamine content was not statistically reduced in either skin or tumors from AdoMetDC/tTA mice relative to control groups (**Fig. 5-8**). This is not unexpected since AdoMetDC transgene is expressed in a very limited number of skin cells, while the polyamine analysis measured levels in the entire skin or tumor tissues, as previously discussed in Chapter IV.

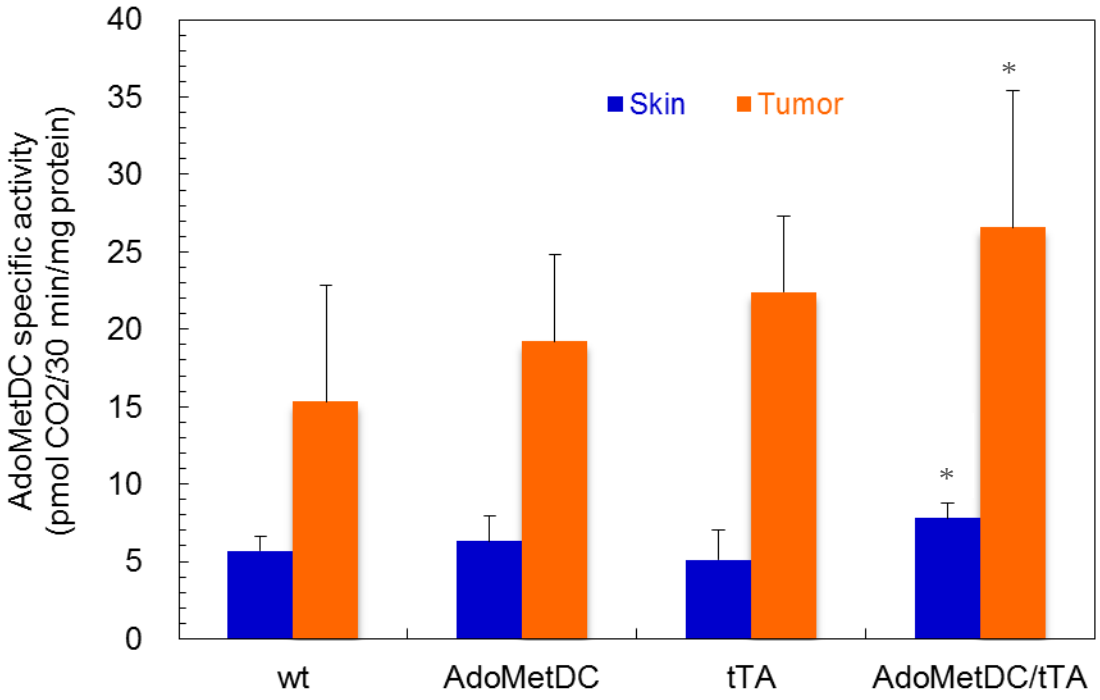

Fig. 5-6 AdoMetDC activity in skin and tumors from DMBA/TPA treated mice

Mice were sacrificed 1 week after the 25-weeks tumor promotion, and tumors and adjacent skin were collected and processed for AdoMetDC activity assay as described in the Materials and Methods. Results (mean ± S.D., n=4-6 for each genotype) are shown for skin and tumors from wild-type, AdoMetDC, tTA and AdoMetDC/tTA mice.
* $p<0.05$ vs. wild type controls.

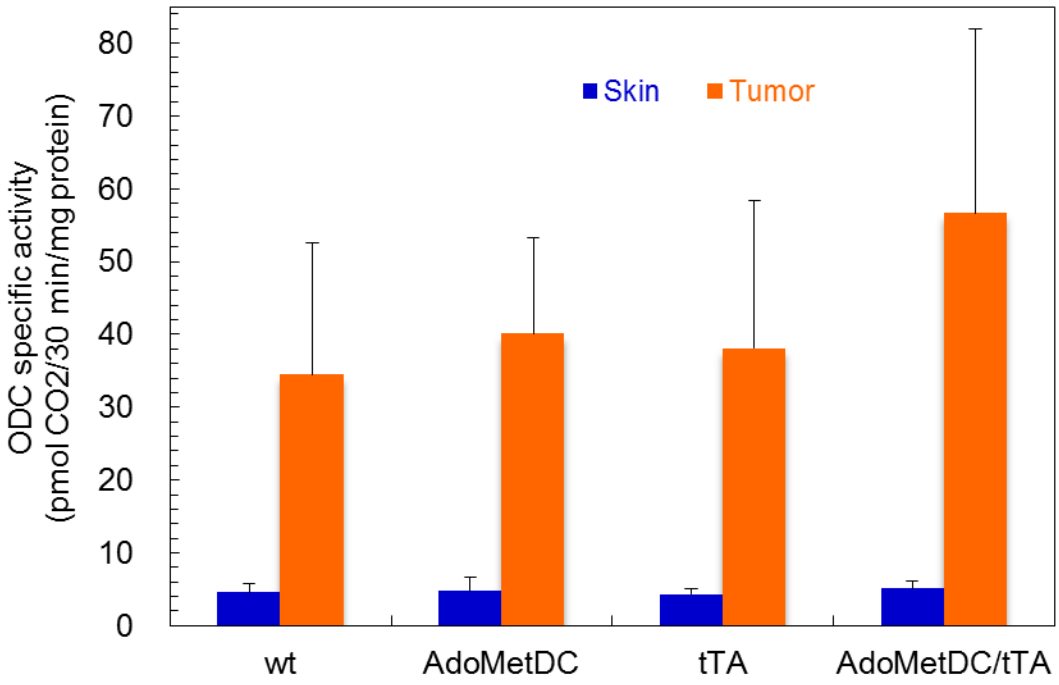

Fig. 5-7 ODC activity in skin and tumors from DMBA/TPA treated mice
Mice were sacrificed 1 week after the 25-weeks tumor promotion, and tumors and adjacent skin were collected and processed for ODC activity assay as described in the Materials and Methods. Results (mean ± S.D., n=4-6 for each genotype) are shown for skin and tumors from wild-type, AdoMetDC, tTA and AdoMetDC/tTA mice. The differences were not statistically significant for skin or tumor between genotypes.

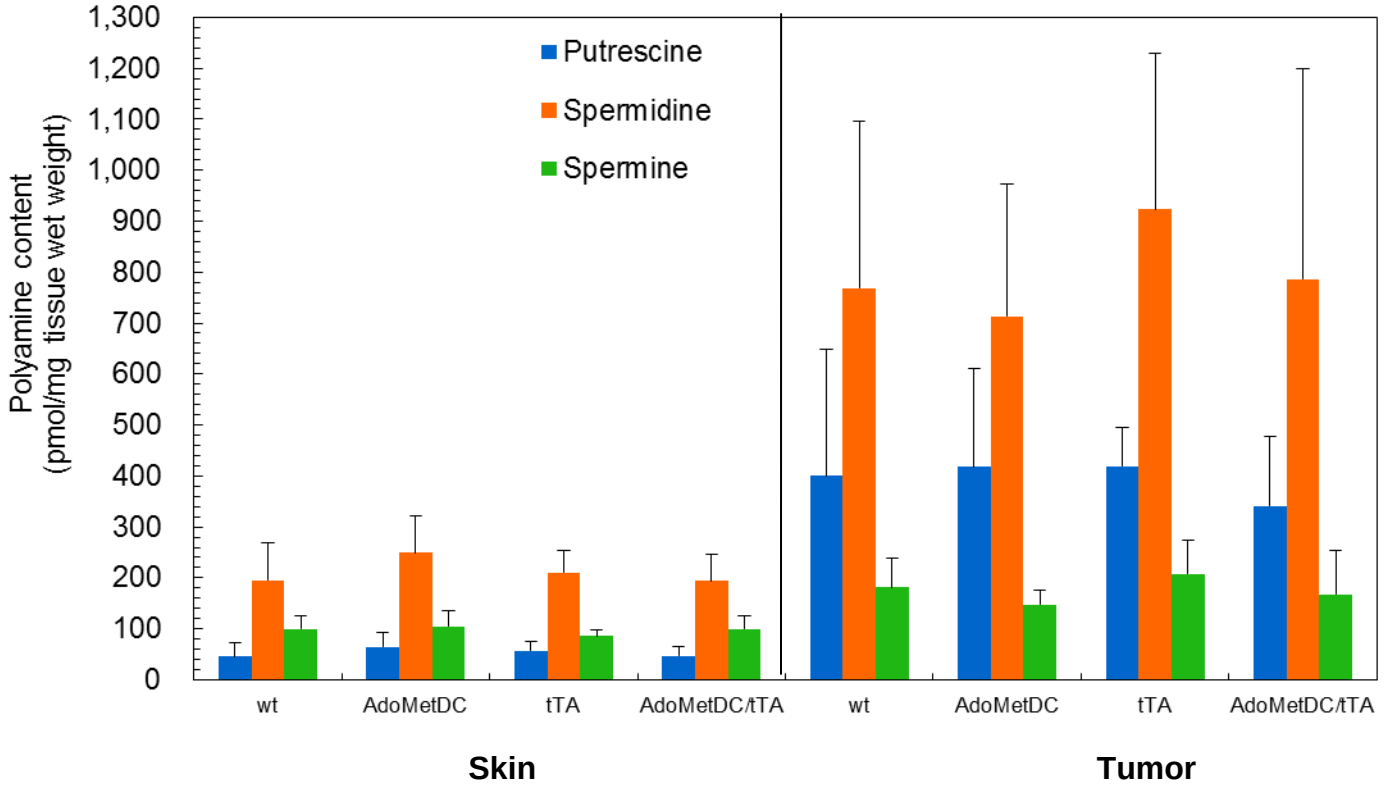

Fig. 5-8 Polyamine Content in skin and tumors from DMBA/TPA treated mice.

Mice were sacrificed 1 week after the 25-weeks tumor promotion, and tumors and adjacent skin were collected and polyamines were measured as described in the Materials and Methods. Results (mean ± S.D., n=4-6 for each genotype) are shown for skin and tumors from wild-type, AdoMetDC, tTA and AdoMetDC/tTA mice. The differences were not statistically significant for skin or tumor between genotypes.

DISCUSSION

In this Chapter, experiments were done to examine the impact of AdoMetDC overexpression on the susceptibility to DMBA/TPA-induced skin carcinogenesis. Our results demonstrated that AdoMetDC/tTA mice with targeted AdoMetDC overexpression resulted in a 46% reduction in tumor multiplicity compared to tTA controls (**Fig. 5-1**). This study utilized DMBA initiation (200 nmol) in newborn mice (1 day old) to prevent the transgene-induced alteration of the synchronized telogen phase at 6 to 8 weeks of age as described in Chapter III, and subsequent TPA promotion (6.8 nmol) began at 8 weeks of age. The low tumor yield is likely due to the fact that newborn mice are more resistant to topical DMBA tumor initiation than adult mice (Hennings et al., 1981). AdoMetDC overexpression tends to decrease tumor incidence (**Fig. 5-2)**, though it does not seem to affect tumor size (**Table 5-1**). After evaluating tumor development in the presence of elevated AdoMetDC, transgene expression was silenced at a late stage of tumor promotion and tumor multiplicity of AdoMetDC/tTA mice increased to match that of tTA controls **(Fig. 5-3)**, which indicates that the promotion of initiated cells to form macroscopic tumors was impaired by AdoMetDC. In agreement with the tumor suppressive effect of AdoMetDC expression, we did not observe any tumors 40 weeks after initiation alone on AdoMetDC/tTA mice, which indicates that elevated AdoMetDC activity is not sufficient for tumor promotion.

The increased tumor burden on AdoMetDC/tTA mice following Dox-mediated transgene silencing (**Fig. 5-3**) has several implications to our study. First of all, it conclusively demonstrated that the tumor suppressive effect is due to increased AdoMetDC activity in AdoMetDC/tTA mice rather than AdoMetDC transgene

integration site, which also excludes the necessity of using a second transgenic line for our study. Secondly, in untreated AdoMetDC/tTA mice, growth of initiated cells was blocked at a microscopic state that is still viable and capable of developing into a macroscopic papilloma. This agrees with previous skin carcinogenesis studies with DFMO (Fischer et al., 2003; Rebel et al., 2002) that indicate initiated cells persist in a dormant but viable state. Also tumors from AdoMetDC/tTA had higher luciferase and AdoMetDC activity than skin, which shows that the tumors from AdoMetDC/tTA mice (no Dox) do maintain transgene expression, and tumor growth is not related to transgene silencing. In other words, tumors from AdoMetDC/tTA mice do not come from cells that have escaped transgene expression. Thirdly, the reduced tumor multiplicity in tTA mice (**Fig. 5-1**), and the small tumor size in tTA and AdoMetDC/tTA mice (**Table 5-1**) are very likely to be caused by tTA transgene itself. The presence of Dox did not affect either tumor growth in tTA mice or tumor size in tTA and AdoMetDC/tTA mice. As mentioned before, another group also observed that tTA mice developed fewer tumors than wild type controls in DMBA/TPA carcinogenesis and Dox treatment did not affect tumor counts over time (Rozenberg et al., 2009), which indicates that the tumor suppression effect is independent of DNA binding of the tTA protein, and more likely to be related to tTA transgene insertion effect, or secondary to tTA protein binding to other factors. The transgene effect results in reduced ODC induction upon TPA treatment (Chapter IV, **Fig. 4-3**), and a consequent reduction in tumor formation.

In Chapter III, we analyzed uninitiated newborn skin histology by established criteria (Hardy, 1992) and did not find any difference between genotype groups in their hair follicle morphogenesis stages. Polyamine measurement of newborn whole skin showed

that there was a decrease in putrescine ($p<0.05$), a trend of increase in spermine, and an increase in Spm/Spd ratio ($p<0.05$) in AdoMetDC/tTA pups compared to wild type and tTA controls (**Table 3-4**). The alterations in polyamine content in the skin of AdoMetDC/tTA mice could potentially affect tumor initiation by altering DMBA metabolism and/or DNA interaction. However, this concern can be largely addressed by the result from the Dox treatment experiment, which indicates that compared with the tTA control group, the reduction in tumor multiplicity in AdoMetDC/tTA mice was due to the effect of AdoMetDC on tumor promotion rather than tumor initiation.

Besides in newborn mice, we also saw a significant increase in Spm/Spd ratio in 4x TPA treated AdoMetDC/tTA mice along with a trend of decrease in putrescine levels. However, the possibility that Spm/Spd ratio decides tumor susceptibility can be ruled out by the finding that increased Spm/Spd ratio in CAG-SpmS mouse skin does not affect susceptibility to DMBA/TPA carcinogenesis (Feith et al., manuscript in preparation).

Since the AdoMetDC/tTA mice have a thin fur phenotype, one may argue that the decreased susceptibility of AdoMetDC/tTA mice to skin carcinogenesis could be the result of thin fur, especially potentially reduced number of hair follicles caused by AdoMetDC overexpression instead of directly relating to transgene expression, and changes in skin structure might affect responses to DMBA and TPA. However, in the 10-weeks of tumor promotion while animals were on Dox, where tumor counts increased, AdoMetDC/tTA mice still exhibit a thin fur phenotype. So it is not the thin fur, but the AdoMetDC overexpression, that causes resistance to DMBA/TPA skin carcinogenesis. Dox treatment can reverse the thin fur phenotype in young mice as discussed in Chapter

III, but not in adult mice, the reason could be that AdoMetDC transgene overexpression, along with time, caused skin stem cell exhaustion in AdoMetDC/tTA mice.

Previous studies have shown that AdoMetDC inhibitors can increase putrescine levels and slow tumor cell growth in various cancer cells and animal systems (reviewed in (Seiler, 2003)). Also it has been found that AdoMetDC overexpression can induce transformation of rodent fibroblasts with an aggressive phenotype (Paasinen-Sohns et al., 2011; Paasinen-Sohns et al., 2000). AdoMetDC inhibitors have been proposed as potential agents for cancer therapy (Janne et al., 1985; McCloskey et al., 2009; Pegg, 2009b; Shantz et al., 1992). However, our data clearly showed that increased AdoMetDC activity suppresses skin carcinogenesis. The explanation for these findings is that AdoMetDC overexpression can inhibit the initial outgrowth of initiated cells during tumor promotion, as seen in our experiment, but on the other hand promote the malignant progression of established tumors. Such a dual role of AdoMetDC in tumor development would be analogous to the effects of TGFβ (Weeks et al., 2001), which has been studied extensively by Dr. Glick (Glick, 2004; Shukla et al., 2008; Tremain et al., 2000). ODC activity is transiently induced by TPA application but is constitutively elevated in papillomas induced by DMBA/TPA carcinogenesis (Koza et al., 1991; O'Brien et al., 1975a). Tumor tissues in our AdoMetDC/tTA mice also showed elevated AdoMetDC activity, and slightly higher ODC activity than control groups, which might be due to further induction by high AdoMetDC activity. Therefore, in the tumor tissues from AdoMetDC/tTA mice, elevated transgene-derived AdoMetDC activity and ODC activity may promote a dramatic accumulation of spermidine and spermine and a compensatory stimulation of the SSAT/PAO catabolic pathway, which is known to promote tumor

progression through generating ROS and reactive aldehydes (Coleman et al., 2002; Wang et al., 2007). Because of the slow growth rate of the tumors in tTA and AdoMetDC/tTA mice, we did not keep those mice for progression study. In future, we can explore the potential dual role of AdoMetDC in tumor development by comparing the progression rate in tTA mice and AdoMetDC/tTA mice, and by conducting additional molecular characterization of archived tumor biopsies to screen for biomarkers that predict papillomas at high risk for progression to SCC (Darwiche et al., 2007).

We were not able to see alterations in polyamine content, either in the tumor or adjacent skin of AdoMetDC/tTA mice. One possible explanation for that is the AdoMetDC transgene is expressed only in limited cell populations within the skin, while polyamine measurements reflect levels in the whole skin or tumor extract. This makes it very difficult to detect even large changes in a small number of cells, while the changes in the initiated cells are the deciding factor in tumor susceptibility.

Because of the same reason as stated above, AdoMetDC activity and the reaction product dcAdoMetDC within the targeted cells might be much higher than what was measured in skin extracts. Typically cellular dcAdoMet (<5%) levels are much lower than AdoMet levels (>95%) because the former is irreversibly committed to polyamine synthesis (Ikeguchi et al., 2006; Pegg, 2009b; Pegg and Michael, 2010). However, dcAdoMet levels can rise to even exceed those of AdoMet with prolonged DFMO treatment (Frostesjo et al., 1997) or massive overexpression of AdoMetDC or AZ (Pegg et al., 2011b; Tsuji et al., 2001; Yamamoto et al., 2010). In this situation dcAdoMet can act as an inhibitor of DNA methyltransferases (Heby et al., 1988), thereby interfering with the methylation of newly replicated DNA (Frostesjo et al., 1997; Heby, 1995). So it

is possible that the increase in dcAdoMet and decrease in AdoMet levels in target cells could influence tumor susceptibility by preventing the growth of initiated cells through effects on methylation reactions.

In summary, our results presented here clearly demonstrate for the first time that AdoMetDC overexpression suppresses tumor development by inhibiting the promotion of initiated cells in the DMBA/TPA skin carcinogenesis model. This finding will provide new perspectives on development of polyamine targeted therapies to prevent and treat cancer.

Chapter VI

Overall conclusion and future perspectives

The main aims of the thesis projects were to examine the impact of elevated spermidine synthase (SpdS) activity on mouse development and physiology, and to elucidate the role of *S*-adenosylmethionine decarboxylase (AdoMetDC) and polyamines in mouse skin carcinogenesis using two transgenic mouse models with altered polyamine metabolism.

We generated and characterized the mouse model with constitutive expression of SpdS utilizing the CAG promoter (Chapter II). CAG-SpdS mice were viable and fertile and tissue SpdS activity was increased up to 9-fold. The increased SpdS activity did not result in a dramatic elevation of spermidine or spermine levels but did lead to a 1.5 to 2-fold reduction in tissue spermine:spermidine ratio in heart, muscle and liver tissues with the highest levels of SpdS activity. This new mouse model enabled simultaneous overexpression of SpdS and other polyamine biosynthetic enzymes by combining transgenic animals. The combined overexpression of both SpdS and SpmS in CAG-SpdS/CAG-SpmS bitransgenic mice did not impair viability or lead to overt developmental abnormalities but instead normalized the elevated tissue spermine:spermidine ratios of CAG-SpmS mice (Ikeguchi et al., 2004). The CAG-SpdS mice were bred to MHC-AdoMetDC mice with a >100-fold increase in cardiac AdoMetDC activity (Nisenberg et al., 2006) to determine if elevated dcAdoMet levels would facilitate greater spermidine accumulation in mice with SpdS overexpression. CAG-SpdS/MHC-AdoMetDC bitransgenic animals were produced at the expected frequency and exhibited cardiac polyamine levels comparable to MHC-AdoMetDC littermates. Taken together, these results indicate that SpdS levels are not rate limiting *in*

vivo for polyamine biosynthesis and are unlikely to exert significant regulatory effects on cellular polyamine content and function.

The CAG-SpdS animals provide additional insight into the regulatory mechanisms that govern polyamine metabolism and are a valuable resource for future studies to explore the role of elevated spermidine levels in physiological or pathological processes. SpdS is a cMyc target gene and elevated SpdS is necessary for Myc-induced B-cell lymphoma (Forshell et al., 2010). CAG-SpdS mice may be useful to determine the effect of elevated SpdS activity and reduced Spm:Spd ratios on tumor development and progression in this model as well as other mouse models of cancer such as skin chemical carcinogenesis. The combination of CAG-SpdS animals with the numerous transgenic and knockout mice with altered polyamine metabolism (Janne et al., 2004; Janne et al., 2006; Pegg et al., 2003) will facilitate the manipulation of polyamine content and ratios to study the role of polyamines in cancer, ion channels function and processes where previous studies propose a role for spermidine (Madeo et al., 2010) or SpdS activity (Cyriac et al., 2002; Korpela et al., 1981; Nishikawa et al., 1997).

CAG-SpdS mice can be bred with Gyro (Gy) mice that harbor a large deletion on the X chromosome that includes most of the SpmS gene (Wang et al., 2004; Wang et al., 2009; Woodward et al., 1993) to evaluate the consequences of SpdS overexpression in the Gy background. The study may provide additional evidence of a role for increased spermidine in the Gy phenotype. Since the human SpdS enzyme displays less substrate specificity than the mouse enzyme (Ikeguchi et al., 2006), CAG-SpdS/Gy mice expressing the human SpdS would also address the provocative question of why spermine is detected in cells from Snyder-Robinson syndrome patients with mutations in the *SMS*

gene that abolish nearly all SpmS activity (Becerra-Solano et al., 2009; Cason et al., 2003; de Alencastro et al., 2008), but not Gy mice.

In a separate project, we developed another transgenic mouse model (AdoMetDC/tTA mice) with tissue-specific and Dox-regulated expression of AdoMetDC using the Tet-regulated system (Chapter III). The basal cell layer of the interfollicular epidermis and the ORS of the hair follicle were targeted with the Keratin 5 promoter. Untreated AdoMetDC/tTA mice displayed a 7 to 8-fold increase in epidermal and dermal AdoMetDC activity and a corresponding increase in dcAdoMet levels. Those mice also exhibited a thin fur phenotype. Transgene expression was silenced by Dox treatment and thin fur phenotype can be abolished by putting nursing dams on Dox. This unique mouse model allowed us to evaluate the role of AdoMetDC and polyamines in skin carcinogenesis.

We next tested the impact of AdoMetDC overexpression on TPA-stimulated enzyme induction and epidermal hyperplasic response in the mouse skin (Chapter IV). We found that AdoMetDC activity in AdoMetDC/tTA mouse skin was constitutively elevated with or without TPA treatment and the high levels of AdoMetDC activity tended to decrease putrescine content after multiple TPA applications. Neither the induction of ODC activity, nor the epidermal thickening following TPA application was affected by AdoMetDC overexpression, but both of them were reduced by tTA transgene in tTA mice and AdoMetDC/tTA mice, which predicts a reduction in skin tumor development in a DMBA/TPA skin carcinogenesis experiment. The difference between tTA and AdoMetDC/tTA mice would be the effect caused by AdoMetDC overexpression.

Lastly, we investigated the effect of AdoMetDC overexpression on susceptibility to

DMBA/TPA carcinogenesis (Chapter V). AdoMetDC/tTA mice were shown to be more resistant to chemical carcinogenesis relative to control groups and elevated AdoMetDC activity suppresses tumor promotion. We also demonstrated that initiated cells that failed to develop into macroscopic tumors persisted in the skin and were capable of developing into macroscopic papillomas upon Dox-mediated transgene silencing. Our finding suggests that putrescine depletion through increased utilization in the presence of elevated AdoMetDC activity suppresses mouse skin tumor promotion, and predicts that AdoMetDC inhibitors may enhance tumor development by elevating putrescine levels instead of inhibiting tumor growth. In addition, this result also suggests that modest alterations in AdoMetDC expression or activity, such as those that may be found within the human population, may contribute to individual tumor susceptibility. AdoMetDC activity determinations could potentially be clinically useful for screening high risk populations for nonmelanoma skin cancer and other epithelial cancers.

Thin fur phenotypes are observed in many mutant mouse models. It can be caused by an abnormally low number of hair follicles, disorders of hair morphogenesis or hair follicle cycling, abnormal follicle structure, or other less likely explanations (Nakamura et al., 2001). Based on the skin histology studies we have done, AdoMetDC/tTA mice show normal follicle structure. We did not count the hair follicle density (e.g. the quantification of hair follicles per linear distance) in newborn or adult mice due to the difficulty of this technique, however, the results from our skin carcinogenesis experiment with Dox-induced transgene silencing suggest that AdoMetDC/tTA mice are likely to have very similar amount of hair follicles as tTA mice, though it is still possible that those two groups of mice both have fewer hair follicles compared with wild type controls

purely due to the tTA transgene. We can further characterize hair follicle morphogenesis at different embryonic and postnatal ages, quantify hair follicle density and analyze hair follicle cycling using established techniques (Nakamura et al., 2001; Sundberg et al., 2005) to elucidate the causes for the thin fur phenotype.

We proposed that elevated AdoMetDC activity may promote the synthesis of higher polyamines at the expense of putrescine and thus suppress tumor promotion. However, since the AdoMetDC transgene was only targeted in the basal keratinocytes, which is a very small cell population within the skin, we were not able to measure directly the putrescine decrease in epidermal, dermal or tumor extracts which consisted of mixed cell populations in AdoMetDC/tTA mice. We can use primary keratinocyte cultures to study the cellular effects of elevated AdoMetDC expression. This *in vitro* experimental model will allow more precise measurements of polyamine content, enzyme activity and polyamine metabolism specifically within the keratinocytes that are expressing AdoMetDC transgene, thereby providing a mechanistic basis for our *in vivo* observations. Alternatively, fluorescence-activated cell sorting (FACS) can be used to isolate basal keratinocytes and polyamine levels can be measured specifically in these transgene-expressing cells, yet so far this is technically challenging because no antibodies have been reported that can be used to isolate all basal keratinocytes, also it is difficult to maintain PA levels intact throughout this process.

Our skin carcinogenesis experiment demonstrated the tumor preventive effect of AdoMetDC expression. To address the ability of AdoMetDC to induce the regression or slow the growth of established tumors, we can put the animals on Dox until they develop tumors and then switch them to normal diet to activate transgene expression and then

quantify the ability of AdoMetDC to induce tumor regression. Alternatively, we can use the K5-rTA strain (Diamond et al., 2000) in which the tetO-AdoMetDC transgene is expressed only in the presence of Dox to prevent the need for long-term maintenance of tTA models on Dox during the promotion phase. DFMO treatment causes tumor regression in a UV-carcinogenesis model, but continued treatment is required to maintain the tumor regression effect (Fischer et al., 2003; Rebel et al., 2002). If we detect tumor regression in our transgenic mice, we can further study if continued transgene expression is required for the effect.

Our studies with the tTA mice indicate that the tTA transgene insertion is very likely to exert an antitumor effect. It will be interesting to identify where the transgene is integrated in the mouse genome. The result could lead to discoveries of a new gene or new regulation mechanisms. The transgene sequence can be localized by established chromosomal mapping method that uses the genomic walking technique in combination with mouse genome database searches (Noguchi et al., 2004).

The AdoMetDC/tTA mouse model we generated can also be used in other skin carcinogenesis protocols to examine the tumor protective effect of AdoMetDC expression, such as repeated application of a low dose of carcinogen/tumor initiator, or UV-carcinogenesis. Additionally, it can be combined with other transgenic mice that are highly sensitive to skin carcinogenesis protocols or predisposed to spontaneous skin tumor development, such as XPA knockout mice (van Steeg et al., 1998) and K14-MEK mouse (Feith et al., 2005) to determine if AdoMetDC can reduce their tumor burden as well as suppress their abnormal phenotype. Moreover, this mouse model can be crossed with other transgenic models with altered polyamine metabolism. For example, they can

be combined with K5-AZ or K6-AZ mice (Feith et al., 2007) to see if putrescine levels could be further depleted and mice are further protected; we can also cross them with K6-ODC to see if AdoMetDC expression would normalize the putrescine increase in those mice and impair tumor development; they can also be combined with K6-SSAT mice (Coleman et al., 2002) to examine how putrescine levels is altered by enhanced utilization and concurrently increased production, and how tumor development is affected by putrescine levels as well as increased metabolic flux. Those cross breeding experiments will enhance our understanding of the role of polyamines in skin carcinogenesis. The AdoMetDC single trangenic mice we developed can be crossed with other transgenic mouse lines with tissue-specific promoter driven tTA/rTA to study AdoMetDC function in other tissues. By silencing transgene expression with Dox during early embryogenesis, this system will also allow AdoMetDC expression in the previously lethal combination of AdoMetDC with other polyamine enzymes (Nisenberg et al., 2006).

BIBLIOGRAPHY

Abel, E.L., Angel, J.M., Kiguchi, K., and DiGiovanni, J. (2009). Multi-stage chemical carcinogenesis in mouse skin: fundamentals and applications. Nat Protoc *4*, 1350-1362.

Alberts, D.S., Dorr, R.T., Einspahr, J.G., Aickin, M., Saboda, K., Xu, M.J., Peng, Y.M., Goldman, R., Foote, J.A., Warneke, J.A., *et al.* (2000). Chemoprevention of human actinic keratoses by topical 2-(difluoromethyl)-dl-ornithine. Cancer Epidemiol Biomarkers Prev *9*, 1281-1286.

Angel, J.M., and DiGiovanni, J. (1999). Genetics of skin tumor promotion. Prog Exp Tumor Res *35*, 143-157.

Anton, D.L., and Kutny, R. (1988). Structural and mechanistic properties of E. coli adenosylmethionine decarboxylase. Adv Exp Med Biol *250*, 81-89.

Bailey, H.H., Kim, K., Verma, A.K., Sielaff, K., Larson, P.O., Snow, S., Lenaghan, T., Viner, J.L., Douglas, J., Dreckschmidt, N.E., *et al.* (2010). A randomized, double-blind, placebo-controlled phase 3 skin cancer prevention study of {alpha}-difluoromethylornithine in subjects with previous history of skin cancer. Cancer Prev Res (Phila) *3*, 35-47.

Balmain, A., Ramsden, M., Bowden, G.T., and Smith, J. (1984). Activation of the mouse cellular Harvey-ras gene in chemically induced benign skin papillomas. Nature *307*, 658-660.

Basuroy, U.K., and Gerner, E.W. (2006). Emerging concepts in targeting the polyamine metabolic pathway in epithelial cancer chemoprevention and chemotherapy. J Biochem *139*, 27-33.

Becerra-Solano, L.E., Butler, J., Castaneda-Cisneros, G., McCloskey, D.E., Wang, X., Pegg, A.E., Schwartz, C.E., Sanchez-Corona, J., and Garcia-Ortiz, J.E. (2009). A missense mutation, p.V132G, in the X-linked spermine synthase gene (SMS) causes Snyder-Robinson syndrome. Am J Med Genet A *149A*, 328-335.

Bickers, D.R., Lim, H.W., Margolis, D., Weinstock, M.A., Goodman, C., Faulkner, E., Gould, C., Gemmen, E., and Dall, T. (2006). The burden of skin diseases: 2004 a joint project of the American Academy of Dermatology Association and the Society for Investigative Dermatology. J Am Acad Dermatol *55*, 490-500.

Bol, D., Kiguchi, K., Beltran, L., Rupp, T., Moats, S., Gimenez-Conti, I., Jorcano, J., and DiGiovanni, J. (1998). Severe follicular hyperplasia and spontaneous papilloma

formation in transgenic mice expressing the neu oncogene under the control of the bovine keratin 5 promoter. Mol Carcinog *21*, 2-12.

Box, N.F., Torchia, E.C., and Roop, D.R. (2010). Are stem cell niches shared for skin cancers? Pigment Cell Melanoma Res *23*, 517-520.

Byrne, C., and Fuchs, E. (1993). Probing keratinocyte and differentiation specificity of the human K5 promoter in vitro and in transgenic mice. Mol Cell Biol *13*, 3176-3190.

Cantoni, G.L. (1975). Biological methylation: selected aspects. Annu Rev Biochem *44*, 435-451.

Casero, R.A., Jr., and Marton, L.J. (2007). Targeting polyamine metabolism and function in cancer and other hyperproliferative diseases. Nat Rev Drug Discov *6*, 373-390.

Cason, A.L., Ikeguchi, Y., Skinner, C., Wood, T.C., Holden, K.R., Lubs, H.A., Martinez, F., Simensen, R.J., Stevenson, R.E., Pegg, A.E., *et al.* (2003). X-linked spermine synthase gene (SMS) defect: the first polyamine deficiency syndrome. Eur J Hum Genet *11*, 937-944.

Chan, K.S., Sano, S., Kataoka, K., Abel, E., Carbajal, S., Beltran, L., Clifford, J., Peavey, M., Shen, J., and Digiovanni, J. (2008). Forced expression of a constitutively active form of Stat3 in mouse epidermis enhances malignant progression of skin tumors induced by two-stage carcinogenesis. Oncogene *27*, 1087-1094.

Chattopadhyay, M.K., Park, M.H., and Tabor, H. (2008). Hypusine modification for growth is the major function of spermidine in Saccharomyces cerevisiae polyamine auxotrophs grown in limiting spermidine. Proc Natl Acad Sci U S A *105*, 6554-6559.

Chattopadhyay, M.K., Tabor, C.W., and Tabor, H. (2002). Absolute requirement of spermidine for growth and cell cycle progression of fission yeast (Schizosaccharomyces pombe). Proc Natl Acad Sci U S A *99*, 10330-10334.

Chiang, P.K., Gordon, R.K., Tal, J., Zeng, G.C., Doctor, B.P., Pardhasaradhi, K., and McCann, P.P. (1996). S-Adenosylmethionine and methylation. FASEB J *10*, 471-480.

Coleman, C.S., and Pegg, A.E. (1998). Assay of mammalian ornithine decarboxylase activity using [14C]ornithine. Methods Mol Biol *79*, 41-44.

Coleman, C.S., Pegg, A.E., Megosh, L.C., Guo, Y., Sawicki, J.A., and O'Brien, T.G. (2002). Targeted expression of spermidine/spermine N1-acetyltransferase increases susceptibility to chemically induced skin carcinogenesis. Carcinogenesis *23*, 359-364.

Cyriac, J., Haleem, R., Cai, X., and Wang, Z. (2002). Androgen regulation of spermidine synthase expression in the rat prostate. Prostate *50*, 252-261.

Darwiche, N., Ryscavage, A., Perez-Lorenzo, R., Wright, L., Bae, D.S., Hennings, H., Yuspa, S.H., and Glick, A.B. (2007). Expression profile of skin papillomas with high cancer risk displays a unique genetic signature that clusters with squamous cell carcinomas and predicts risk for malignant conversion. Oncogene *26*, 6885-6895.

de Alencastro, G., McCloskey, D.E., Kliemann, S.E., Maranduba, C.M., Pegg, A.E., Wang, X., Bertola, D.R., Schwartz, C.E., Passos-Bueno, M.R., and Sertie, A.L. (2008). New SMS mutation leads to a striking reduction in spermine synthase protein function and a severe form of Snyder-Robinson X-linked recessive mental retardation syndrome. J Med Genet *45*, 539-543.

Diamond, I., Owolabi, T., Marco, M., Lam, C., and Glick, A. (2000). Conditional gene expression in the epidermis of transgenic mice using the tetracycline-regulated transactivators tTA and rTA linked to the keratin 5 promoter. J Invest Dermatol *115*, 788-794.

DiGiovanni, J. (1992). Multistage carcinogenesis in mouse skin. Pharmacol Ther *54*, 63-128.

Dingledine, R., Borges, K., Bowie, D., and Traynelis, S.F. (1999). The glutamate receptor ion channels. Pharmacol Rev *51*, 7-61.

Ekstrom, J.L., Tolbert, W.D., Xiong, H., Pegg, A.E., and Ealick, S.E. (2001). Structure of a human S-adenosylmethionine decarboxylase self-processing ester intermediate and mechanism of putrescine stimulation of processing as revealed by the H243A mutant. Biochemistry *40*, 9495-9504.

Fashe, T.M., Keinanen, T.A., Grigorenko, N.A., Khomutov, A.R., Janne, J., Alhonen, L., and Pietila, M. (2010). Cutaneous application of alpha-methylspermidine activates the growth of resting hair follicles in mice. Amino Acids *38*, 583-590.

Feith, D.J., Bol, D.K., Carboni, J.M., Lynch, M.J., Sass-Kuhn, S., Shoop, P.L., and Shantz, L.M. (2005). Induction of ornithine decarboxylase activity is a necessary step for mitogen-activated protein kinase kinase-induced skin tumorigenesis. Cancer Res *65*, 572-578.

Feith, D.J., Origanti, S., Shoop, P.L., Sass-Kuhn, S., and Shantz, L.M. (2006). Tumor suppressor activity of ODC antizyme in MEK-driven skin tumorigenesis. Carcinogenesis *27*, 1090-1098.

Feith, D.J., Shantz, L.M., and Pegg, A.E. (2001). Targeted antizyme expression in the skin of transgenic mice reduces tumor promoter induction of ornithine decarboxylase and decreases sensitivity to chemical carcinogenesis. Cancer Res *61*, 6073-6081.

Feith, D.J., Shantz, L.M., Shoop, P.L., Keefer, K.A., Prakashagowda, C., and Pegg, A.E. (2007). Mouse skin chemical carcinogenesis is inhibited by antizyme in promotion-sensitive and promotion-resistant genetic backgrounds. Mol Carcinog *46*, 453-465.

Feuerstein, B.G., Pattabiraman, N., and Marton, L.J. (1989). Molecular dynamics of spermine-DNA interactions: sequence specificity and DNA bending for a simple ligand. Nucleic Acids Res *17*, 6883-6892.

Feuerstein, B.G., Pattabiraman, N., and Marton, L.J. (1990). Molecular mechanics of the interactions of spermine with DNA: DNA bending as a result of ligand binding. Nucleic Acids Res *18*, 1271-1282.

Finch, J.S., Albino, H.E., and Bowden, G.T. (1996). Quantitation of early clonal expansion of two mutant 61st codon c-Ha-ras alleles in DMBA/TPA treated mouse skin by nested PCR/RFLP. Carcinogenesis *17*, 2551-2557.

Fischer, S.M., Conti, C.J., Viner, J., Aldaz, C.M., and Lubet, R.A. (2003). Celecoxib and difluoromethylornithine in combination have strong therapeutic activity against UV-induced skin tumors in mice. Carcinogenesis *24*, 945-952.

Fleidervish, I.A., Libman, L., Katz, E., and Gutnick, M.J. (2008). Endogenous polyamines regulate cortical neuronal excitability by blocking voltage-gated Na+ channels. Proc Natl Acad Sci U S A *105*, 18994-18999.

Fontecave, M., Atta, M., and Mulliez, E. (2004). S-adenosylmethionine: nothing goes to waste. Trends Biochem Sci *29*, 243-249.

Forshell, T.P., Rimpi, S., and Nilsson, J.A. (2010). Chemoprevention of B-cell lymphomas by inhibition of the Myc target spermidine synthase. Cancer Prev Res (Phila) *3*, 140-147.

Frostesjo, L., Holm, I., Grahn, B., Page, A.W., Bestor, T.H., and Heby, O. (1997). Interference with DNA methyltransferase activity and genome methylation during F9 teratocarcinoma stem cell differentiation induced by polyamine depletion. J Biol Chem *272*, 4359-4366.

Fuchs, E. (2009). The tortoise and the hair: slow-cycling cells in the stem cell race. Cell *137*, 811-819.

Fujisawa, S., and Kadoma, Y. (2005). Kinetic evaluation of polyamines as radical scavengers. Anticancer Res *25*, 965-969.

Gerdes, M.J., and Yuspa, S.H. (2005). The contribution of epidermal stem cells to skin cancer. Stem Cell Rev *1*, 225-231.

Gerner, E.W., and Meyskens, F.L., Jr. (2004). Polyamines and cancer: old molecules, new understanding. Nat Rev Cancer *4*, 781-792.

Gerner, E.W., and Meyskens, F.L., Jr. (2009). Combination chemoprevention for colon cancer targeting polyamine synthesis and inflammation. Clin Cancer Res *15*, 758-761.

Gilmour, S.K. (2007). Polyamines and nonmelanoma skin cancer. Toxicol Appl Pharmacol *224*, 249-256.

Glick, A.B. (2004). TGFbeta1, back to the future: revisiting its role as a transforming growth factor. Cancer Biol Ther *3*, 276-283.

Hardy, M.H. (1992). The secret life of the hair follicle. Trends Genet *8*, 55-61.

Hayes, C.S., DeFeo, K., Lan, L., Paul, B., Sell, C., and Gilmour, S.K. (2006). Elevated levels of ornithine decarboxylase cooperate with Raf/ERK activation to convert normal keratinocytes into invasive malignant cells. Oncogene *25*, 1543-1553.

Heby, O. (1995). DNA methylation and polyamines in embryonic development and cancer. Int J Dev Biol *39*, 737-757.

Heby, O., Persson, L., and Rentala, M. (2007). Targeting the polyamine biosynthetic enzymes: a promising approach to therapy of African sleeping sickness, Chagas' disease, and leishmaniasis. Amino Acids *33*, 359-366.

Heby, O., Persson, L., and Smith, S.S. (1988). Polyamines, DNA methylation and cell differentiation. Adv Exp Med Biol *250*, 291-299.

Hennings, H., Devor, D., Wenk, M.L., Slaga, T.J., Former, B., Colburn, N.H., Bowden, G.T., Elgjo, K., and Yuspa, S.H. (1981). Comparison of two-stage epidermal carcinogenesis initiated by 7,12-dimethylbenz(a)anthracene or N-methyl-N'-nitro-N-nitrosoguanidine in newborn and adult SENCAR and BALB/c mice. Cancer Res *41*, 773-779.

Hennings, H., Glick, A.B., Lowry, D.T., Krsmanovic, L.S., Sly, L.M., and Yuspa, S.H. (1993). FVB/N mice: an inbred strain sensitive to the chemical induction of squamous cell carcinomas in the skin. Carcinogenesis *14*, 2353-2358.

Hibasami, H., Hoffman, J.L., and Pegg, A.E. (1980). Decarboxylated S-adenosylmethionine in mammalian cells. J Biol Chem *255*, 6675-6678.

Hoyt, M.A., Williams-Abbott, L.J., Pitkin, J.W., and Davis, R.H. (2000). Cloning and expression of the S-adenosylmethionine decarboxylase gene of Neurospora crassa and processing of its product. Mol Gen Genet *263*, 664-673.

Huang, Y., Pledgie, A., Casero, R.A., Jr., and Davidson, N.E. (2005). Molecular mechanisms of polyamine analogs in cancer cells. Anticancer Drugs *16*, 229-241.

Ikeguchi, Y., Bewley, M.C., and Pegg, A.E. (2006). Aminopropyltransferases: function, structure and genetics. J Biochem *139*, 1-9.

Ikeguchi, Y., Wang, X., McCloskey, D.E., Coleman, C.S., Nelson, P., Hu, G., Shantz, L.M., and Pegg, A.E. (2004). Characterization of transgenic mice with widespread overexpression of spermine synthase. Biochem J *381*, 701-707.

Janne, J., Alhonen-Hongisto, L., Nikula, P., and Elo, H. (1985). S-adenosylmethionine decarboxylase as target of chemotherapy. Adv Enzyme Regul *24*, 125-139.

Janne, J., Alhonen, L., Pietila, M., and Keinanen, T.A. (2004). Genetic approaches to the cellular functions of polyamines in mammals. Eur J Biochem *271*, 877-894.

Janne, J., Alhonen, L., Pietila, M., Keinanen, T.A., Uimari, A., Hyvonen, M.T., Pirinen, E., and Jarvinen, A. (2006). Genetic manipulation of polyamine catabolism in rodents. J Biochem *139*, 155-160.

Jones, P.H., and Watt, F.M. (1993). Separation of human epidermal stem cells from transit amplifying cells on the basis of differences in integrin function and expression. Cell *73*, 713-724.

Kagoura, M., Toyoda, M., Matsui, C., and Morohashi, M. (2000). Immunohistochemical localization of ornithine decarboxylase in skin tumors. J Cutan Pathol *27*, 338-343.

Kameji, T., and Pegg, A.E. (1987). Effect of putrescine on the synthesis of S-adenosylmethionine decarboxylase. Biochem J *243*, 285-288.

Korpela, H., Holtta, E., Hovi, T., and Janne, J. (1981). Response of enzymes involved in the metabolism of polyamines to phytohaemagglutinin-induced activation of human lymphocytes. Biochem J *196*, 733-738.

Koza, R., Megosh, L., Palmieri, M., and O'Brien, T. (1991). Constitutively elevated levels of ornithine and polyamines in mouse epidermal papillomas. Carcinogenesis *12*, 1619-1625.

Kusano, T., Berberich, T., Tateda, C., and Takahashi, Y. (2008). Polyamines: essential factors for growth and survival. Planta *228*, 367-381.

Lin, X., and Veenstra, R.D. (2007). Effect of transjunctional KCl gradients on the spermine inhibition of connexin40 gap junctions. Biophys J *93*, 483-495.

Liu, X., Alexander, V., Vijayachandra, K., Bhogte, E., Diamond, I., and Glick, A. (2001). Conditional epidermal expression of TGFbeta 1 blocks neonatal lethality but causes a reversible hyperplasia and alopecia. Proc Natl Acad Sci U S A *98*, 9139-9144.

Loenen, W.A. (2006). S-adenosylmethionine: jack of all trades and master of everything? Biochem Soc Trans *34*, 330-333.

Mackintosh, C.A., and Pegg, A.E. (2000). Effect of spermine synthase deficiency on polyamine biosynthesis and content in mice and embryonic fibroblasts, and the sensitivity of fibroblasts to 1,3-bis-(2-chloroethyl)-N-nitrosourea. Biochem J *351 Pt 2*, 439-447.

Madeo, F., Eisenberg, T., Buttner, S., Ruckenstuhl, C., and Kroemer, G. (2010). Spermidine: a novel autophagy inducer and longevity elixir. Autophagy *6*, 160-162.

McCloskey, D.E., Bale, S., Secrist, J.A., 3rd, Tiwari, A., Moss, T.H., 3rd, Valiyaveettil, J., Brooks, W.H., Guida, W.C., Pegg, A.E., and Ealick, S.E. (2009). New insights into the design of inhibitors of human S-adenosylmethionine decarboxylase: studies of adenine C8 substitution in structural analogues of S-adenosylmethionine. J Med Chem *52*, 1388-1407.

Meyskens, F.L., Jr., and Gerner, E.W. (1999). Development of difluoromethylornithine (DFMO) as a chemoprevention agent. Clin Cancer Res *5*, 945-951.

Meyskens, F.L., Jr., McLaren, C.E., Pelot, D., Fujikawa-Brooks, S., Carpenter, P.M., Hawk, E., Kelloff, G., Lawson, M.J., Kidao, J., McCracken, J., *et al.* (2008). Difluoromethylornithine plus sulindac for the prevention of sporadic colorectal adenomas: a randomized placebo-controlled, double-blind trial. Cancer Prev Res (Phila Pa) *1*, 32-38.

Miller, S.J., Wei, Z.G., Wilson, C., Dzubow, L., Sun, T.T., and Lavker, R.M. (1993). Mouse skin is particularly susceptible to tumor initiation during early anagen of the hair cycle: possible involvement of hair follicle stem cells. J Invest Dermatol *101*, 591-594.

Morris, R.J. (2004). A perspective on keratinocyte stem cells as targets for skin carcinogenesis. Differentiation *72*, 381-386.

Muller-Rover, S., Handjiski, B., van der Veen, C., Eichmuller, S., Foitzik, K., McKay, I.A., Stenn, K.S., and Paus, R. (2001). A comprehensive guide for the accurate classification of murine hair follicles in distinct hair cycle stages. J Invest Dermatol *117*, 3-15.

Muller, S., Da'dara, A., Luersen, K., Wrenger, C., Das Gupta, R., Madhubala, R., and Walter, R.D. (2000). In the human malaria parasite Plasmodium falciparum, polyamines are synthesized by a bifunctional ornithine decarboxylase, S-adenosylmethionine decarboxylase. J Biol Chem *275*, 8097-8102.

Nakamura, M., Sundberg, J.P., and Paus, R. (2001). Mutant laboratory mice with abnormalities in hair follicle morphogenesis, cycling, and/or structure: annotated tables. Exp Dermatol *10*, 369-390.

Nancarrow, M.J., Nesci, A., Hynd, P.I., and Powell, B.C. (1999). Dynamic expression of ornithine decarboxylase in hair growth. Mech Dev *84*, 161-164.

Nisenberg, O., Pegg, A.E., Welsh, P.A., Keefer, K., and Shantz, L.M. (2006). Overproduction of cardiac S-adenosylmethionine decarboxylase in transgenic mice. Biochem J *393*, 295-302.

Nishikawa, Y., Kar, S., Wiest, L., Pegg, A.E., and Carr, B.I. (1997). Inhibition of spermidine synthase gene expression by transforming growth factor-beta 1 in hepatoma cells. Biochem J *321 (Pt 2)*, 537-543.

Noguchi, A., Takekawa, N., Einarsdottir, T., Koura, M., Noguchi, Y., Takano, K., Yamamoto, Y., Matsuda, J., and Suzuki, O. (2004). Chromosomal mapping and zygosity check of transgenes based on flanking genome sequences determined by genomic walking. Exp Anim *53*, 103-111.

Nowotarski, S.L., and Shantz, L.M. (2010). Cytoplasmic accumulation of the RNA-binding protein HuR stabilizes the ornithine decarboxylase transcript in a murine nonmelanoma skin cancer model. J Biol Chem *285*, 31885-31894.

O'Brien, T., Simsiman, R., and Boutwell, R. (1975a). Induction of the polymine-biosynthetic enzymes in mouse epidermis by tumor-promoting agents. Cancer Res *35*, 1662-1670.

O'Brien, T.G. (1976a). The induction of ornithine decarboxylase as an early, possibly obligatory, event in mouse skin carcinogenesis. Cancer Res *36*, 2644-2653.

O'Brien, T.G. (1976b). The induction of ornithine decarboxylase as an early, possibly obligatory, event in mouse skin carcinogenesis. Cancer Res *36*, 2644-2653.

O'Brien, T.G., Megosh, L.C., Gilliard, G., and Soler, A.P. (1997). Ornithine decarboxylase overexpression is a sufficient condition for tumor promotion in mouse skin. Cancer Res *57*, 2630-2637.

O'Brien, T.G., Simsiman, R.C., and Boutwell, R.K. (1975b). Induction of the polyamine-biosynthetic enzymes in mouse epidermis by tumor-promoting agents. Cancer Res *35*, 1662-1670.

Okabe, M., Ikawa, M., Kominami, K., Nakanishi, T., and Nishimune, Y. (1997). 'Green mice' as a source of ubiquitous green cells. FEBS Lett *407*, 313-319.

Paasinen-Sohns, A., Kaariainen, E., Yin, M., Jarvinen, K., Nummela, P., and Holtta, E. (2011). Chaotic neovascularization induced by aggressive fibrosarcoma cells overexpressing S-adenosylmethionine decarboxylase. Int J Biochem Cell Biol *43*, 441-454.

Paasinen-Sohns, A., Kielosto, M., Kaariainen, E., Eloranta, T., Laine, A., Janne, O.A., Birrer, M.J., and Holtta, E. (2000). c-Jun activation-dependent tumorigenic transformation induced paradoxically by overexpression or block of S-adenosylmethionine decarboxylase. J Cell Biol *151*, 801-810.

Pajunen, A., Crozat, A., Janne, O.A., Ihalainen, R., Laitinen, P.H., Stanley, B., Madhubala, R., and Pegg, A.E. (1988). Structure and regulation of mammalian S-adenosylmethionine decarboxylase. J Biol Chem *263*, 17040-17049.

Panagiotidis, C.A., Artandi, S., Calame, K., and Silverstein, S.J. (1995). Polyamines alter sequence-specific DNA-protein interactions. Nucleic Acids Res *23*, 1800-1809.

Panteleyev, A.A., Christiano, A.M., O'Brien, T.G., and Sundberg, J.P. (2000). Ornithine decarboxylase transgenic mice as a model for human atrichia with papular lesions. Exp Dermatol *9*, 146-151.

Park, M.H. (2006). The post-translational synthesis of a polyamine-derived amino acid, hypusine, in the eukaryotic translation initiation factor 5A (eIF5A). J Biochem *139*, 161-169.

Park, M.H., Nishimura, K., Zanelli, C.F., and Valentini, S.R. (2010). Functional significance of eIF5A and its hypusine modification in eukaryotes. Amino Acids *38*, 491-500.

Paus, R., Muller-Rover, S., Van Der Veen, C., Maurer, M., Eichmuller, S., Ling, G., Hofmann, U., Foitzik, K., Mecklenburg, L., and Handjiski, B. (1999). A comprehensive guide for the recognition and classification of distinct stages of hair follicle morphogenesis. J Invest Dermatol *113*, 523-532.

Pegg, A.E. (1984). S-adenosylmethionine decarboxylase: a brief review. Cell Biochem Funct *2*, 11-15.

Pegg, A.E. (1986). Recent advances in the biochemistry of polyamines in eukaryotes. Biochem J *234*, 249-262.

Pegg, A.E. (1988). Polyamine metabolism and its importance in neoplastic growth and a target for chemotherapy. Cancer Res *48*, 759-774.

Pegg, A.E. (2006). Regulation of ornithine decarboxylase. J Biol Chem *281*, 14529-14532.

Pegg, A.E. (2008). Spermidine/spermine-N(1)-acetyltransferase: a key metabolic regulator. Am J Physiol Endocrinol Metab *294*, E995-1010.

Pegg, A.E. (2009a). Mammalian polyamine metabolism and function. IUBMB Life *61*, 880-894.

Pegg, A.E. (2009b). S-Adenosylmethionine decarboxylase. Essays Biochem *46*, 25-45.

Pegg, A.E., and Feith, D.J. (2007). Polyamines and neoplastic growth. Biochem Soc Trans *35*, 295-299.

Pegg, A.E., Feith, D.J., Fong, L.Y., Coleman, C.S., O'Brien, T.G., and Shantz, L.M. (2003). Transgenic mouse models for studies of the role of polyamines in normal, hypertrophic and neoplastic growth. Biochem Soc Trans *31*, 356-360.

Pegg, A.E., and McCann, P.P. (1982). Polyamine metabolism and function. Am J Physiol *243*, C212-221.

Pegg, A.E., and Michael, A.J. (2010). Spermine synthase. Cell Mol Life Sci *67*, 113-121.

Pegg, A.E., and Wang, X. (2009). Mouse models to investigate the function of spermine. Commun Integr Biol *2*, 271-274.

Pegg, A.E., Wang, X., Schwartz, C.E., and McCloskey, D.E. (2011a). Spermine synthase activity affects the content of decarboxylated S-adenosylmethionine. Biochem J *433*, 139-144.

Pegg, A.E., Wang, X., Schwartz, C.E., and McCloskey, D.E. (2011b). Spermine synthase activity affects the content of decarboxylated S-adenosylmethionine. Biochem J *433*, 139-144.

Pegg, A.E., Wechter, R., Poulin, R., Woster, P.M., and Coward, J.K. (1989). Effect of S-adenosyl-1,12-diamino-3-thio-9-azadodecane, a multisubstrate adduct inhibitor of spermine synthase, on polyamine metabolism in mammalian cells. Biochemistry *28*, 8446-8453.

Pegg, A.E., Xiong, H., Feith, D.J., and Shantz, L.M. (1998). S-adenosylmethionine decarboxylase: structure, function and regulation by polyamines. Biochem Soc Trans *26*, 580-586.

Peng, H.F., and Jackson, V. (2000). In vitro studies on the maintenance of transcription-induced stress by histones and polyamines. J Biol Chem *275*, 657-668.

Peralta Soler, A., Gilliard, G., Megosh, L., George, K., and O'Brien, T.G. (1998). Polyamines regulate expression of the neoplastic phenotype in mouse skin. Cancer Res *58*, 1654-1659.

Pietila, M., Parkkinen, J.J., Alhonen, L., and Janne, J. (2001). Relation of skin polyamines to the hairless phenotype in transgenic mice overexpressing spermidine/spermine N-acetyltransferase. J Invest Dermatol *116*, 801-805.

Probst, E., and Krebs, A. (1975). Ornithine decarboxylase activity in relation to DNA synthesis in mouse interfollicular epidermis and hair follicles. Biochim Biophys Acta *407*, 147-157.

Quintanilla, M., Brown, K., Ramsden, M., and Balmain, A. (1986). Carcinogen-specific mutation and amplification of Ha-ras during mouse skin carcinogenesis. Nature *322*, 78-80.

Ramirez, A., Bravo, A., Jorcano, J.L., and Vidal, M. (1994). Sequences 5' of the bovine keratin 5 gene direct tissue- and cell-type-specific expression of a lacZ gene in the adult and during development. Differentiation *58*, 53-64.

Rebel, H., van Steeg, H., Beems, R.B., Schouten, R., de Gruijl, F.R., and Terleth, C. (2002). Suppression of UV carcinogenesis by difluoromethylornithine in nucleotide excision repair-deficient Xpa knockout mice. Cancer Res *62*, 1338-1342.

Rider, J.E., Hacker, A., Mackintosh, C.A., Pegg, A.E., Woster, P.M., and Casero, R.A., Jr. (2007). Spermine and spermidine mediate protection against oxidative damage caused by hydrogen peroxide. Amino Acids *33*, 231-240.

Roberts, S.C., Scott, J., Gasteier, J.E., Jiang, Y., Brooks, B., Jardim, A., Carter, N.S., Heby, O., and Ullman, B. (2002). S-adenosylmethionine decarboxylase from Leishmania donovani. Molecular, genetic, and biochemical characterization of null mutants and overproducers. J Biol Chem *277*, 5902-5909.

Rozenberg, J., Rishi, V., Orosz, A., Moitra, J., Glick, A., and Vinson, C. (2009). Inhibition of CREB function in mouse epidermis reduces papilloma formation. Mol Cancer Res *7*, 654-664.

Russell, D.H., and McVicker, T.A. (1972). Polyamine biogenesis in the rat mammary gland during pregnancy and lactation. Biochem J *130*, 71-76.

Sawicki, J.A., Morris, R.J., Monks, B., Sakai, K., and Miyazaki, J. (1998). A composite CMV-IE enhancer/beta-actin promoter is ubiquitously expressed in mouse cutaneous epithelium. Exp Cell Res *244*, 367-369.

Scalabrino, G., and Ferioli, M.E. (1985). Degree of enhancement of polyamine biosynthetic decarboxylase activities in human tumors: a useful new index of degree of malignancy. Cancer Detect Prev *8*, 11-16.

Schmidt-Ullrich, R., and Paus, R. (2005). Molecular principles of hair follicle induction and morphogenesis. Bioessays *27*, 247-261.

Schneider, M.R., Schmidt-Ullrich, R., and Paus, R. (2009). The hair follicle as a dynamic miniorgan. Curr Biol *19*, R132-142.

Seiler, N. (2003). Thirty years of polyamine-related approaches to cancer therapy. Retrospect and prospect. Part 1. Selective enzyme inhibitors. Curr Drug Targets *4*, 537-564.

Shah, N., Thomas, T.J., Lewis, J.S., Klinge, C.M., Shirahata, A., Gelinas, C., and Thomas, T. (2001). Regulation of estrogenic and nuclear factor kappa B functions by polyamines and their role in polyamine analog-induced apoptosis of breast cancer cells. Oncogene *20*, 1715-1729.

Shantz, L.M., Holm, I., Janne, O.A., and Pegg, A.E. (1992). Regulation of S-adenosylmethionine decarboxylase activity by alterations in the intracellular polyamine content. Biochem J *288 (Pt 2)*, 511-518.

Shantz, L.M., and Levin, V.A. (2007). Regulation of ornithine decarboxylase during oncogenic transformation: mechanisms and therapeutic potential. Amino Acids *33*, 213-223.

Shantz, L.M., and Pegg, A.E. (1998). Ornithine decarboxylase induction in transformation by H-Ras and RhoA. Cancer Res *58*, 2748-2753.

Shantz, L.M., and Pegg, A.E. (1999). Translational regulation of ornithine decarboxylase and other enzymes of the polyamine pathway. Int J Biochem Cell Biol *31*, 107-122.

Shirahata, A., and Pegg, A.E. (1985). Regulation of S-adenosylmethionine decarboxylase activity in rat liver and prostate. J Biol Chem *260*, 9583-9588.

Shukla, A., Ho, Y., Liu, X., Ryscavage, A., and Glick, A.B. (2008). Cripto-1 alters keratinocyte differentiation via blockade of transforming growth factor-beta1 signaling: role in skin carcinogenesis. Mol Cancer Res *6*, 509-516.

Smith, M.K., Trempus, C.S., and Gilmour, S.K. (1998). Co-operation between follicular ornithine decarboxylase and v-Ha-ras induces spontaneous papillomas and malignant conversion in transgenic skin. Carcinogenesis *19*, 1409-1415.

Soininen, T., Liisanantti, M.K., and Pajunen, A.E. (1996). S-adenosylmethionine decarboxylase gene expression in rat hepatoma cells: regulation by insulin and by inhibition of protein synthesis. Biochem J *316 (Pt 1)*, 273-277.

Soler, A.P., Gilliard, G., C., M.L., and O'Brien, L.G. (1996). Modulations of murine hair follicle function by alterations in ornithine decarboxylase activity. J Invest Dermatol *106*, 1108-1113.

Soulet, D., Gagnon, B., Rivest, S., Audette, M., and Poulin, R. (2004). A fluorescent probe of polyamine transport accumulates into intracellular acidic vesicles via a two-step mechanism. J Biol Chem *279*, 49355-49366.

Stanfield, P.R., and Sutcliffe, M.J. (2003). Spermine is fit to block inward rectifier (Kir) channels. J Gen Physiol *122*, 481-484.

Stenback, F., Peto, R., and Shubik, P. (1981). Initiation and promotion at different ages and doses in 2200 mice. I. Methods, and the apparent persistence of initiated cells. Br J Cancer *44*, 1-14.

Sundberg, J.P., Erickson, A.A., Roop, D.R., and Binder, R.L. (1994a). Ornithine decarboxylase expression in cutaneous papillomas in SENCAR mice is associated with altered expression of keratins 1 and 10. Cancer Res *54*, 1344-1351.

Sundberg, J.P., Erickson, A.E., Roop, D.R., and Binder, R.L. (1994b). Ornithine decarboxylase expression in cutaneous papillomas in SENCAR mice is associated with altered expression of keratins 1 and 10. Cancer Res *54*, 1344-1351.

Sundberg, J.P., Peters, E.M., and Paus, R. (2005). Analysis of hair follicles in mutant laboratory mice. J Investig Dermatol Symp Proc *10*, 264-270.

Tabor, C.W., and Tabor, H. (1984). Polyamines. Annu Rev Biochem *53*, 749-790.

Takigawa, M., Verma, A.K., Simsiman, R.C., and Boutwell, R.K. (1982). Polyamine biosynthesis and skin tumor promotion: inhibition of 12-O-tetradecanoylphorbol-13-acetate-promoted mouse skin tumor formation by the irreversible inhibitor of ornithine decarboxylase alpha-difluoromethylornithine. Biochem Biophys Res Commun *105*, 969-976.

Tang, X., Kim, A.L., Feith, D.J., Pegg, A.E., Russo, J., Zhang, H., Aszterbaum, M., Kopelovich, L., Epstein, E.H., Jr., Bickers, D.R., *et al.* (2004). Ornithine decarboxylase is a target for chemoprevention of basal and squamous cell carcinomas in Ptch1+/- mice. J Clin Invest *113*, 867-875.

Tani, H., Morris, R.J., and Kaur, P. (2000). Enrichment for murine keratinocyte stem cells based on cell surface phenotype. Proc Natl Acad Sci U S A *97*, 10960-10965.

Tempero, M.A., Nishioka, K., Knott, K., and Zetterman, R.K. (1989). Chemoprevention of mouse colon tumors with difluoromethylornithine during and after carcinogen treatment. Cancer Res *49*, 5793-5797.

Tolbert, W.D., Ekstrom, J.L., Mathews, II, Secrist, J.A., 3rd, Kapoor, P., Pegg, A.E., and Ealick, S.E. (2001). The structural basis for substrate specificity and inhibition of human S-adenosylmethionine decarboxylase. Biochemistry *40*, 9484-9494.

Tolbert, W.D., Zhang, Y., Cottet, S.E., Bennett, E.M., Ekstrom, J.L., Pegg, A.E., and Ealick, S.E. (2003). Mechanism of human S-adenosylmethionine decarboxylase proenzyme processing as revealed by the structure of the S68A mutant. Biochemistry *42*, 2386-2395.

Tomayko, M.M., and Reynolds, C.P. (1989). Determination of subcutaneous tumor size in athymic (nude) mice. Cancer Chemother Pharmacol *24*, 148-154.

Tremain, R., Marko, M., Kinnimulki, V., Ueno, H., Bottinger, E., and Glick, A. (2000). Defects in TGF-beta signaling overcome senescence of mouse keratinocytes expressing v-Ha-ras. Oncogene *19*, 1698-1709.

Tsuji, T., Usui, S., Aida, T., Tachikawa, T., Hu, G.F., Sasaki, A., Matsumura, T., Todd, R., and Wong, D.T. (2001). Induction of epithelial differentiation and DNA demethylation in hamster malignant oral keratinocyte by ornithine decarboxylase antizyme. Oncogene *20*, 24-33.

van Steeg, H., Klein, H., Beems, R.B., and van Kreijl, C.F. (1998). Use of DNA repair-deficient XPA transgenic mice in short-term carcinogenicity testing. Toxicol Pathol *26*, 742-749.

Vance, J.E., and Vance, D.E. (2004). Phospholipid biosynthesis in mammalian cells. Biochem Cell Biol *82*, 113-128.

Wallace, H.M., and Fraser, A.V. (2004). Inhibitors of polyamine metabolism: review article. Amino Acids *26*, 353-365.

Wallace, H.M., Fraser, A.V., and Hughes, A. (2003). A perspective of polyamine metabolism. Biochem J *376*, 1-14.

Wang, X., Feith, D.J., Welsh, P., Coleman, C.S., Lopez, C., Woster, P.M., O'Brien, T.G., and Pegg, A.E. (2007). Studies of the mechanism by which increased spermidine/spermine N1-acetyltransferase activity increases susceptibility to skin carcinogenesis. Carcinogenesis *28*, 2404-2411.

Wang, X., Ikeguchi, Y., McCloskey, D.E., Nelson, P., and Pegg, A.E. (2004). Spermine synthesis is required for normal viability, growth, and fertility in the mouse. J Biol Chem *279*, 51370-51375.

Wang, X., Levic, S., Gratton, M.A., Doyle, K.J., Yamoah, E.N., and Pegg, A.E. (2009). Spermine synthase deficiency leads to deafness and a profound sensitivity to alpha-difluoromethylornithine. J Biol Chem *284*, 930-937.

Wang, X., and Pegg, A.E. (2011). Use of (Gyro) Gy and spermine synthase transgenic mice to study functions of spermine. Methods Mol Biol *720*, 159-170.

Warters, R.L., Newton, G.L., Olive, P.L., and Fahey, R.C. (1999). Radioprotection of human cell nuclear DNA by polyamines: radiosensitivity of chromatin is influenced by tightly bound spermine. Radiat Res *151*, 354-362.

Weeks, B.H., He, W., Olson, K.L., and Wang, X.J. (2001). Inducible expression of transforming growth factor beta1 in papillomas causes rapid metastasis. Cancer Res *61*, 7435-7443.

Weeks, C.E., Herrmann, A.L., Nelson, F.R., and Slaga, T.J. (1982). alpha-Difluoromethylornithine, an irreversible inhibitor of ornithine decarboxylase, inhibits tumor promoter-induced polyamine accumulation and carcinogenesis in mouse skin. Proc Natl Acad Sci U S A *79*, 6028-6032.

Wiest, L., and Pegg, A.E. (1998). Assay of spermidine and spermine synthases. Methods Mol Biol *79*, 51-57.

Wolff, E.C., Kang, K.R., Kim, Y.S., and Park, M.H. (2007). Posttranslational synthesis of hypusine: evolutionary progression and specificity of the hypusine modification. Amino Acids *33*, 341-350.

Woodward, J.E., Meyer, M.H., Gray, R.W., and Meyer, R.A., Jr. (1993). Intestinal malabsorption of 45calcium in young Gy mice, a second model for X-linked hypophosphatemia. J Bone Miner Res *8*, 1281-1290.

Wu, H., Min, J., Ikeguchi, Y., Zeng, H., Dong, A., Loppnau, P., Pegg, A.E., and Plotnikov, A.N. (2007). Structure and mechanism of spermidine synthases. Biochemistry *46*, 8331-8339.

Xiong, H., Stanley, B.A., Tekwani, B.L., and Pegg, A.E. (1997). Processing of mammalian and plant S-adenosylmethionine decarboxylase proenzymes. J Biol Chem *272*, 28342-28348.

Yamamoto, D., Shima, K., Matsuo, K., Nishioka, T., Chen, C.Y., Hu, G.F., Sasaki, A., and Tsuji, T. (2010). Ornithine decarboxylase antizyme induces hypomethylation of genome DNA and histone H3 lysine 9 dimethylation (H3K9me2) in human oral cancer cell line. PLoS One *5*, e12554.

Yuspa, S.H. (1994). The pathogenesis of squamous cell cancer: lessons learned from studies of skin carcinogenesis--thirty-third G. H. A. Clowes Memorial Award Lecture. Cancer Res *54*, 1178-1189.

Yuspa, S.H. (1998). The pathogenesis of squamous cell cancer: lessons learned from studies of skin carcinogenesis. J Dermatol Sci *17*, 1-7.

Yuspa, S.H., Lichti, U., Ben, T., Patterson, E., Hennings, H., Slaga, T.J., Colburn, N., and Kelsey, W. (1976). Phorbol esters stimulate DNA synthesis and ornithine decarboxylase activity in mouse epidermal cell cultures. Nature *262*, 402-404.

Zhu, Z., Zheng, T., Lee, C.G., Homer, R.J., and Elias, J.A. (2002). Tetracycline-controlled transcriptional regulation systems: advances and application in transgenic animal modeling. Semin Cell Dev Biol *13*, 121-128.

VITA

Chenxu Shi

Education

2005-2011 PhD Candidate, Physiology Graduate Program
Pennsylvania State University College of Medicine

2000-2005 Bachelor of Medicine (MD equivalent)
Peking University Health Science Center, Beijing, China

Publications

Chenxu Shi, Patricia A. Welsh, Suzanne Sass-Kuhn, Xiaojing Wang, Diane E. McCloskey, Anthony E. Pegg, David J. Feith. Characterization of Transgenic Mice with Overexpression of Spermidine Synthase. *Amino Acids,* Epub 2011 Aug. PMID: 21809077

Chenxu Shi, Diane E. McCloskey, Anthony E. Pegg, David J. Feith. S-adenosylmethionine Decarboxylase Overexpression in the Skin of Transgenic Mice Reduces Sensitivity to Skin Chemical Carcinogenesis. *Manuscript prepared for submission.*

Abstracts and Presentations

Chenxu Shi, Diane E. McCloskey, Anthony E. Pegg, David J. Feith. Transgenic Mice to Evaluate the Role of S-adenosylmethionine Decarboxylase in Skin Carcinogenesis.
Abstract, *Proc. Am. Assoc. Cancer Res*. 2010, 19:2483.
Poster Presentation, *9th International Skin Carcinogenesis Conference* University Park, PA. June, 2010.

Chenxu Shi, Diane E. McCloskey, Anthony E. Pegg, David J. Feith. Development of Transgenic Mice with Regulated AdoMetDC Expression in the Skin.
Poster Presentation, *Gordon Research Conference on Polyamines* Waterville Valley, NH. June, 2009.

Chenxu Shi, David J. Feith, Diane E. McCloskey, Anthony E. Pegg. DNA Construct to Make Transgenic Mice with Regulated AdoMetDC Expression.
Poster Presentation, *Gordon Research Conference on Polyamines* Waterville Valley, NH. June, 2007.